N O T I C E

THIS DOCUMENT HAS BEEN REPRODUCED FROM
MICROFICHE. ALTHOUGH IT IS RECOGNIZED THAT
CERTAIN PORTIONS ARE ILLEGIBLE, IT IS BEING RELEASED
IN THE INTEREST OF MAKING AVAILABLE AS MUCH
INFORMATION AS POSSIBLE

Lox/Gox Mechanical Impact Tester Assessment

By J. W. Bransford, C. J. Bryan, G. W. Frye, and S. L Stohler

FEBRUARY 1980

NASA

John F. Kennedy Space Center

STANDARD TITLE PAGE

1. Report No. NASA TM 74106	2. Government Accession No.	3. Recipient's Catalog No.
4. Title and Subtitle LOX/GOX Mechanical Impact Tester Assessment		5. Report Date February, 1980
		6. Performing Organization Code
7. Author(s) J.W.Bransford*,C.J. Bryan**,G.W.Frye[+], & S.L.Stohler[++]		8. Performing Organization Report No.
9. Performing Organization Name and Address John F. Kennedy Space Center Kennedy Space Center, Florida 32899		10. Work Unit No.
		11. Contract or Grant No.
		13. Type of Report and Period Covered
12. Sponsoring Agency Name and Address National Aeronautics and Space Administration Washington, D. C. 20546		
		14. Sponsoring Agency Code

15. Abstract

This report presents a description of a test program evaluating the performance of three existing high-pressure oxygen mechanical impact test systems located at Marshall Space Flight Center, Rocketdyne Santa Susana Field Laboratory, and White Sands Test Facility. The Marshall and Rocketdyne systems were fabricated from the same design drawing, whereas, the White Sands system, even though similar, was of different design. The ABMA impact testers located at Kennedy Space Center and the above three facilities were also evaluated.

This test program was a two-phase project evaluating and comparing energy delivered to the test sample for each test system and comparing those results to the reaction rates obtained during a material test program.

*NASA, Marshall Space Flight Center, Alabama
**NASA, Kennedy Space Center, Florida
 NASA, Johnson Space Center, White Sands Test
        Facility

[++]Rockwell Intermational Corp.
    Rocketdyne Division

16. Key Words

Oxygen compatibility
Mechanical Impact Tester

17. Bibliographic Control	18. Distribution
	Unclassified — Unlimited Star Category 23

19. Security Classif.(of this report)	20. Security Classif.(of this page)	21. No. of Pages	22. Price
Unclassified	Unclassified	104	NTIS

KSC FORM 16-272NS (REV 7/78)

FOREWORD

This is the final report describing the work accomplished in a 2-year period to evaluate the ABMA and high pressure oxygen impact testers for energy delivery and reproducibility for a given tester and among testers of the same design.

TABLE OF CONTENTS

LIST OF ILLUSTRATIONS

iv

LIST OF ILLUSTRATIONS (Continued)

LIST OF ILLUSTRATIONS (Concluded)

LIST OF TABLES

LOX/GOX MECHANICAL IMPACT TESTER ASSESSMENT

SUMMARY

In support of the Space Shuttle program, two different high-pressure mechanical impact testers were developed for determining reaction sensitivity of materials in oxygen at pressures up to 6.9×10^7 Pa (10000 psig) by White Sands Test Facility (WSTF) and Rockwell International, Rocketdyne Division. This report examines the differences of these two designs together with the reproducibility of the test results. Each test performed on the high pressure systems was also performed on ABMA testers located at Marshall Space Flight Center (MSFC), WSTF, Kennedy Space Center (KSC), and Rocketdyne.

The program was set up in two phases. Phase I was an energy input study and Phase II was a material round-robin test series. It was found that all ABMA testers produced essentially identical results for Phase I and Phase II, demonstrating the capacity for excellent reproducibility under standardized conditions. Results from Phase I showed that the MSFC and Rocketdyne high pressure testers delivered nearly the same amount of energy to the test samples in LOX and GOX at 3.4×10^7 Pa (5000 psi), but the WSTF high pressure tester delivered only one-third as much energy in 3.4×10^7 Pa LOX and only two-thirds as much energy in 3.4×10^7 Pa GOX for any given plummet height. However, when materials were tested under identical conditions (Phase II), the WSTF tester produced material reactions at the same or lower plummet heights than did the MSFC and Rocketdyne testers. This is contrary to the trend suggested by the energy input study and indicates that factors other than total input energy to the sample influenced the results.

INTRODUCTION

The most widely used technique within NASA to evaluate the compatibility of materials in LOX and GOX has been the test method which determines the reaction sensitivity of materials under mechanical impact conditions. The most familiar impact device has been the ABMA dropweight tester. This tester has been utilized extensively in the evaluation of materials for oxygen service in many space programs such as Apollo and Space Shuttle. This ABMA tester, which used unpressurized LOX, was standardized by the establishment of MSFC-SPEC-106B [1] and industrial specifications such as ASTM-D-2512 [2].

Because of the obvious temperature and pressure limitations of the ABMA impact tester, two different high-pressure oxygen impact test systems were developed: one by the Johnson Space Center's (JSC) WSTF and another by Rockwell International Corporation, Rocketdyne Division, under contract to MSFC in support of the Space Shuttle program. Both designs were based upon the ABMA test method and provided the capability to test in LOX or GOX at pressures up to 6.9×10^7 Pa (10000 psig) to simulate the maximum operating conditions of the Space Shuttle.

An enormous amount of data has been generated over the years from the ABMA tester by various test facilities which provided information regarding the reproducibility of test results. However, no studies have been performed to date to evaluate the tester-to-tester reproducibility of the high-pressure mechanical impact testers located at WSTF, MSFC, and Rocketdyne's Santa Susana Field Laboratory (SSFL). Therefore, efforts were initiated in 1976 to study the high-pressure oxygen impact tester variability noted between the three test facilities, previously listed, resulting from a preliminary test program reported in Appendix A. This study supported the proposed theory that the Rocketdyne-designed impact tester at MSFC had the highest material reaction rate. Next in observed reactivity was the identically designed and built Rocketdyne tester at SSFL and then the WSTF-designed tester. To understand and correlate high-pressure oxygen compatibility impact test data for the Space Shuttle program, it became apparent that an effort should be initiated to determine the tester-to-tester reproducibility along with an analysis of the observed test result discrepancies between the Rocketdyne-designed and the WSTF-designed impact testers. A two-phase study was subsequently developed with the following objectives:

1) Determine impact test data reproducibility for the three existing high-pressure testers.

2) Determine and compare energy delivery for each high-pressure tester and ABMA test system (with the participation of KSC).

3) Correlate material reactivity with energy delivery in the high-pressure and ABMA testers.

4) Determine guidelines for high-pressure impact testing standardization.

5) Develop a calibration method for impact testers.

2

Phase I of this evaluation was to examine the amount of energy delivered by the individual test system to the test sample. Phase II involved a round-robin impact test program between all test facilities (KSC, MSFC, SSFL, and WSTF) on identical lots of materials under standardized conditions.

This report presents all the procedures, test results, data, and conclusions of this extensive 2-year program. Due to the importance placed upon the oxygen compatibility batch test program for the use of materials in all components in the Space Shuttle oxygen systems, it is hoped that the information presented herein will prove valuable for assessing, understanding, standardizing, and improving oxygen mechanical impact testing.

EXPERIMENTAL PROCEDURES AND TEST RESULTS

Phase I: Energy Input Study

Discussion and Experimental Procedure. During the initial discussions, in which the Round Robin Test Series (Phase II) was set up, it was decided that an experiment should be included to determine the energy delivered to a test sample. The necessity of this study can be seen by viewing the detail of the various testers (Figs. 1, 2, and 3). As seen in Figure 1, the ABMA tester has a rigid base configuration and an unrestrained striker pin and, therefore, was expected to produce the greatest impact stress upon a test specimen for any given plummet drop height. The MSFC/SSFL high pressure tester (Fig. 2) has a base equally as rigid as the ABMA tester, but the friction effects of the three seals upon dynamic response of the balance piston was not totally understood. Even though the seal effects were unknown, it was expected that the impact results for the MSFC/SSFL testers would approach those of the ABMA tester. The WSTF high-pressure tester design (Fig. 3) is completely different from the Rocketdyne-designed tester. Its response was not known but was believed by some to produce smaller impact loads on the test specimen than either the ABMA or MSFC/SSFL tester because of its base design and smaller diameter striker pin shaft.

It was recognized that an absolute value for the energy absorbed by a sample could probably not be found but that a relative energy could be determined. A method suggested by WSTF was used to examine the amount of energy transferred from the 9.07-kg (20 lb) plummet to the test sample. This method was to impact a metal disc of sufficient thickness with a 1.27-cm (0.500 in.) diameter hemispherical striker tip instead of the usual 1.27-cm (0.500 in.)

PLUMMET

STRIKER PIN
GUIDE

STRIKER PIN

LOX

CUP

TOP PLATE

SAMPLE

ANVIL

BASE PLATE

CONCRETE
PEDESTAL
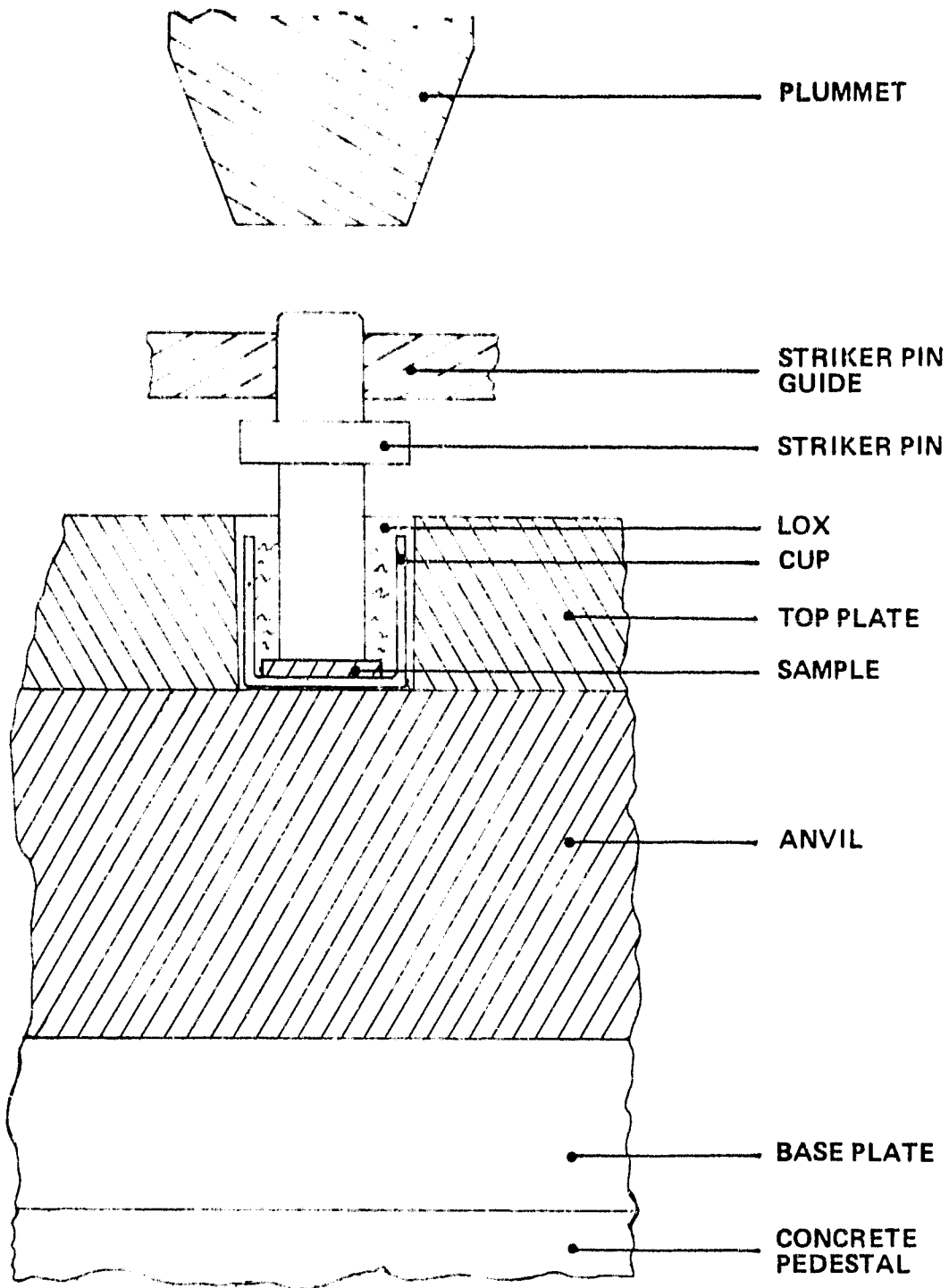
Figure 1. ABMA tester detail.

4
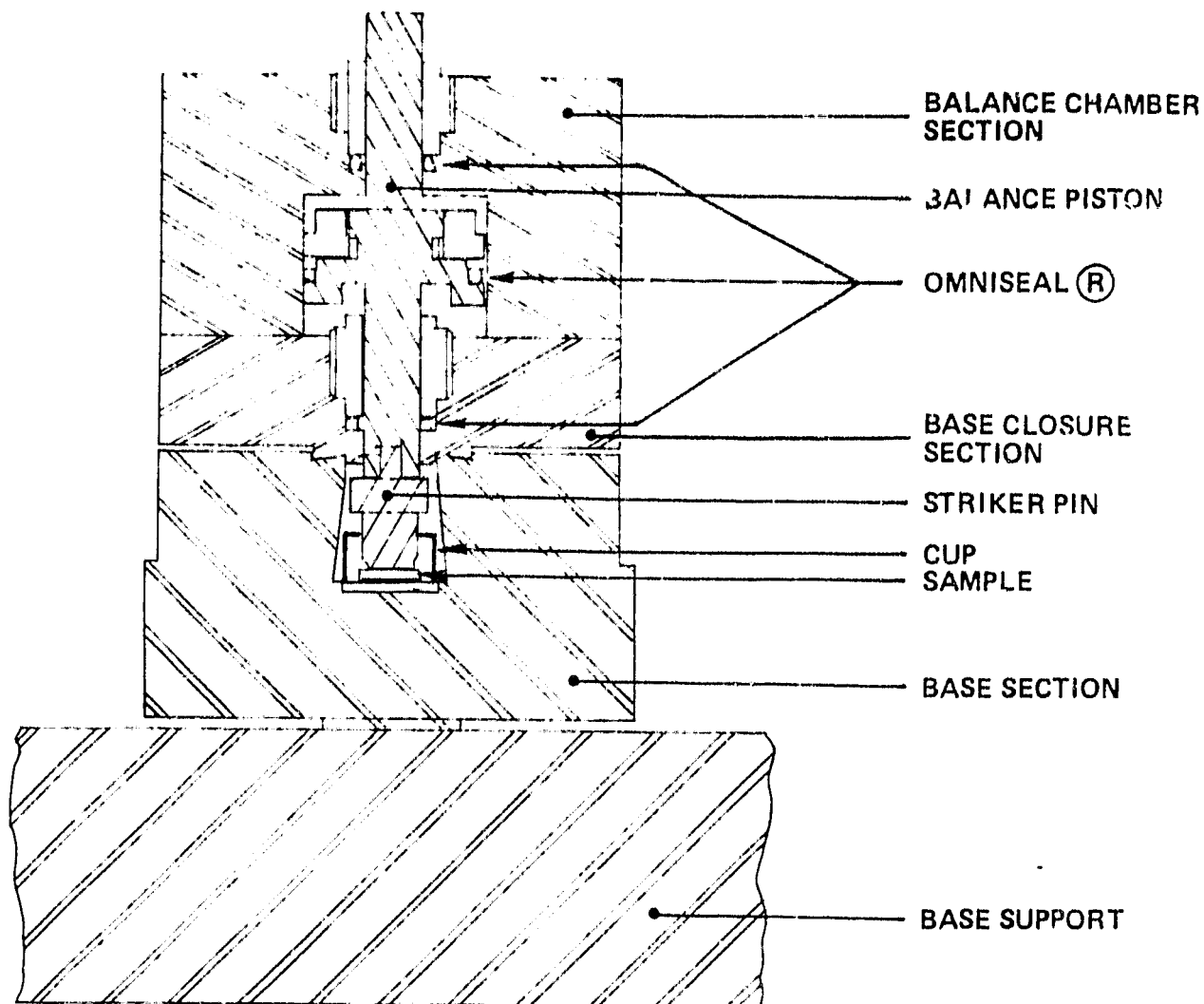
Figure 2. MSFC/SSFL high pressure tester detail.

diameter flat striker tip. The penetration or diameter of the indentation produced by a given tester at various energy levels (plummet drop heights) could then be measured and compared to data generated by the other testers. It was also decided that the ABMA tester should serve as a reference since this tester has a rigid base and a minimum of mechanical constraints on the striker and should, therefore, give the maximum indentation.

With the method of comparison decided, a test matrix was developed in which variables to be studied were detailed. For the ABMA impact tester, the principal variable was temperature so that a reference for GOX temperatures
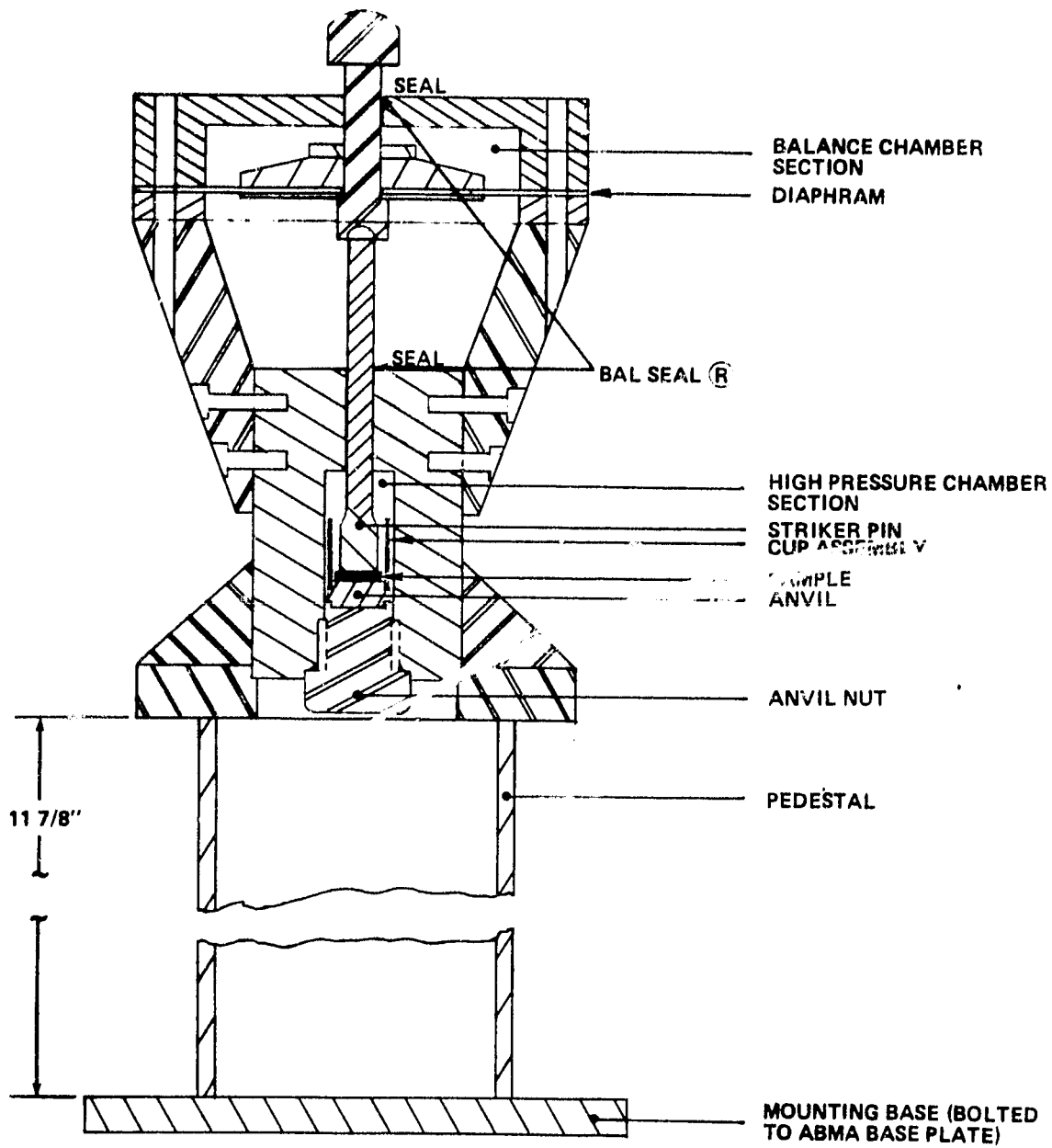
Figure 3. WSTF high pressure tester detail.

SEAL

BALANCE CHAMBER
SECTION

DIAPHRAM

SEAL

BAL SEAL ®

HIGH PRESSURE CHAMBER
SECTION

STRIKER PIN
CUP ASSEMBLY

SAMPLE
ANVIL

ANVIL NUT

PEDESTAL

11 7/8"

MOUNTING BASE (BOLTED
TO ABMA BASE PLATE)

6

could be established. For the high-pressure tester, the principal variables were temperature and pressure. The effect of these variables on the dynamic balance piston seals was also studied in the MSFC/SSFL high pressure test systems (Fig. 2). The test matrix as implemented by each facility is shown in Figure 4.

Facility	ABMA TESTER	HIGH PRESSURE TESTER	HIGH TEMP (73°C)	AMB TEMP	LOX TEMP	AMB PRESS	3.4 X 10⁷ Pa	SEALS IN	Notes
K			•		•				INITIAL DATA (BAD BASE PLATE)
K			•		•				FINAL DATA
K				•	•				
M			•		•				
M				•	•				
S			•		•				NO CUPS
S			•		•				WITH CUPS
W			•		•				
M			•		•		•		
M			•		•			•	
M			•			•	•		
M				•	•		•		
M				•		•	•		
S		•			•		•		
S			•		•		•		
S				•	•		•		
S		•			•			•	
S			•		•			•	
S				•	•			•	
S		•				•	•		
S			•			•	•		
S				•		•	•		
W			•		•		•		
W			•			•	•		
W				•		•	•		

K — KSC
M — MSFC
S — SSFL
W — WSTF

Figure 4. Energy input study test matrix.

could be established. For the high-pressure tester, the principal variables were temperature and pressure. The effect of these variables on the dynamic balance piston seals was also studied in the MSFC/SSFL high pressure test systems (Fig. 2). The test matrix as implemented by each facility is shown in Figure 4.

	ABMA TESTER	HIGH PRESSURE TESTER	HIGH TEMP (73°C)	AMB TEMP	LOX TEMP	AMB PRESS	3.4 X 10⁷ Pa	SEALS IN	SEALS OUT	
K			•		•					INITIAL DATA (BAD BASE PLATE)
K			•		•					FINAL DATA
K				•	•					
M			•		•					
M				•	•					
S			•		•					NO CUPS
S			•		•					WITH CUPS
W			•		•					
M			•		•		•			
M			•		•			•		
M			•			•	•			
M				•	•		•			
M				•		•	•			
S	•				•		•			
S			•		•		•			
S				•	•		•			
S	•				•			•		
S			•		•			•		
S				•	•			•		
S	•					•	•			
S			•			•	•			
S				•		•	•			
W			•		•		•			
W			•			•	•			
W				•		•	•			

K — KSC
M — MSFC
S — SSFL
W — WSTF

Figure 4. Energy input study test matrix.

7

The discs used in the penetration tests were fabricated from an available rod of 304 stainless steel. The discs were annealed to remove work hardening and to produce uniform hardness. Figure 5 gives the disc specifications and shows an exaggerated view of an impacted disc.

MATERIAL: 304 S. S.
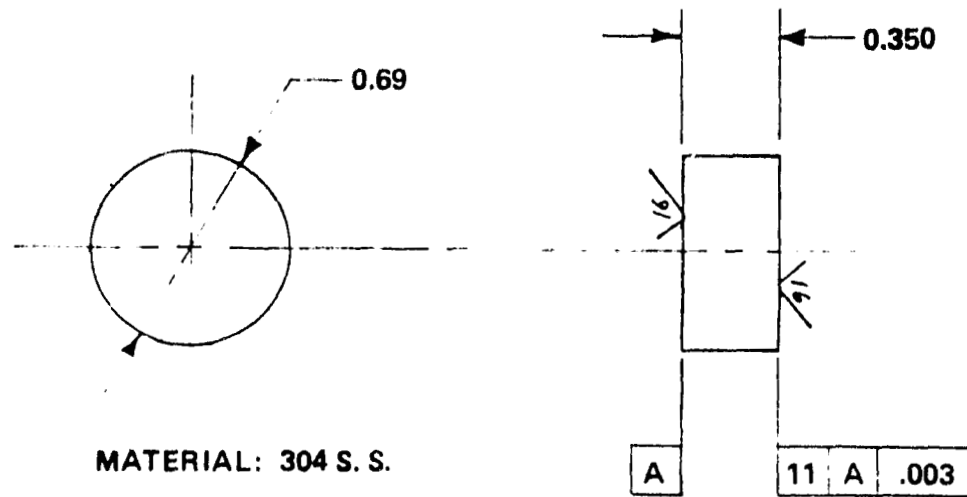
a. Detail.
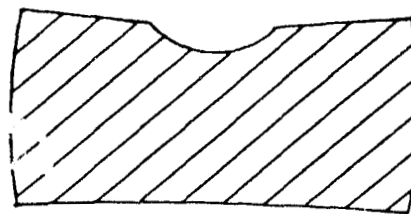
EXAGGERATED

b. Impacted specimen cross section

Figure 5. Energy input test specimen.

The diameter of the indentation was determined to be the most error-free measurement that could be made from which the penetration could be calculated. This measurement was made using an optical comparator and then converted into a penetration depth by assuming that the indentation was a perfect hemispherical section. Figure 6 shows the conversion derivation.
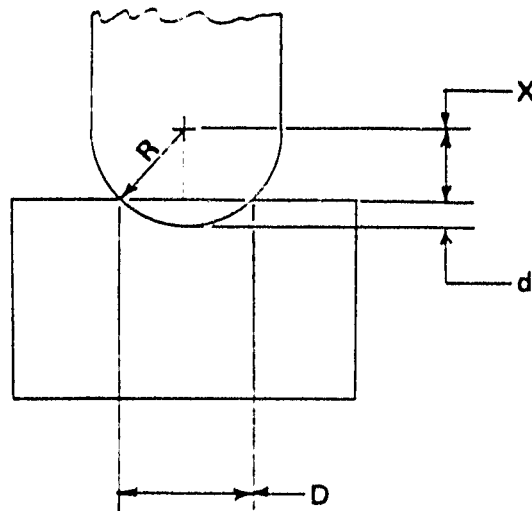
R — STRIKER RADIUS (6.35 MM)
D — DENT DIAMETER
d — PENETRATION

$$d = R - X$$
$$d^2 = R^2 - 2 X R + X^2$$
$$X^2 = R^2 - (D/2)^2$$
$$d^2 = R^2 - 2R [R^2 - (D/2)^2]^{\frac{1}{2}} + R^2 - (D/2)^2$$
$$= 2R^2 - (D/2)^2 - 2R [R^2 - (D/2)^2]^{\frac{1}{2}}$$

$$F(D) = [d \ (mm)]^2 = 80.645 - 0.25 \ D^2 - 12.7 \ (40.3225 - 0.25 \ D^2)^{\frac{1}{2}}$$

WHERE D IS IN mm

Figure 6. Derivation of penetration function.

The identation tests were conducted in substantially the same manner as regular impact tests with the following exceptions:

1) No oxvgen was used.

2) Plummet rebound was eliminated when possible.

3) No sample cups were used, except where noted in Figure 4, to prevent any reduction of the indentation in the sample.

9

Since no catcher was used to prevent rebounding of the plummet on the ABMA tester, indentation samples were examined to verify that diameters could still be measured accurately. No appreciable effect was noted on measurements due to rebounding. The data generated at LOX and ambient temperatures for all testers at various energy levels are presented graphically in Figures 7 through 29.

The abbreviation LOX (liquid oxygen) as used in this report represents several temperatures. For the ABMA tester it represents the boiling point at test site atmospheric pressure, nominally -183°C. For the SSFL high pressure tester, it represents -145+5°C [1]. For the WSTF high pressure tester, it represents a temperature between -183°C and the critical temperature of LOX.

Test Results

ABMA Testers - The identation diameter measurements and calculated penetrations are listed in Table 2 of Appendix B and are presented graphically in Figures 7 through 15.

The results for the ABMA testers were in excellent agreement with the exception of the initial KSC results at ambient temperature. This difference in results proved to be fortuitous; in resolving the cause, KSC and MSFC were able to resolve previously observed anomalous results. The cause of the difference in material and penetration test results was an improperly supported base plate on the KSC tester. This allowed the base plate to deflect during the impact process and thus reduce the peak stress on the test specimen, giving the lower penetrations and erroneous material test results. During the problem resolution period it was noted that the measured plummet rebound height (on sample cups only) was also an excellent method for comparing the performance of identical testers.

The ABMA tester behaved as expected giving greater penetrations at ambient temperature than at LOX temperature. The dent diameter versus energy level data are presented graphically in Figures 7, 9, 11, and 13. The data were fitted to a second degree polynomial over the data interval. These curves have no theoretical basis and are shown to indicate the trend of the data only. The grouping of the data points, in most cases, indicates excellent reproducibility and proper functioning of the four testers. From the diameter of the indentation, the theoretical penetration (Pc) was calculated. The square of this value is called the penetration function F (D) and is a linear function with respect to the energy level. The penetration function was used to compare the test results from all testers.

10
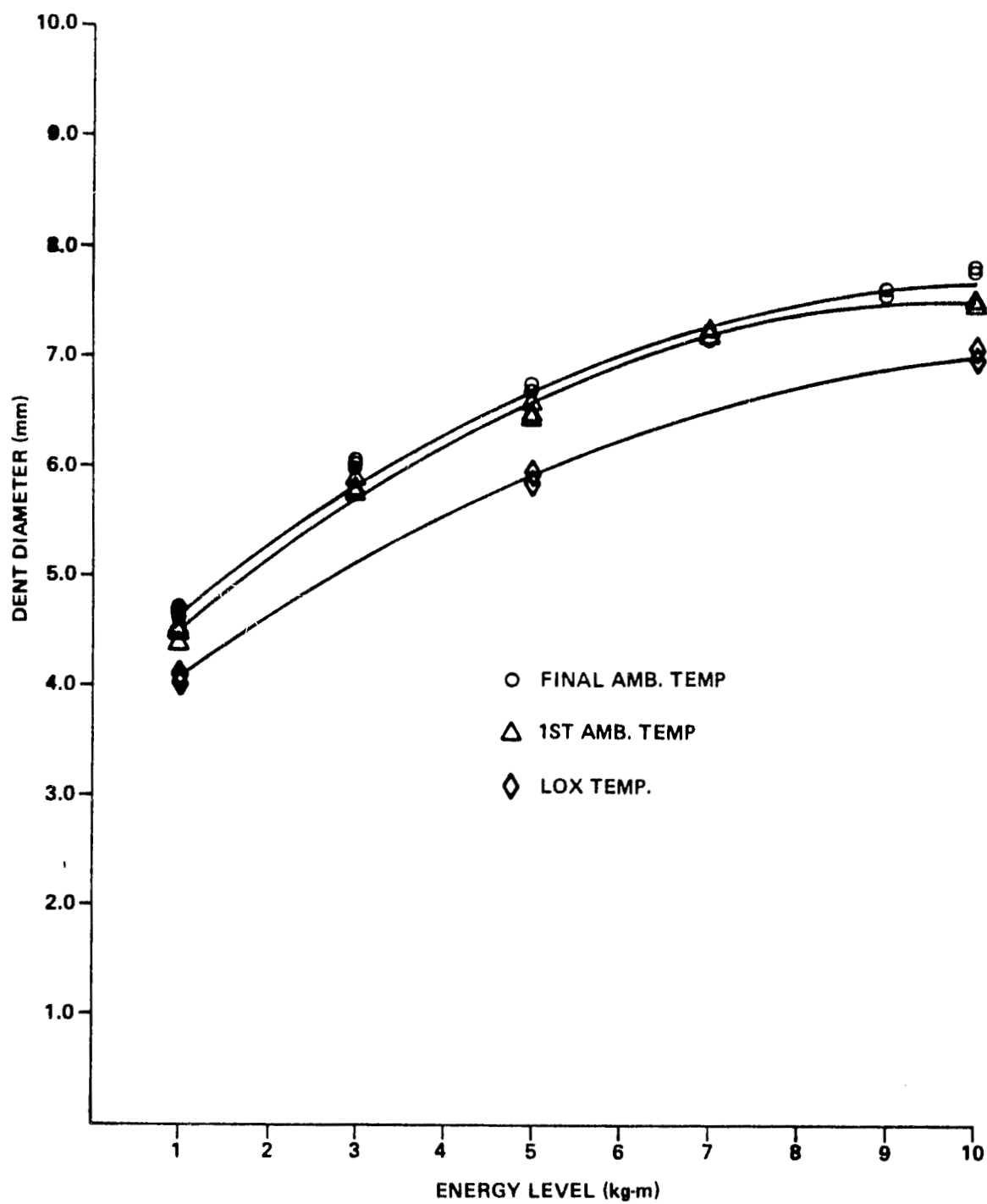
Figure 7. Dent diameter versus energy level KSC ABMA tester.
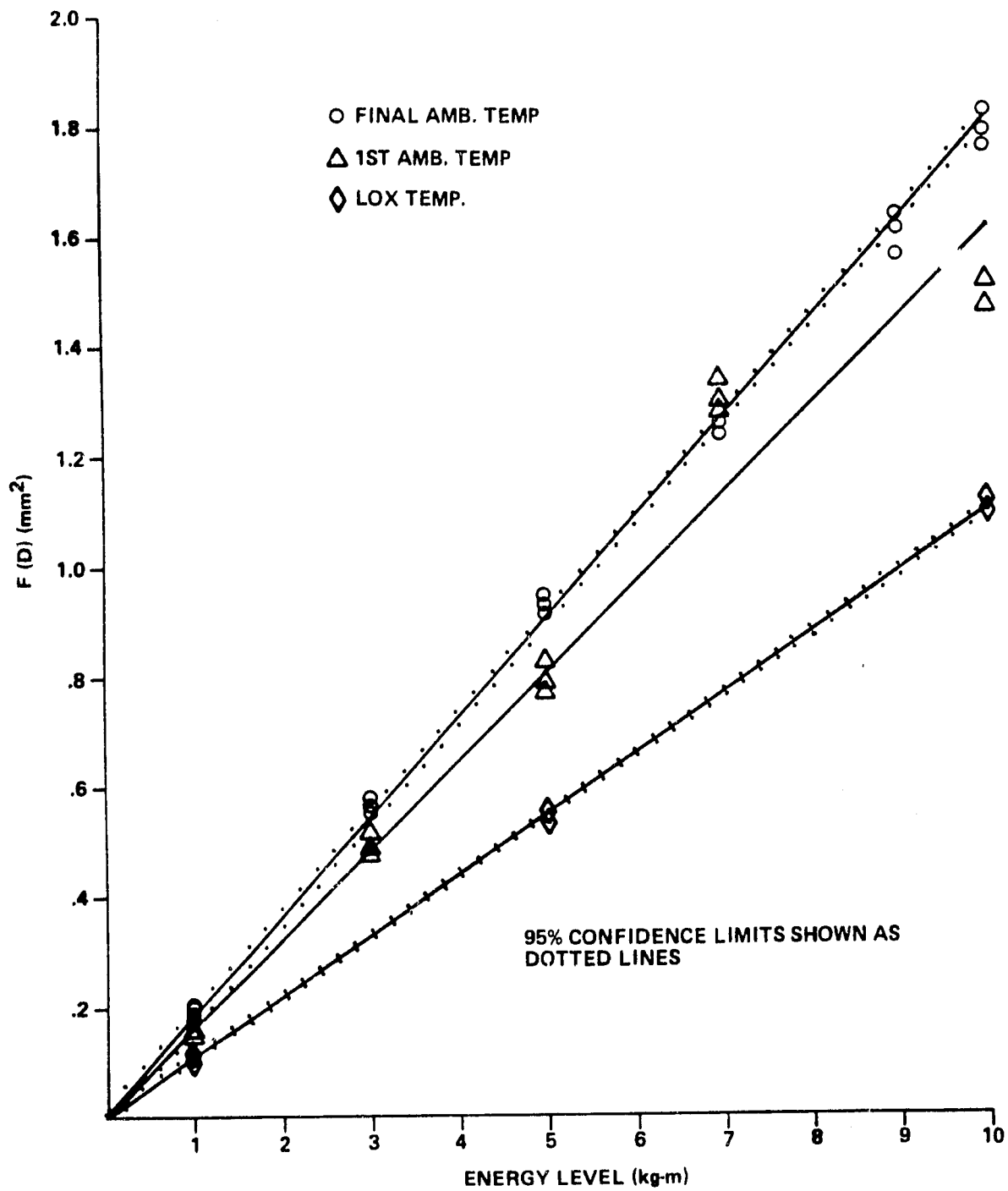
Figure 8. Penetration function versus energy level KSC ABMA tester.
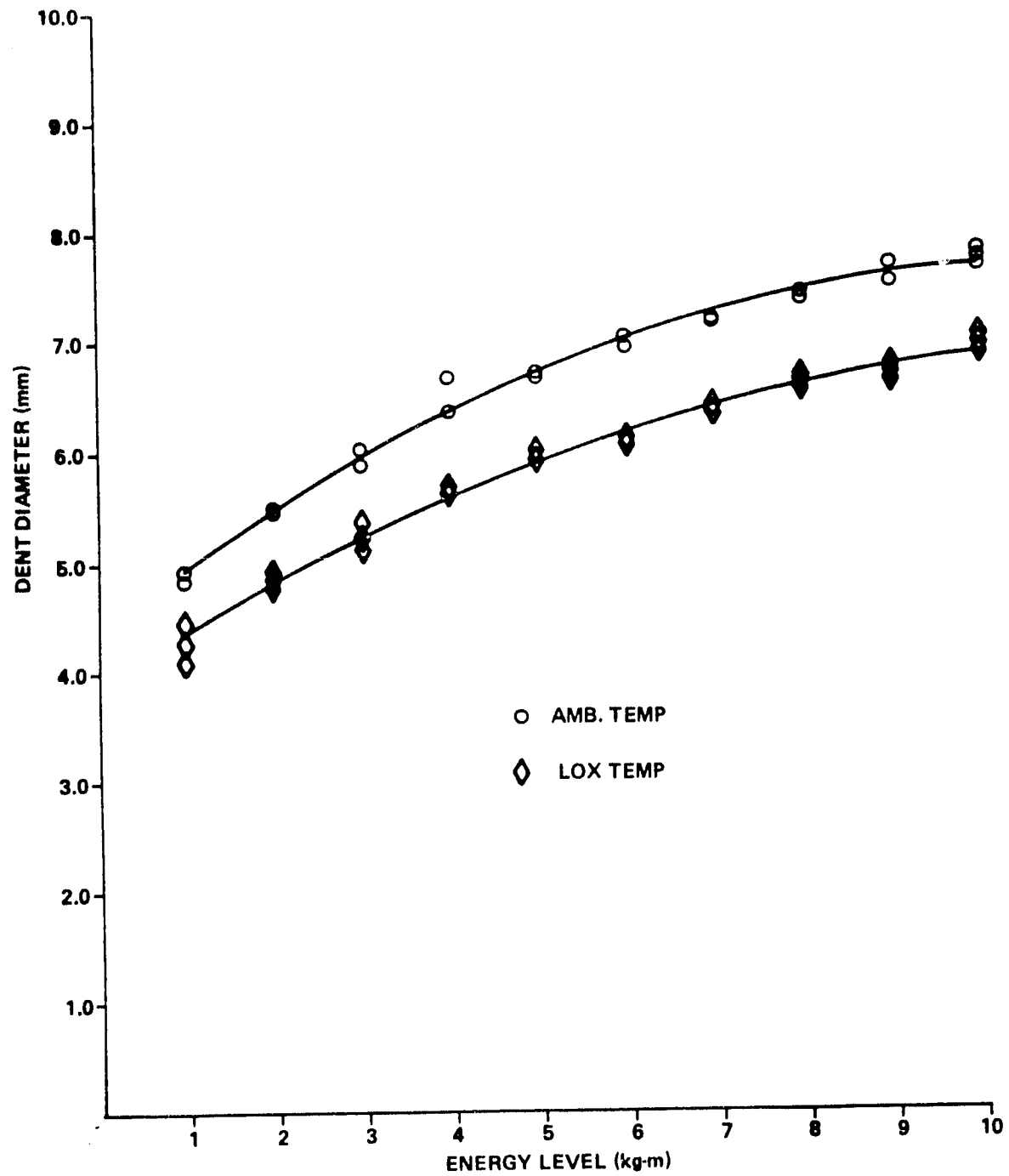
Figure 9. Dent diameter versus energy level MSFC ABMA tester.
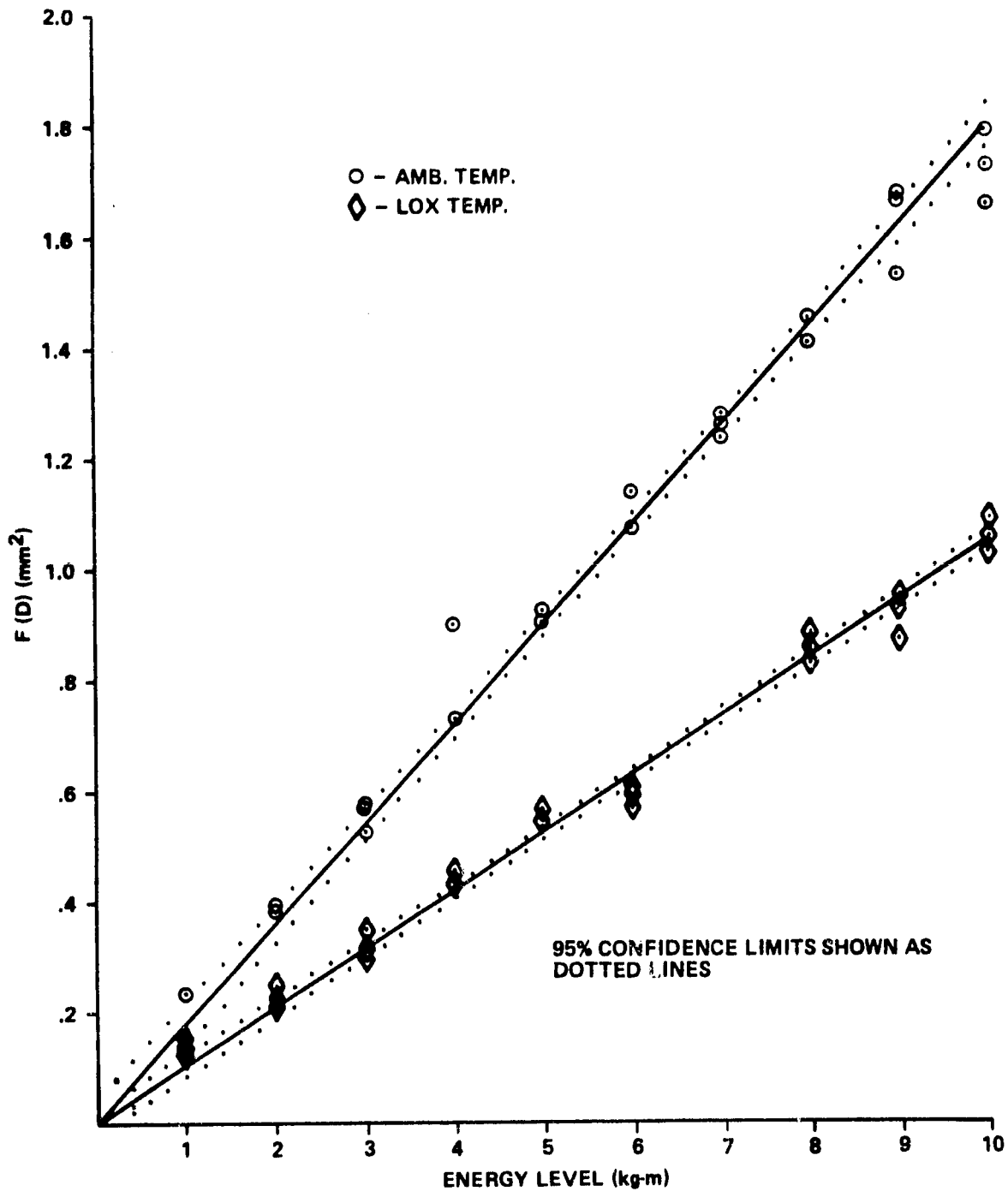
Figure 10. Penetration function versus energy level
MSFC ABMA tester.
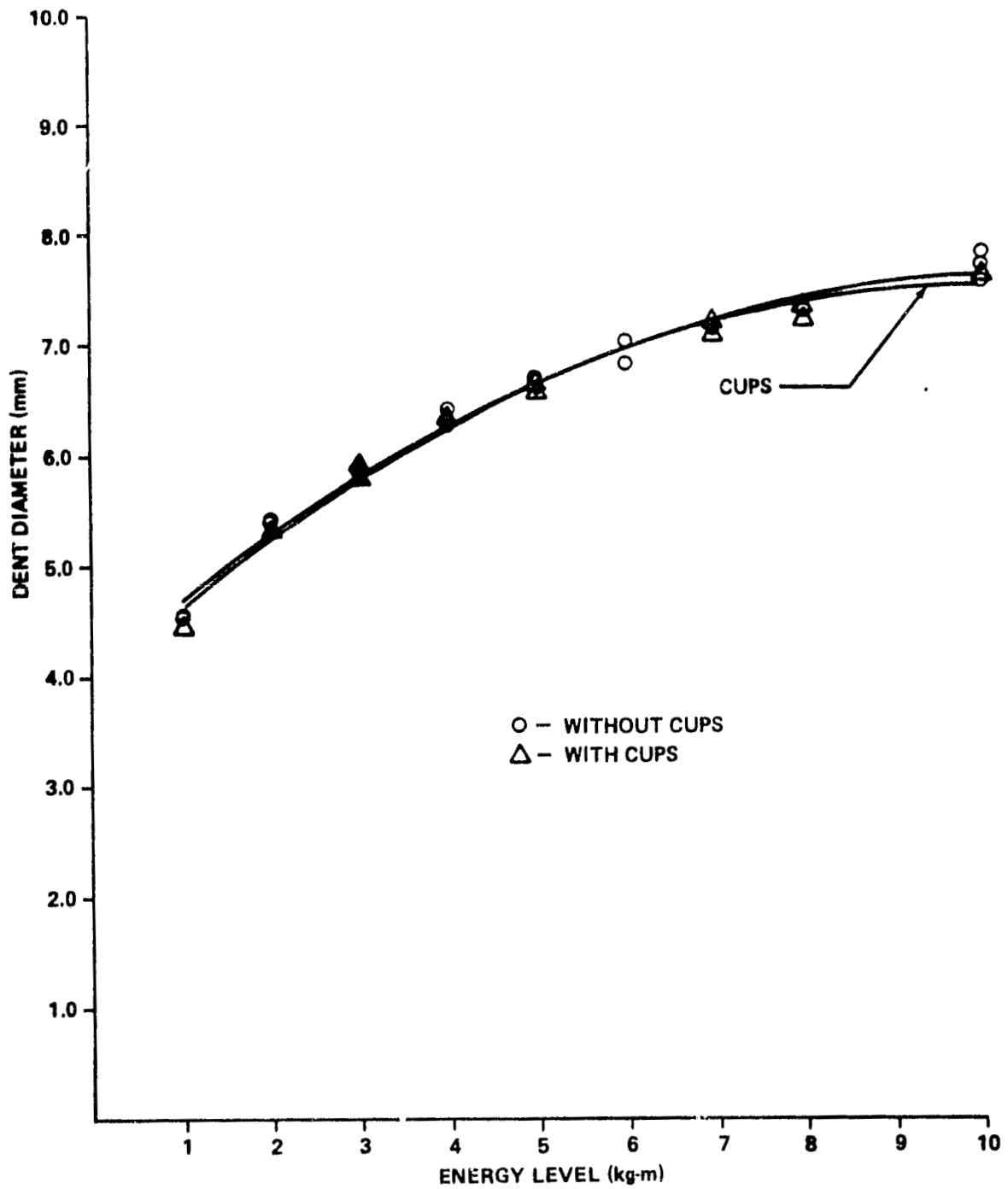
Figure 11. Dent diameter versus energy level SSFL ABMA
tester, ambient temperature.
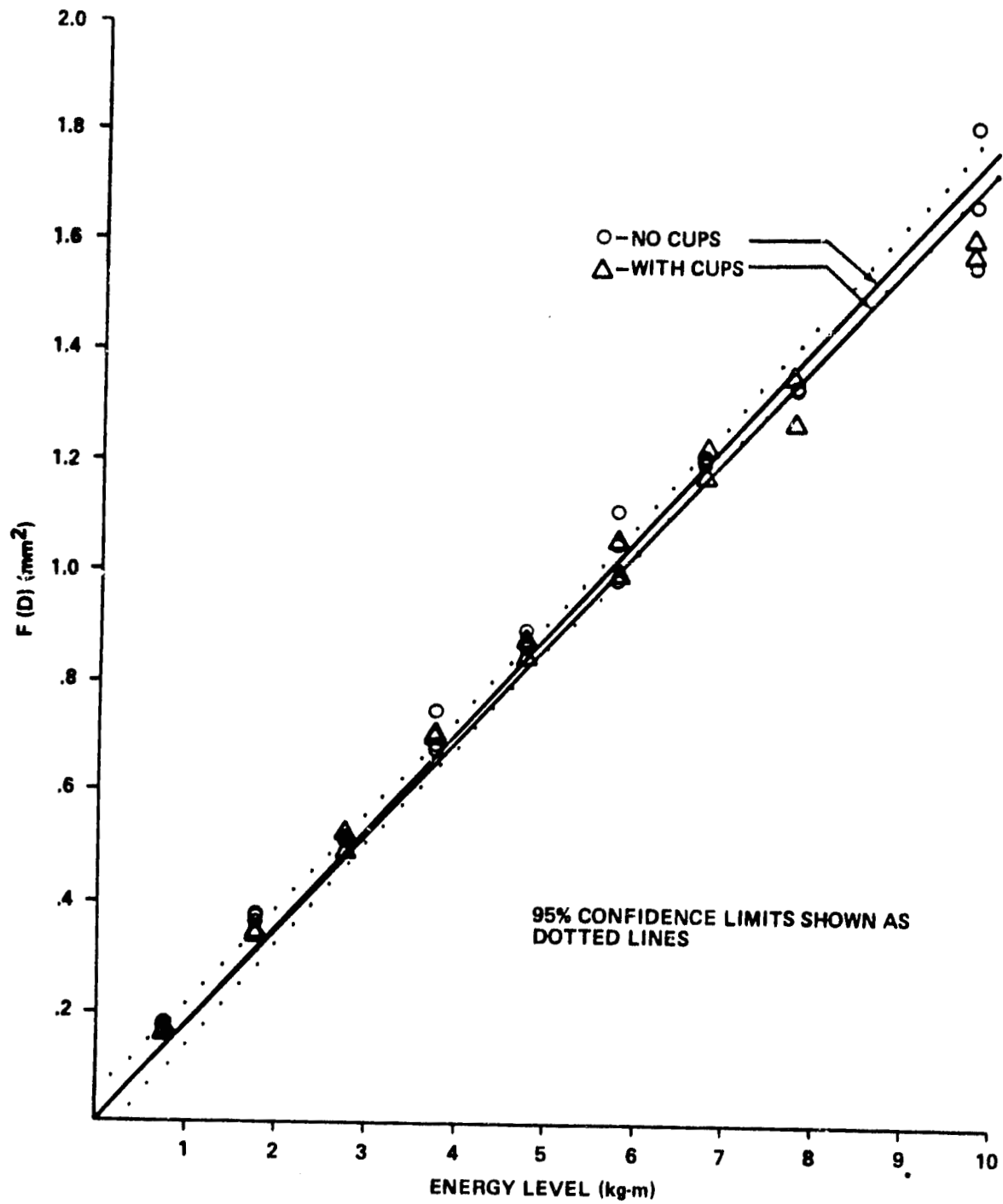
Figure 12.   Penetration function versus energy level SSFL ABMA
tester, ambient temperature.

16
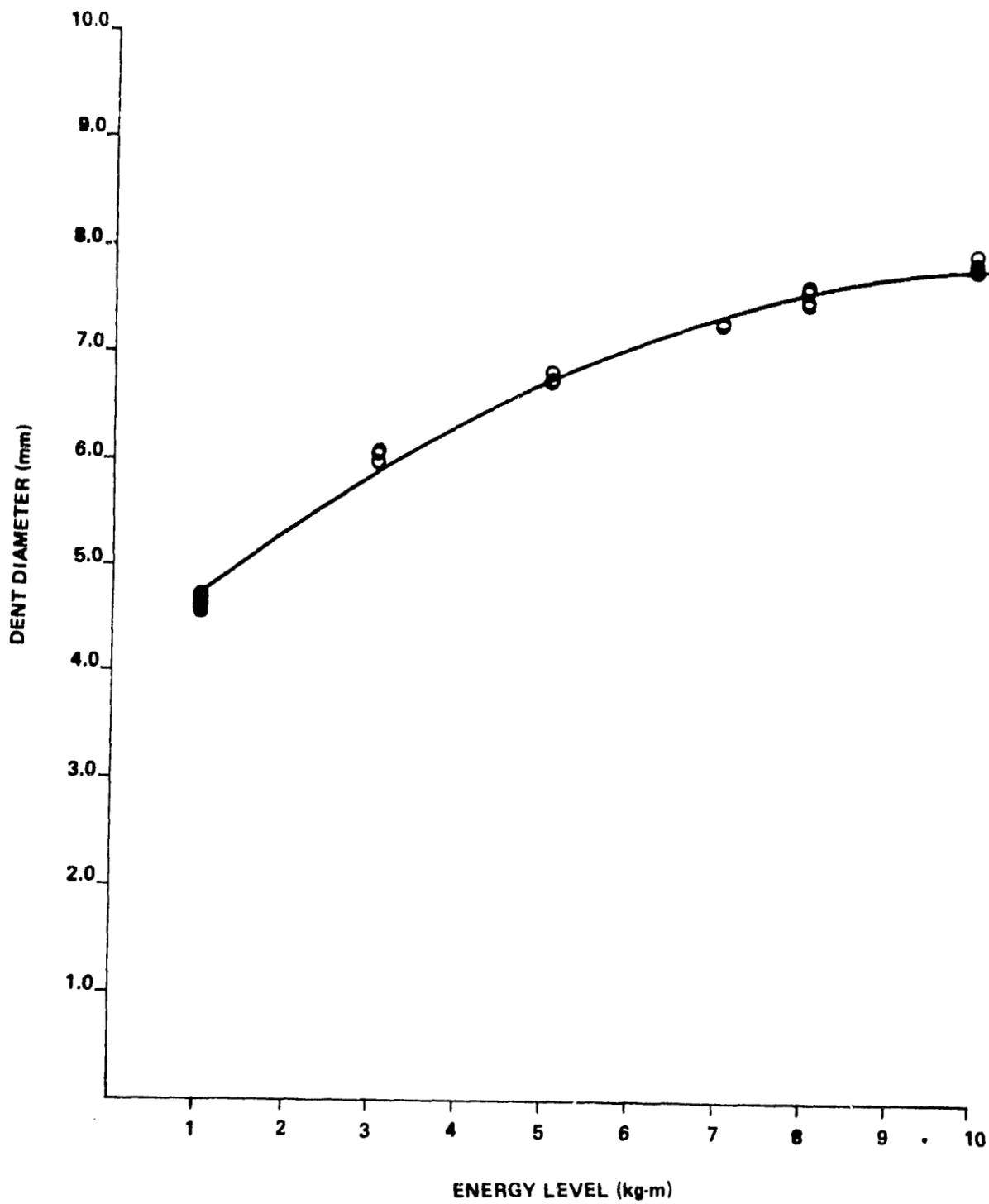
Figure 13. Dent diameter versus energy level WSTF ABMA
tester, ambient temperature.
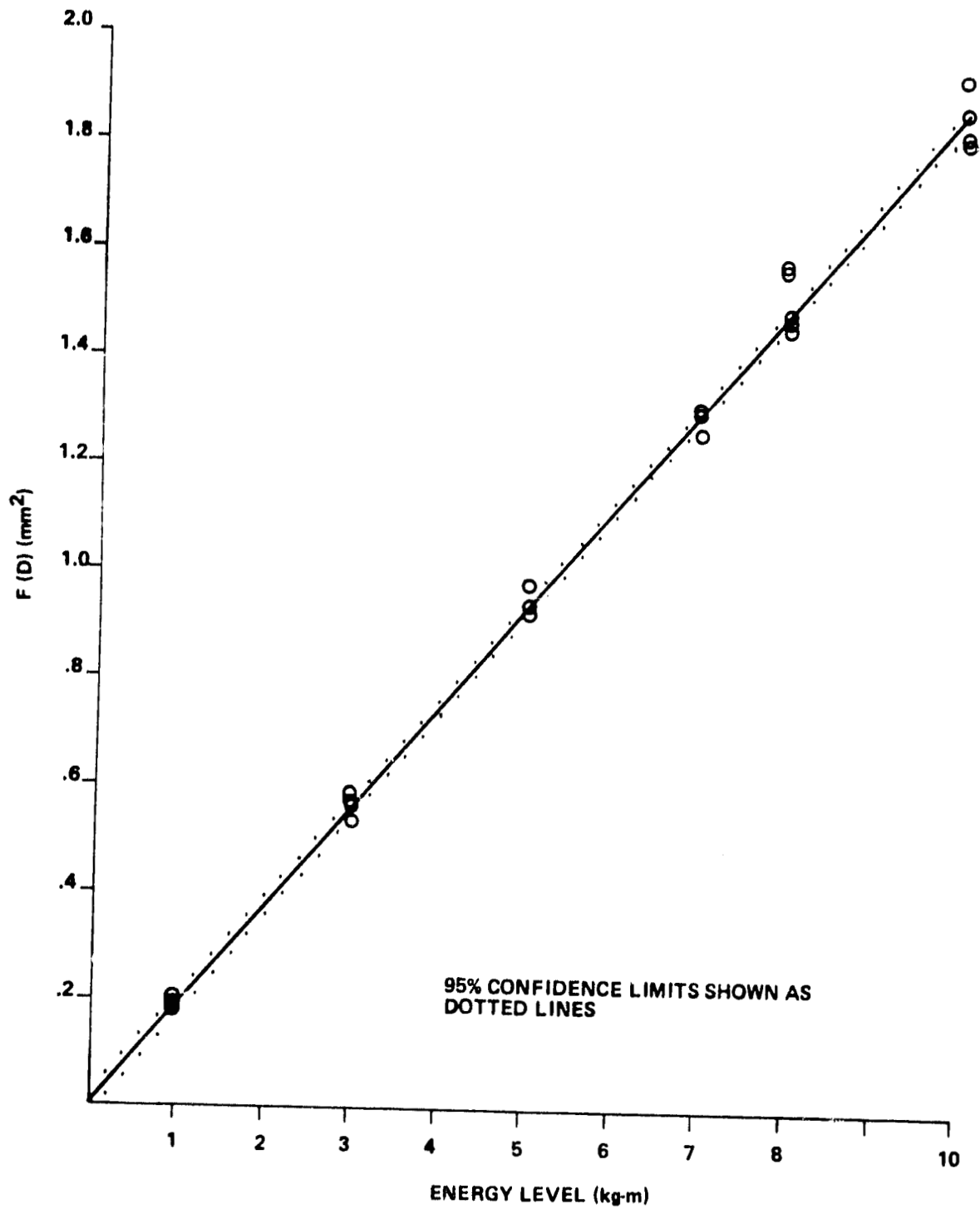
Figure 14. Penetration function versus energy level WSTF ABMA tester, ambient temperature.

18
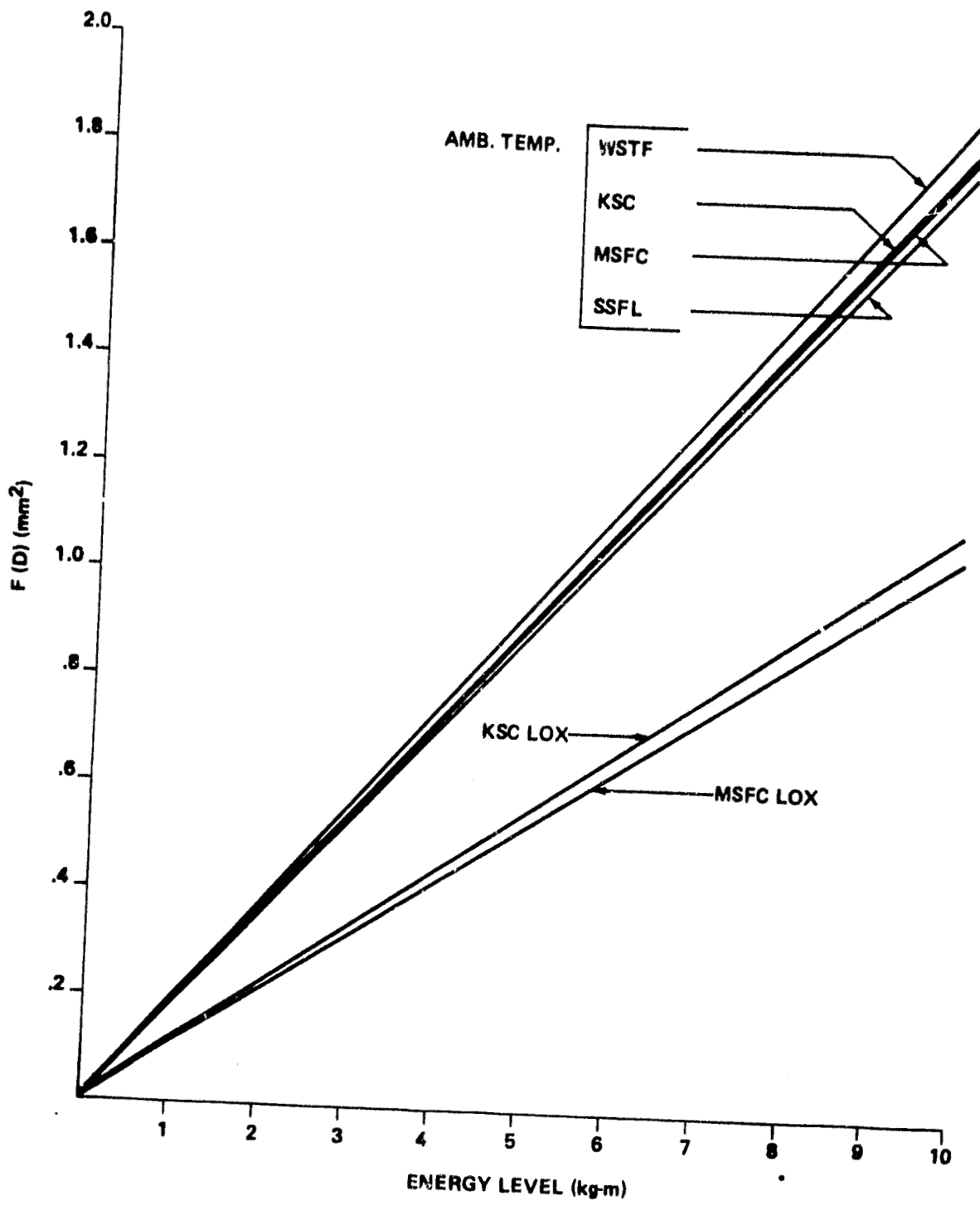
Figure 15.   Penetration function versus energy level, all ABMA testers.
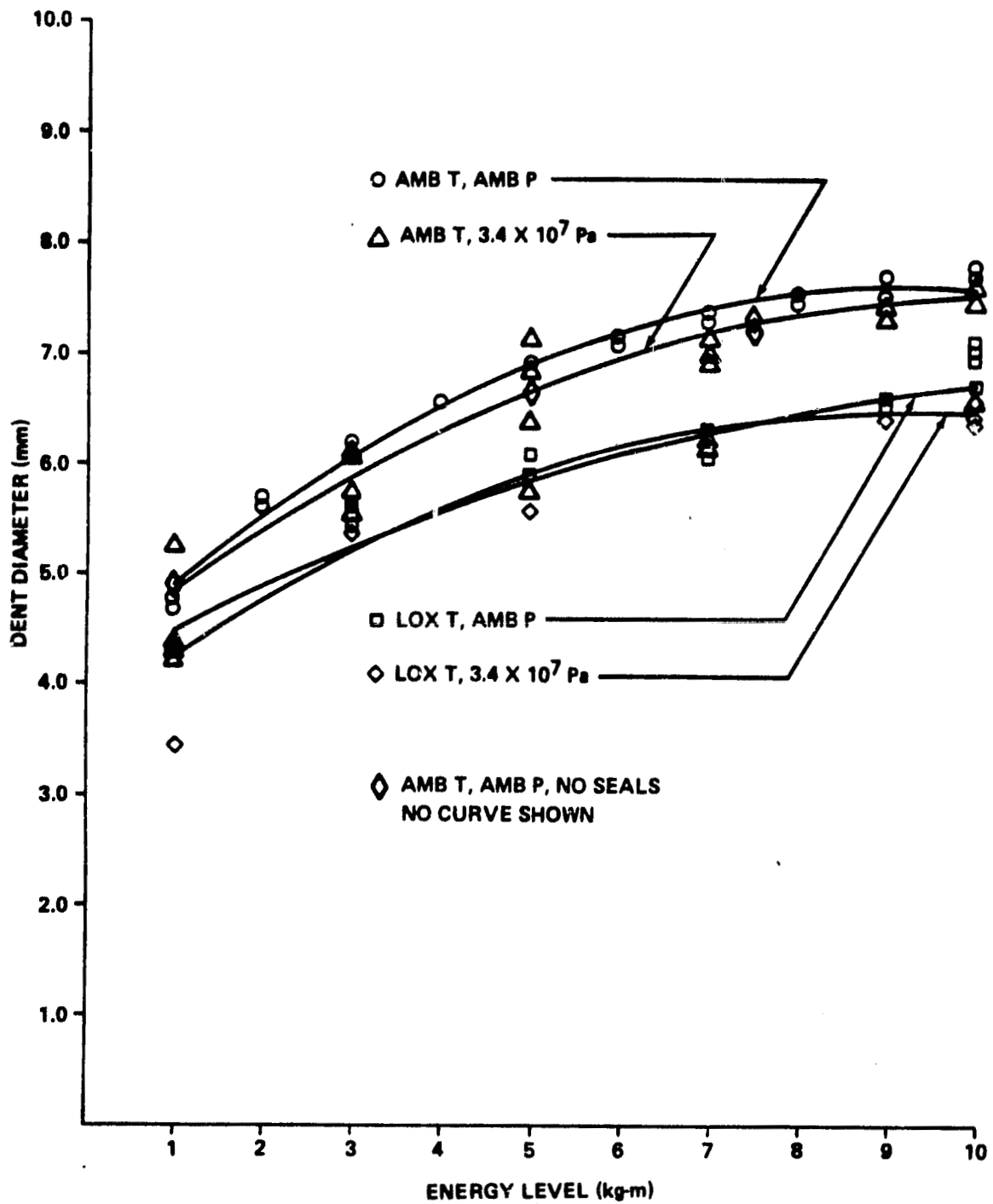
Figure 16. Dent diameter versus energy level MSFC high
pressure tester.
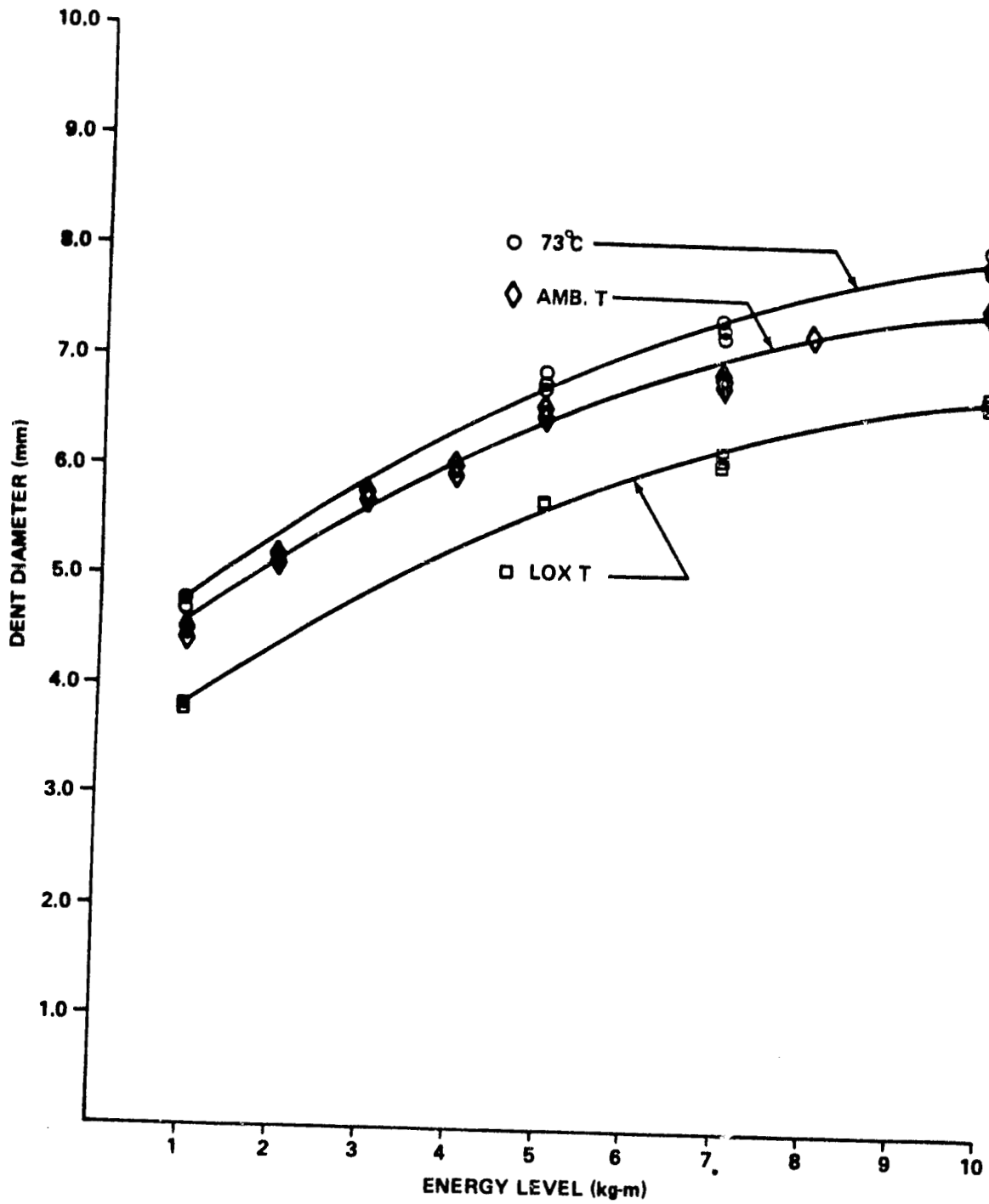
Figure 17.   Dent diameter versus energy level SSFL high
pressure tester, ambient pressure.
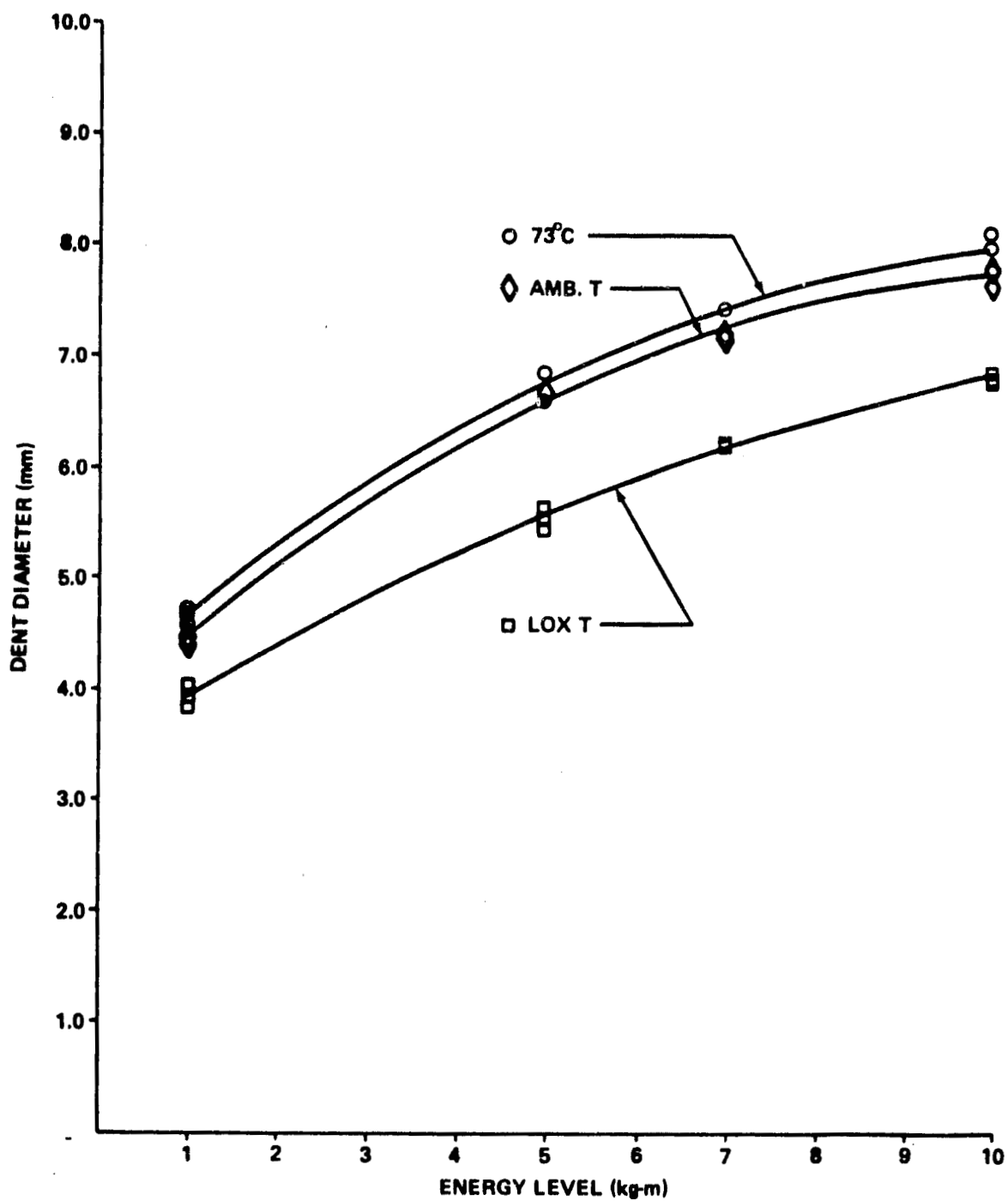
Figure 18. Dent diameter versus energy level SSFL high pressure tester, ambient pressure, no seals.
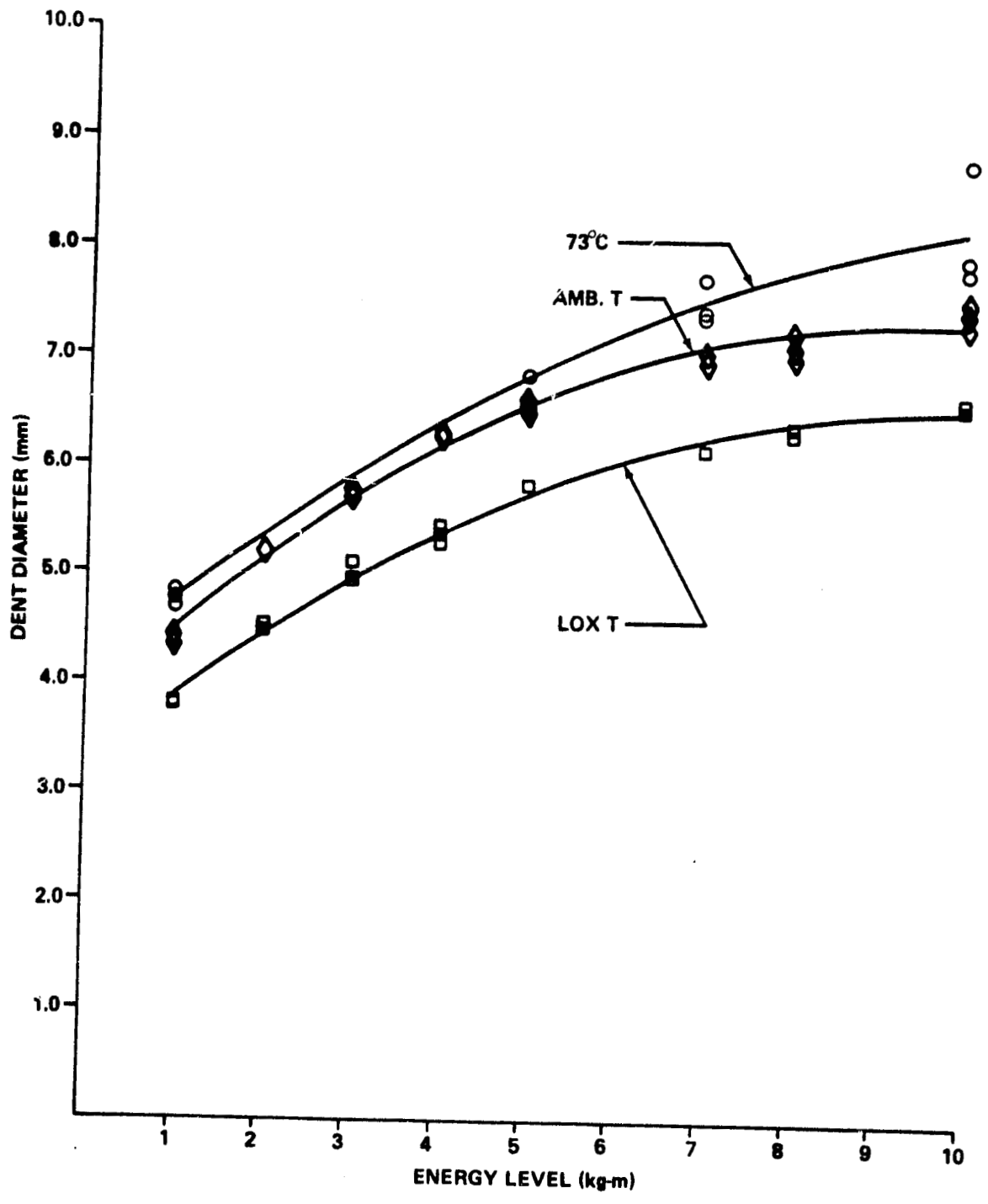
Figure 19. Dent diameter versus energy level SSFL high pressure
tester, 3.0×10^7 Pa.
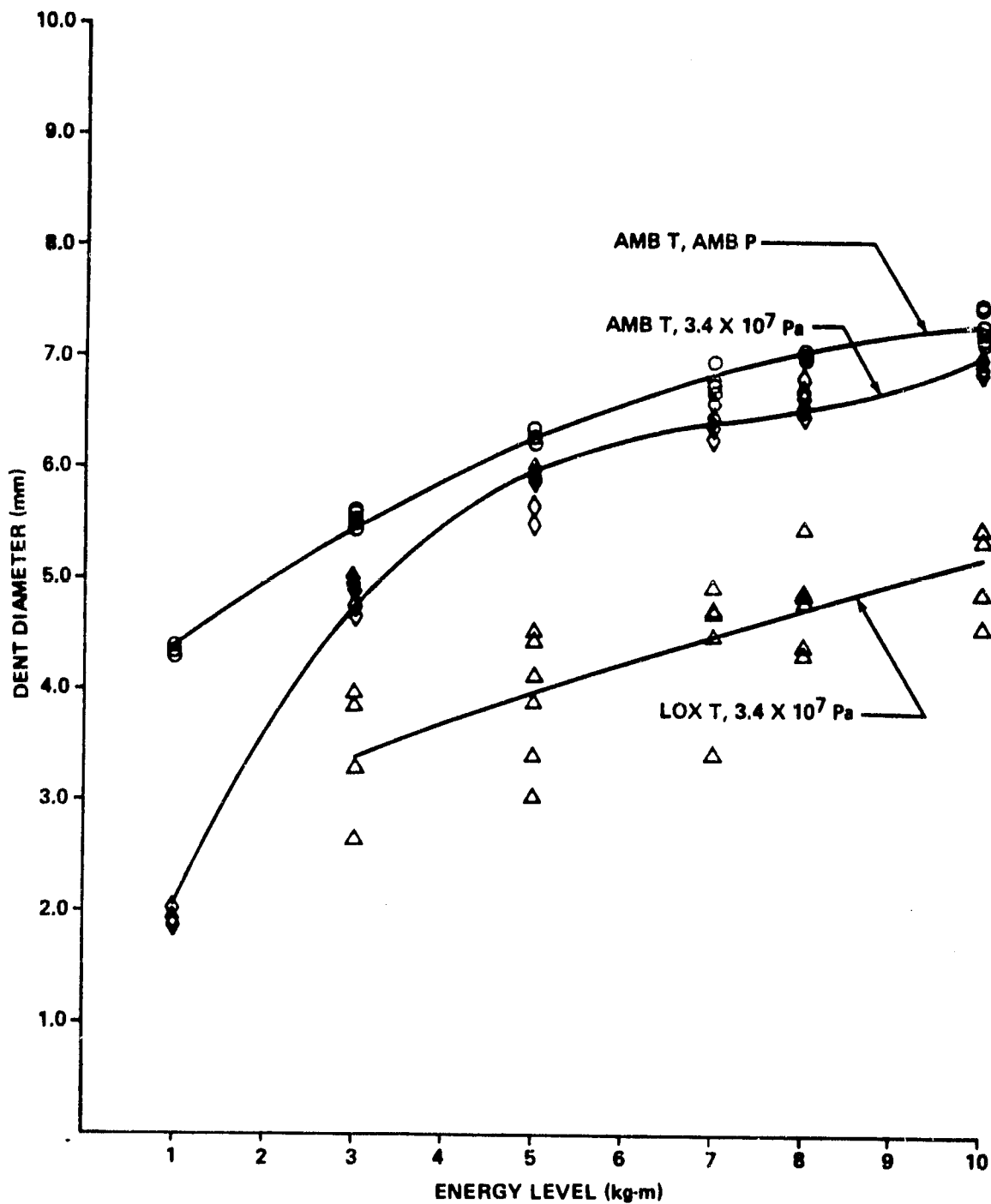
Figure 20. Dent diameter versus energy level WSTF high pressure tester.
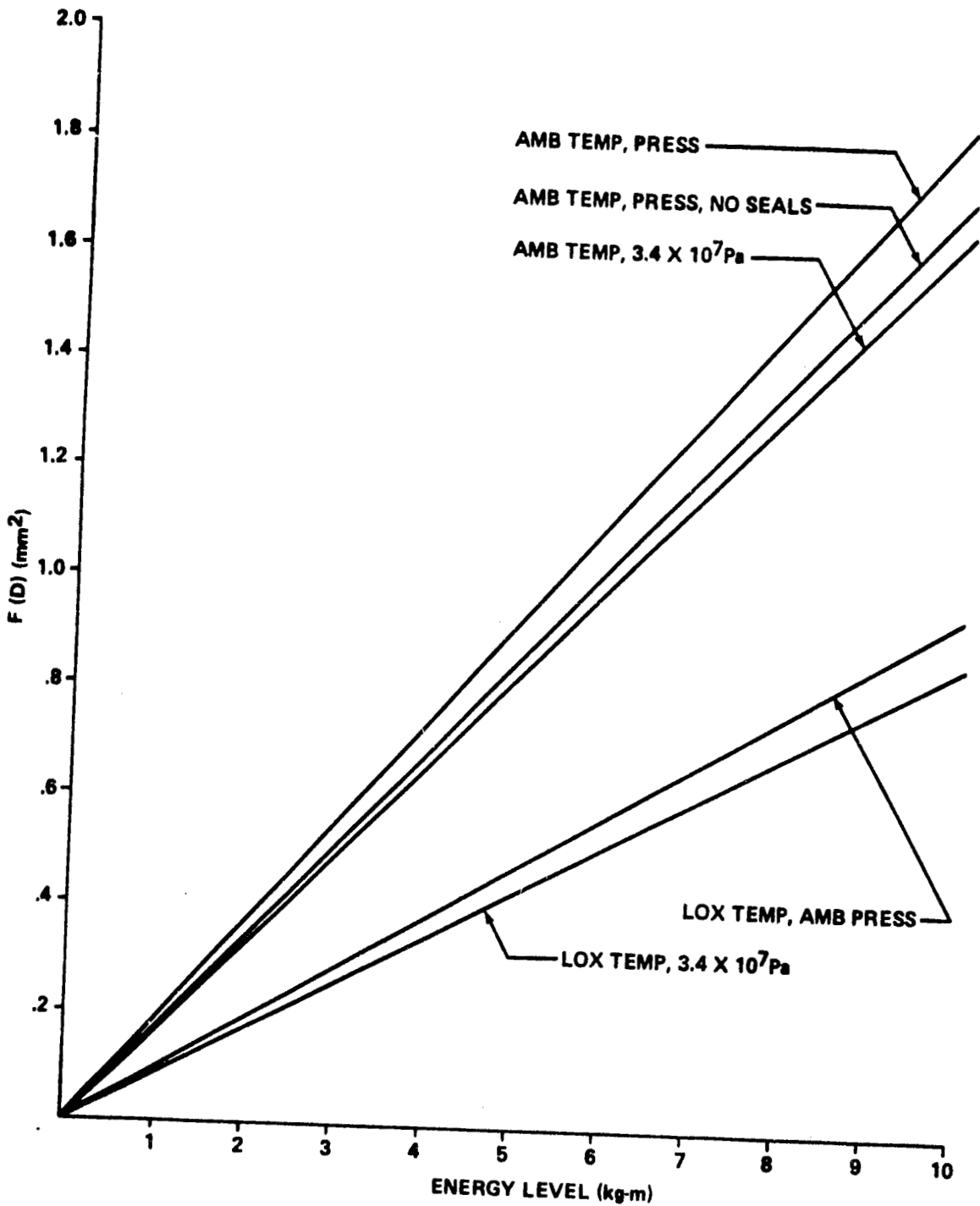
Figure 21. Penetration function versus energy level
MSFC high pressure tester.
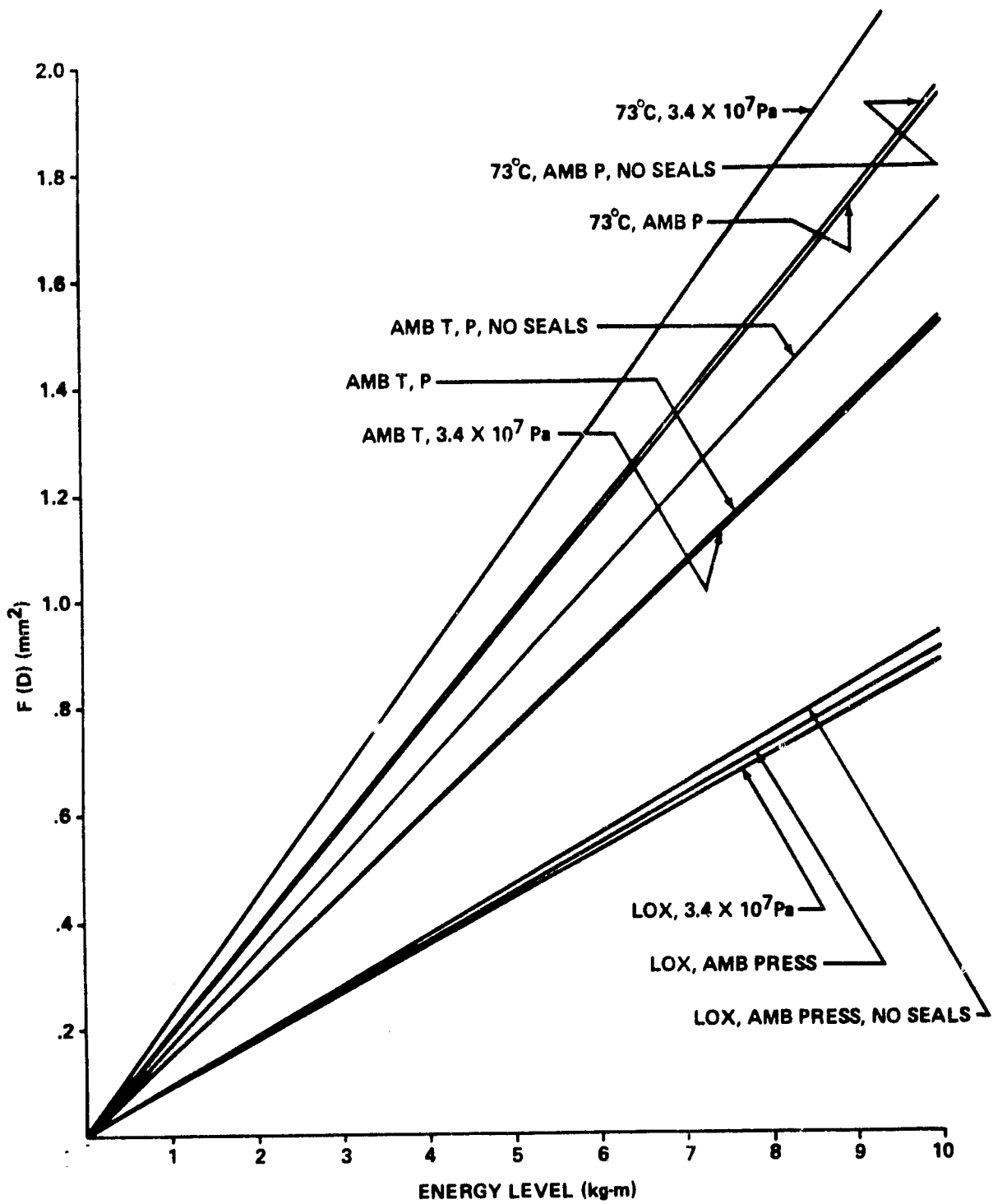
Figure 22. Penetration function versus energy level
SSFL high pressure tester.
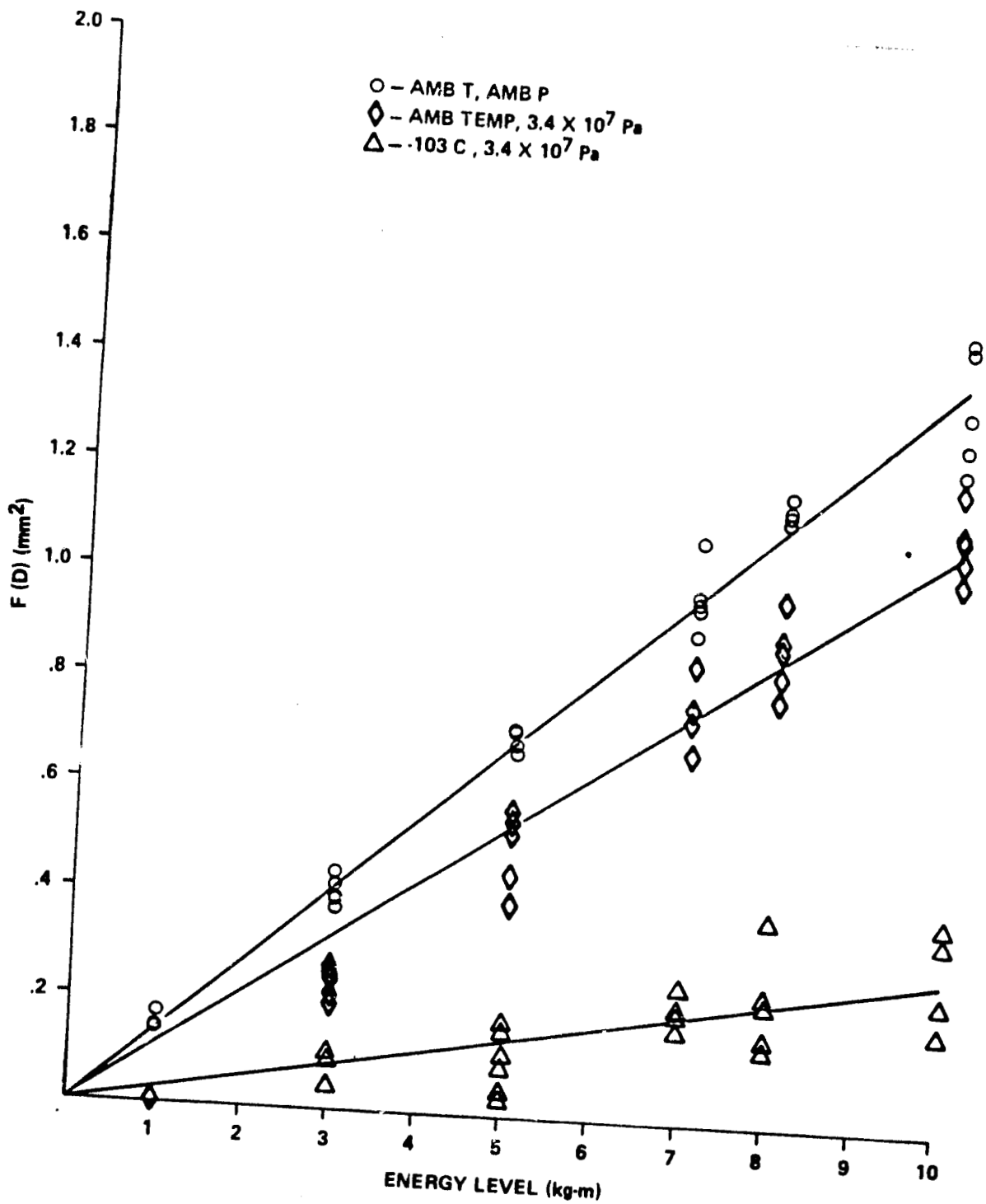
Figure 23. Penetration function versus energy level WSTF high pressure tester.
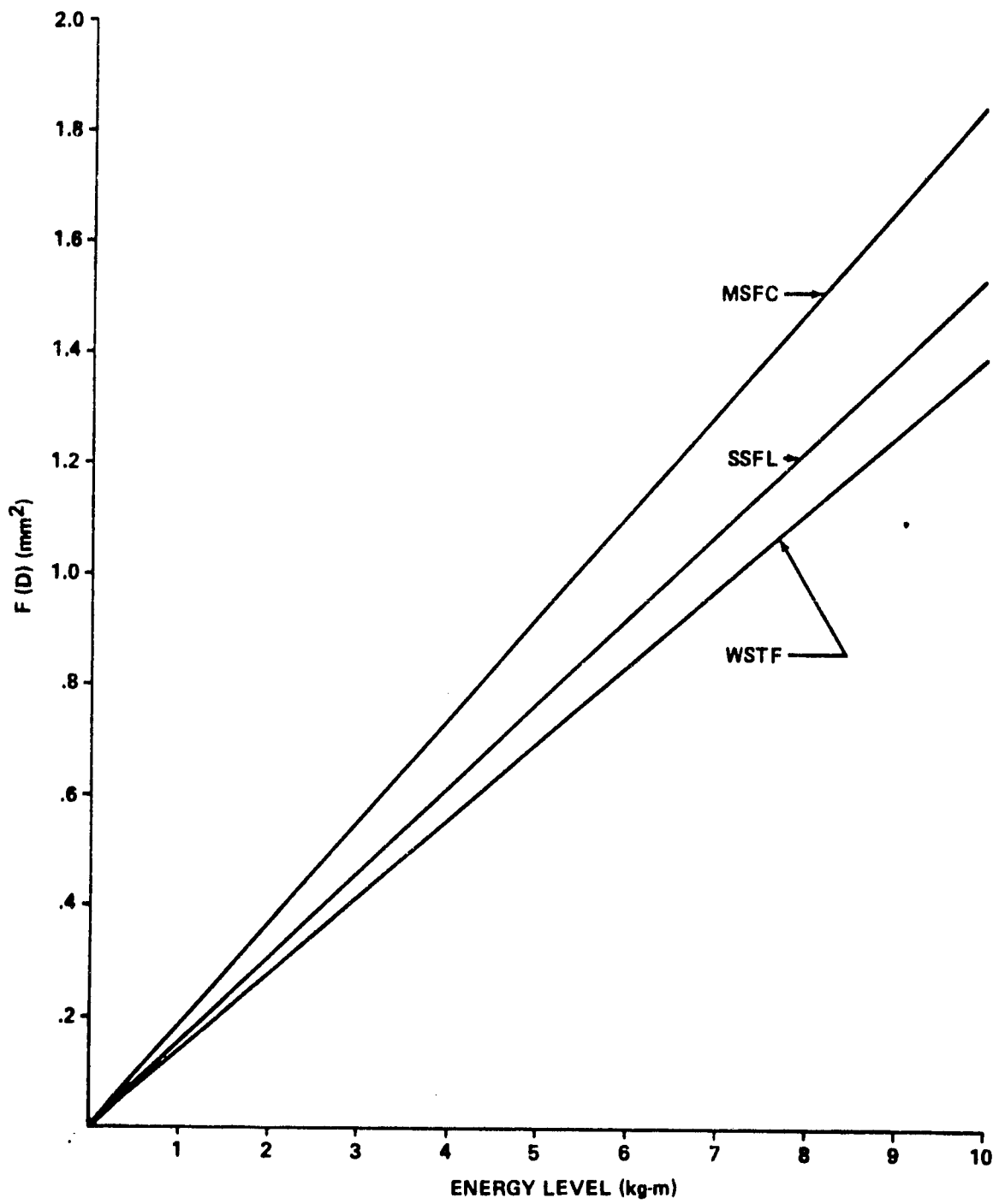
Figure 24. Comparison of high pressure testers at
ambient temperature and pressure.
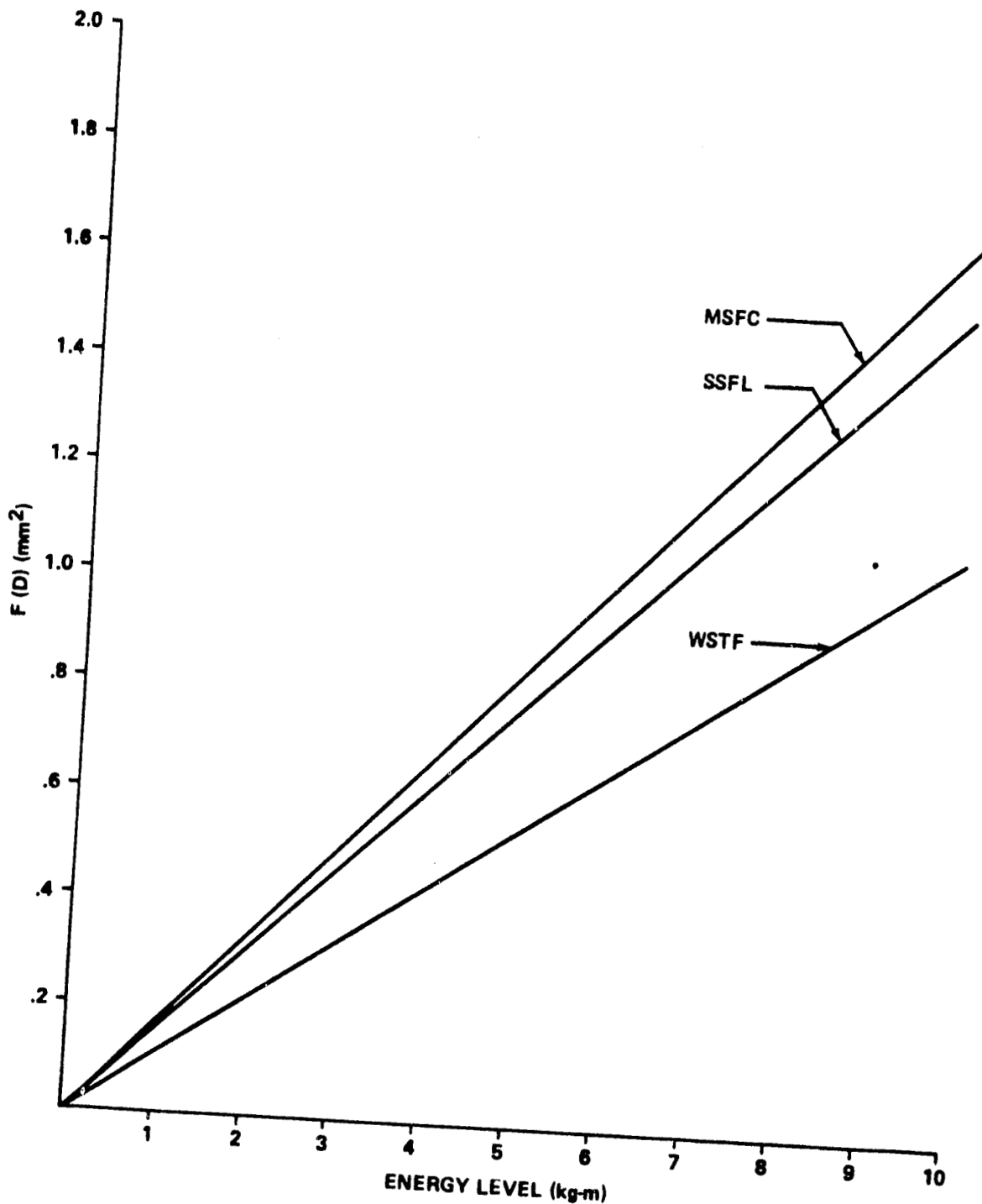
Figure 25. Comparison of high pressure testers at ambient temperature and 3.4×10^7 Pa.
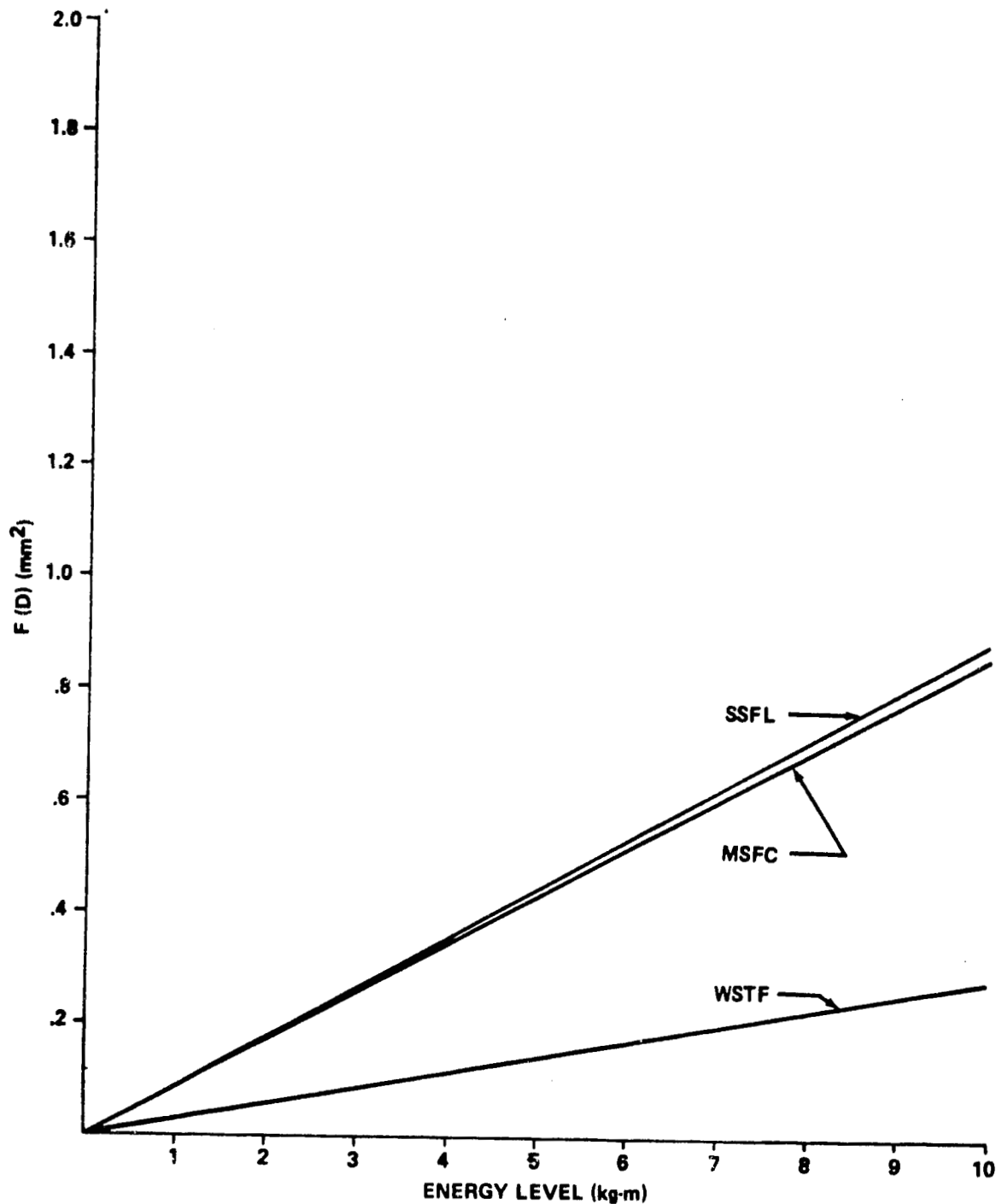
Figure 26. Comparison of high pressure testers at cryogenic temperature and 3.4×10^7 Pa.
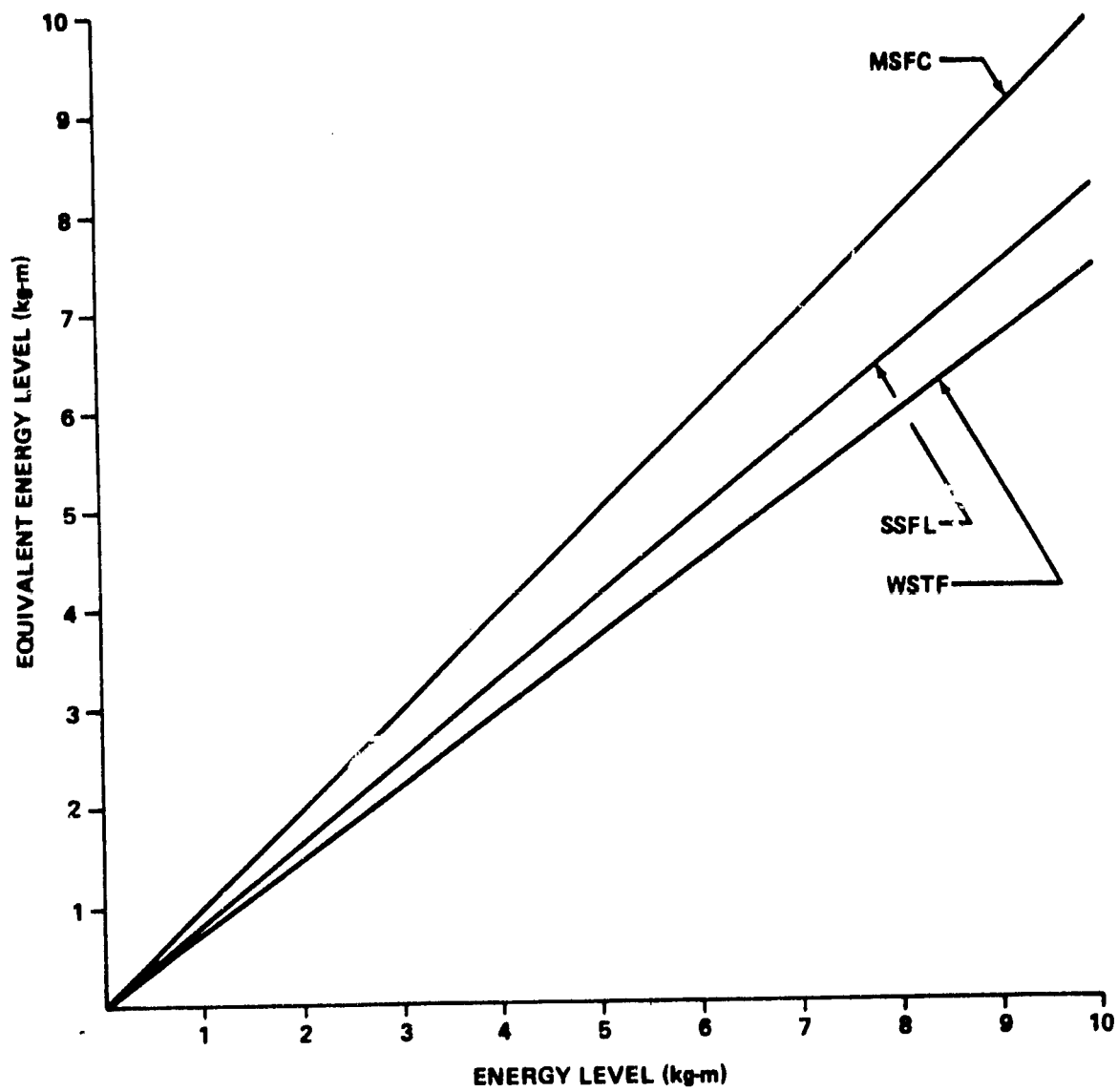
Figure 27. Equivalent energy of high pressure testers at
ambient temperature and pressure.
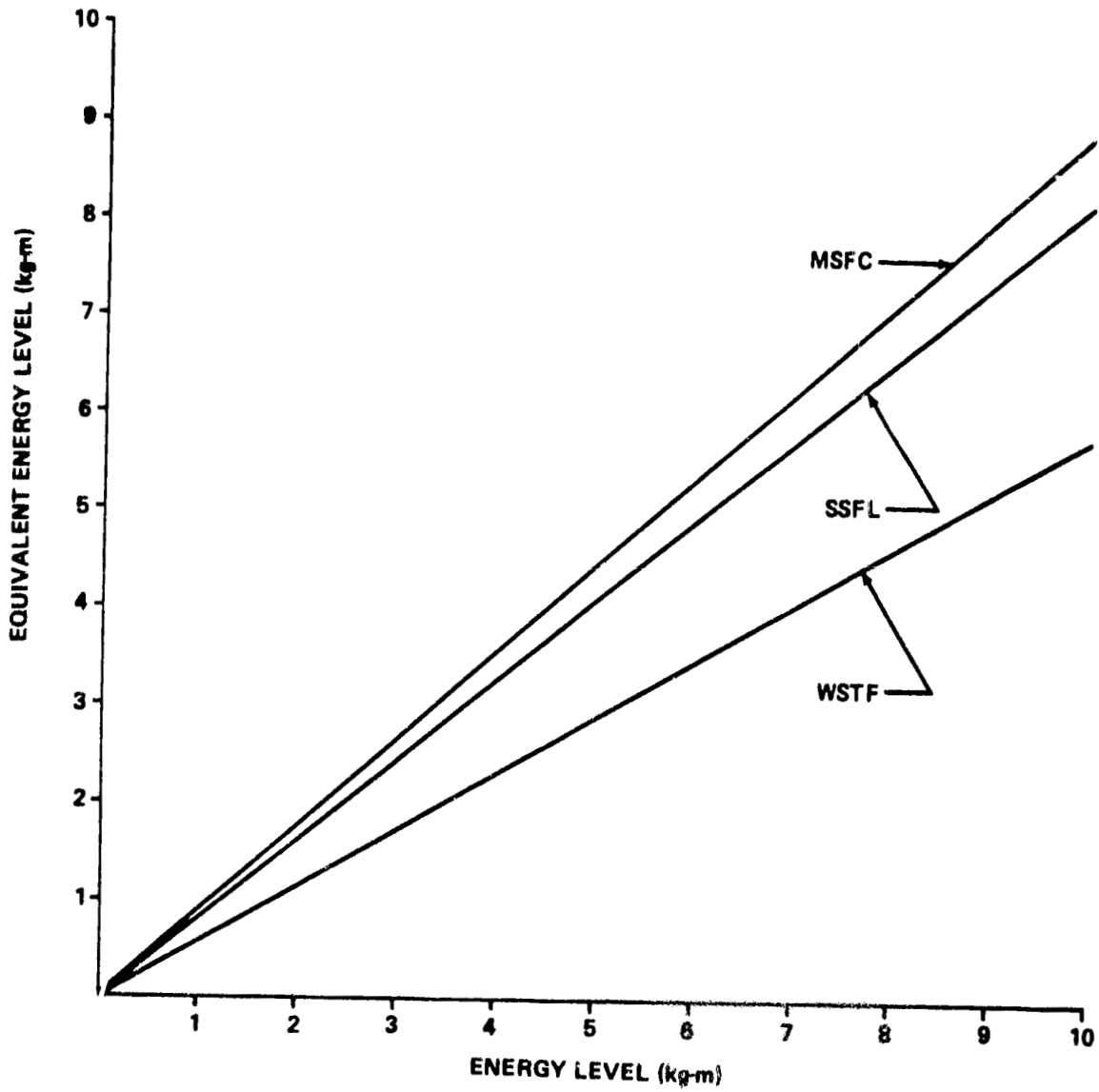
Figure 28. Equivalent energy of high pressure testers at
ambient temperature and 3.4×10^7 Pa.
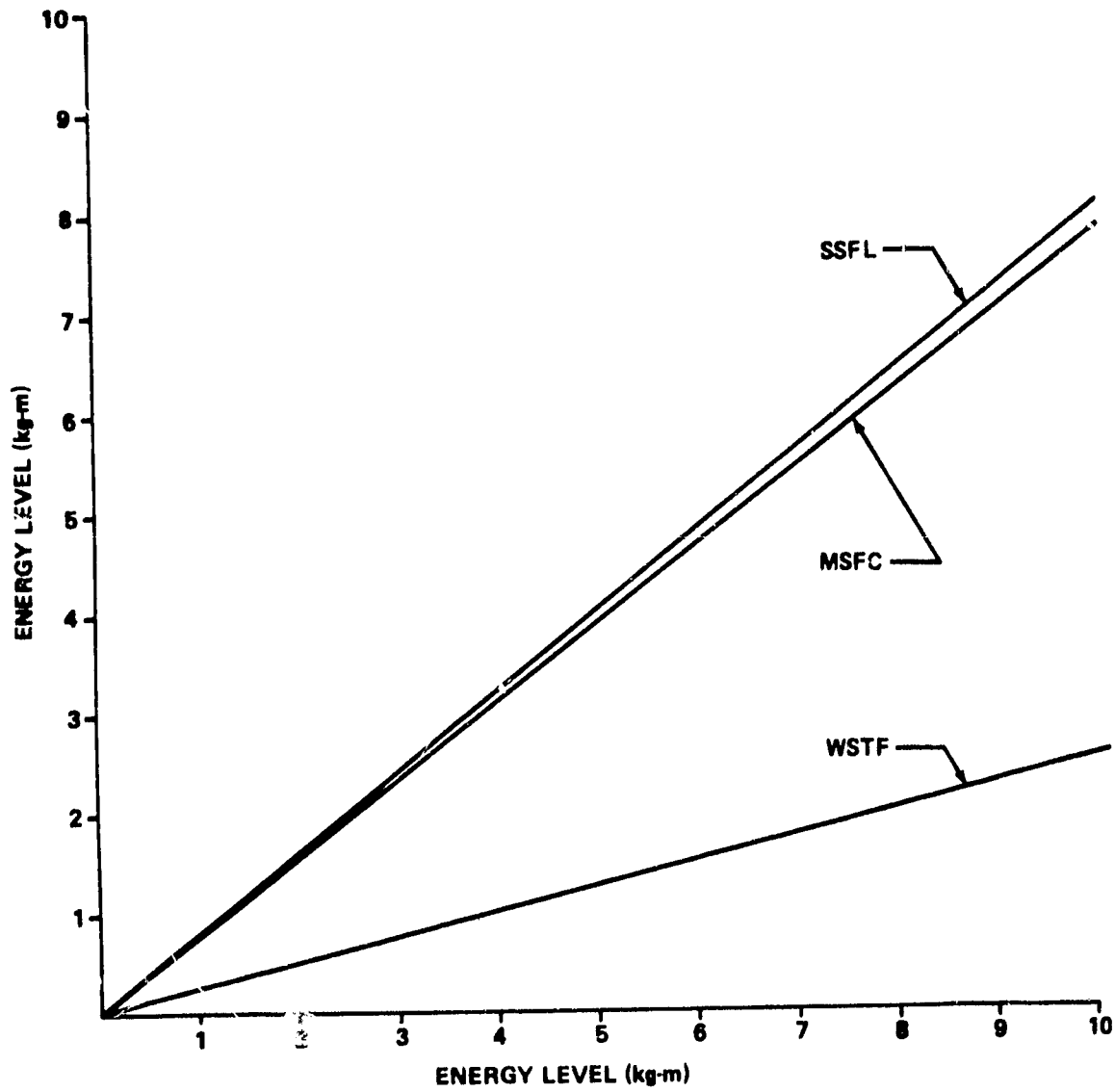
Figure 29. Equivalent energy of high pressure testers at LOX temperature and 3.4×10^7 Pa.

A linear curve fit forced through the origin, a common point to all testers, was determined and the curve statistics generated (Table 1). The dotted lines on various plots represent the 95 percent confidence limits. As seen from the plots of the penetration function of the ABMA testers (Figs. 8, 10, 12, and 14), excellent correlation to the linear assumption exists (Table 1). The comparative energy input test results for all ABMA testers are presented in Figure 15. The results are considered to be excellent considering the age and use history of several of these testers.

A determination was made of the effect of the aluminum cups upon the impact results (Figs. 11 and 12). The lower curves represent the data for impact tests using aluminum cups. The linear least squares curve from data taken with cups falls within the 95 percent confidence limits of the data taken without cups (Fig. 12). This would indicate that the cups absorb little of the impact energy and thus do not affect the impact test results in a significant manner.

High Pressure Testers - The indentation diameter measurements, calculated penetrations, and penetration functions for the high pressure tester study are listed in Table 2 of Appendix B. The dent diameter versus energy level data are presented graphically in Figures 16 through 20. The results of the linear curve fits of the penetration function versus energy level are listed in Table 2 and presented graphically in Figures 21 through 26.

The indentation data generated by the MSFC and SSFL testers are shown graphically in Figures 16 through 19, and for the WSTF tester in Figure 20. An extensive evaluation of the effects of the piston seals on the Rocketdyne-designed tester performance was carried out by SSFL and, to a lessor degree, by MSFC. It was expected that removal of the piston seals would result in an increase in indentation of the sample disc; however, as shown by the penetration function data plotted in Figures 21 and 22, indentations obtained were not consistent with expectations. At high temperature, the greatest indentation occurred at high pressure. At high temperature and ambient pressure, the indentations produced by the SSFL tester with no seals installed were only slightly greater than with seals. However, the reverse was seen on the MSFC tester under the same conditions. The WSTF tester produced smaller indentations at any given condition than either the MSFC or SSFL testers (Figs. 20 and 23). On all testers the penetration function was least at LOX temperature and high pressure.

When all testers were compared at the same conditions, by the penetration function (Figs.24, 25, and 26), it was found that the MSFC/SSFL testers gave a greater impact indentation than the WSTF tester and that the MSFC gave

34

TABLE 1. ABMA TESTER PENETRATION FUNCTION CURVE PARAMETERS

Source	Temperature	Pressure	Additional Conditions	Forced Regression Line					Unforced Regression Line	
				A0	A1	σ^2 Line	$\sigma^2 A_1$	R	A0	A1
KSC	Amb	Amb	Initial test data	0.0	0.162152	9.9994 E-03	6.8305 E-05	0.99103	0.039143	0.156619
KSC	Amb	Amb		0.0	0.151129	6.8775 E-04	2.26112 E-06	0.99995	0.032924	0.15757~9
KSC	LOX	Amb		0.0	0.110304	6.04657 E-05	2.97372 E-07	0.9993	-0.002705	0.110604
MSFC	Amb	Amb		0.0	0.150073	3.14897 E-03	1.27724 E-05	0.99341	0.050112	0.150014
MSFC	LOX	Amb		0.0	0.105272	5.34224 E-04	3.4069 E-06	0.99556	0.026947	0.101493
SSFL	Amb	Amb	No cups	0.0	0.177261	3.02593 E-03	1.46416 E-05	0.99320	0.066844	0.166890
SSFL	Amb	Amb	Cups	0.0	0.172949	2.69577 E-03	1.95879 E-05	0.99365	0.072736	0.16170~
WSTF	Amb	Amb		0.0	0.156931	7.62285 E-04	2.40303 E-06	0.99493	0.006255	0.156606

TABLE 2. HIGH PRESSURE TESTER PENETRATION FUNCTION CURVE PARAMETERS

Source	Temperature	Pressure	Additional Conditions	Forced Regression Line					Unforced Regression Line	
				A0	A1	c^2 Line	σ^2 A1	R	A0	A1
MSFC	Amb	Amb		0.0	0.184807	1.26172 E-02	5.61595 E-05	0.97345	0.140462	0.18419
MSFC	Amb	Amb	No seals	0.0	0.171700	1.90783 E-03	3.27057 E-05	0.99690	0.078073	0.182243
MSFC	Amb	3.4×10^7		0.0	0.165884	1.73585 E-02	6.55806 E-05	0.96075	0.121739	0.149731
MSFC	LOX	Amb		0.0	0.095314	9.84905 E-03	3.84671 E-05	0.93818	0.086493	0.08543
MSFC	LOX	3.4×10^7		0.0	0.086283	1.10980 E-02	4.88592 E-05	0.90664	0.134443	0.06970
SSFL	73	Amb		0.0	0.195317	3.50820 E-03	2.73544 E-05	0.99601	0.012867	0.19362
SSFL	Amb	Amb		0.0	0.153333	2.56528 E-03	1.25749 E-05	0.99381	0.007628	0.17219
SSFL	LOX	Amb		0.0	0.091043	2.91479 E-04	2.27274 E-06	0.99853	-0.008504	0.09210
SSFL	73	Amb	No seals	0.0	0.196746	8.11862 E-03	6.33031 E-05	0.99117	-0.003755	0.197240
SSFL	Amb	Amb	No seals	0.0	0.175434	2.21107 E-03	1.72403 E-05	0.99694	-0.000992	0.177564
SSFL	LOX	Amb	No seals	0.0	0.094189	1.91312 E-03	1.49171 E-05	0.99161	-0.031825	0.09832
SSFL	73	3.4×10^7		0.0	0.223546	1.18817 E-01	9.30902 E-04	0.92302	-0.06337	0.231653
SSFL	Amb	3.4×10^7		0.0	0.152961	4.13695 E-03	2.02792 E-05	0.98919	0.047262	0.14790
SSFL	LOX	3.4×10^7		0.0	0.089118	6.98296 E-04	2.98184 E-06	0.96001	0.00323	0.08646
WSTF	Amb	Amb		0.0	0.139128	2.71317 E-03	9.80665 E-06	0.99264	0.006231	0.138274
WSTF	Amb	3.4×10^7		0.0	0.107795	5.89091 E-03	2.56127 E-05	0.97806	-0.126135	0.125912
WSTF	LOX	3.4×10^7		0.0	0.028318	4.88802 E-03	3.52501 E-05	0.76201	-0.063213	0.036706

a greater impact indentation than the SSFL tester except at LOX conditions.
The LOX temperature data were generated at -145±5°C for the MSFC/SSFL
testers and at temperatures between -183°C and -119°C for the WSTF tester.
Therefore, a direct comparison of the data does contain some error; however,
this error is not believed to be large.

It was found that the ABMA tester produced the largest indentation at a
given temperature; therefore, reference testers were selected. The WSTF
ABMA tester was chosen as the ambient temperature reference tester and the
KSC ABMA tester as the LOX temperature reference tester because each gave
the largest indentation at the respective temperatures. Using the penetration
function, equivalent energy plots were made. The results of the comparisons
of the high pressure testers with the respective reference testers are given in
Figures 27, 28, and 29. As seen from these figures, it is clear that the
pressurized testers do not place the same magnitude of stress on a sample as
does the ABMA tester. Of the two types of testers, the Rocketdyne design
approaches more closely the ABMA tester in specimen penetration than does
the WSTF tester, especially at LOX conditions.

Phase II: Material Round-Robin Tests

Discussion and Experimental Procedure. The purpose of this round-
robin test program was to determine reaction sensitivity and energy threshold
levels of several materials under standardized conditions in the high-pressure
and ABMA test systems. Material procurement and sample fabrication were
done by MSFC. WSTF cleaned, packaged, and submitted all test samples to
participating test facilities. Each type of material was from one lot and samples
were randomly distributed. The selected materials were chosen according to
past history of reaction rates. The test materials were as follows:

Highly Reactive — Nylon 6/6

Moderately Reactive — Rulon A® and FEP Teflon® [1]

Minimally Reactive — TFE Teflon® and 15 percent graphite filled
TFE Teflon® [1]

Exact procedures were established for all test facilities to eliminate as
many variables as possible that could effect test results. A number of precau-
tions such as purging, running blanks, and changing striker pins and cups were

---

1. Testing of these materials was optional.

taken to enhance cleanliness of the test systems. Energy threshold determinations were made for each of the selected materials at 3.4×10^7 Pa in LOX and ambient temperature GOX. Energy thresholds were also determined for each of the materials on the ABMA testers with similar precautions. Reaction rates were generally determined by making 20 drops at 10 kg-m at each test condition, regardless of the number of reactions.

Test Results

ABMA LOX Impact Tests - The results of the ABMA ambient pressure LOX round-robin impact tests are summarized in Table 3. These tests reveal that the four ABMA testers produced essentially identical results. In part, the four threshold levels determined for Nylon 6/6 were in exceptionally good agreement. The single reaction for the graphite-filled TFE at WSTF is not sufficient cause for rejection since one more reaction in an additional 40 drops is required by either MSFC-SPEC-106B [1] or NHB 8060.1A [3] before the material is considered to be reactive at this energy level.

High Pressure Impact Tests - The threshold energy level determined for the five test materials at 3.4×10^7 Pa are summarized in Table 4. Because of its high degree of reactivity and damage potential to the test systems, Nylon 6/6 was not fully evaluated.

The detailed test results at each energy level are shown in Table 5. All three impact testers had essentially the same threshold levels for graphite-filled TFE in LOX and ambient temperature GOX, and for Rulon A® in LOX. For the remaining materials and test conditions, the MSFC and Rocketdyne impact testers produced essentially identical threshold energy levels while the WSTF impact tester produced lower threshold energy levels. Several retest test series were conducted by WSTF because of test results obtained with TFE Teflon® in 3.4×10^7 Pa, ambient temperature GOX. An energy threshold of 1 kg-m was determined during the initial test series which strongly disagreed with the MSFC/SSFL result of 10 kg-m as an energy threshold. WSTF performed two more test series of 20 drops each at the same conditions and obtained a threshold of 10 kg-m each time. The reason for this wide difference in data from the WSTF tester remains unknown. All variables such as packaging, contamination of the samples or test system, and surface anomalies of the strikers and/or cups were discounted as a possible cause for the reactions in the first test series. Consequently, all three TFE Teflon® test results were considered valid. In addition, WSTF retested the majority of the other materials in high pressure oxygen at 10 kg-m. These additional test data seemed to support the previous test results. Table 4 presents a summary of these threshold data.

38

TABLE 3. ABMA IMPACT TESTER TEST RESULTS

Material	Temperature (°C)	Level (kg-m)	Test Results			
			KSC	WSTF	MSFC	SSFL
Teflon®, TFR	-183	10	0/100	0/20	0/20	0/20
Nylon 6/6	-183	10	8/20	7/20	5/20	3/20
		9	9/20	1/1	3/20	2/20
		8	9/20	8/22	5/20	5/20
		7	4/20	1/20	4/20	2/20
		6	0/20	0/20	2/20 2/20	0/20
		5	—	—	0/20	—
Teflon®, FEP	-183	10	0/100	0/20	0/20	—
15 percent Graphite TFE	-183	10	0/100	1/20	0/20	—
Rulon A®	-183	10	0/10	0/20	0/20	0/20

TABLE 4. SUMMARY OF HIGH PRESSURE IMPACT TEST ENERGY
THRESHOLD DETERMINATIONS AT 3.4×10^7 Pa

Material	WSTF (kg-m)	MSFC (kg-m)	SSFL (kg-m)
15 percent Graphite Filled TFE, amb	10	10	—
15 percent Graphite Filled TFE, -145°C	10	9	—
Nylon 6/6, 6.9×10^6 Pa, amb	7	7	—
Rulon A®, amb	1, 4[a]	7	7
Rulon A®, -145°C	3, 3[a]	4	5
Teflon®, TFE, amb	1, 10[a], 10[a]	9	9
Teflon®, TFE, -145°C	10, 10[a]	9	10
Teflon®, FEP, amb	2, 3[a]	5, 5[a]	5
Teflon®, FEP, -145°C	6	9	9
a. Retest			

TABLE 5. HIGH PRESSURE IMPACT TEST RESULTS AT 3.4×10^7 Pa

Material	Temperature (°C)	Level (kg-m)	Test Results		
			WSTF	MSFC	SSFL
Teflon®, TFE	amb	10	1/4, 0/20[a], 0/20[a]	3/20, 2/20[b]	1/20, 0/20[b]
		9	1/4	0/20	0/20
		8	1/2	—	—
		7	1/16	—	—
		6	1/8	—	—
		5	2/4	—	—
		4	1/20	—	—
		3	1/20	—	—
		2	1/20	—	—
		1	0/20	—	—
Teflon®, TFE	-145	10	0/20	9/20, 5/20[b]	0/20
		9	—	0/20	—
15 percent Graphite TFE	amb	10	0/20	0/20	—
15 percent Graphite TFE	-145	10	0/20	1/20, 0/20[b]	—
		9	—	0/20	—
Nylon 6/6 at 6.9 × 10⁶ Pa	amb	10	3/20	4/7	—
		9	1/20	2/5	—
		8	1/20	2/8, 2/10[b]	—
		7	1/20	0/20	—
		6	0/3	—	—

41

TABLE 5. (Continued)

Material	Temperature (°C)	Level (kg-m)	Test Results		
			WSTF	MSFC	SSFL
Teflon®, FEP	amb	10	1/1, 19/20	10/20	10/20
		9	1/1	2/4, 9/9[a]	—
		8	1/1	2/2, 16/20[a]	2/14
		7	1/1	2/12, 13/20[a]	2/8
		6	1/1	2/17, 2/5, 12/20[a], 2/5[ab]	0/20
		5	1/1	0/20, 0/20[a]	—
		4	2/3, 1/1[a]	—	—
		3	1/20, 0/20[a]	—	—
		2	0/20	—	—
Teflon®, FEP	-145	10	10/20	5/20, 6/20[b]	1/20, 0/20[b]
		9	—	0/20	0/20
		8	—	—	—
		7	2/4	—	—
		6	0/2	—	—
Rulon A®	-145	10	2/5	12/20	15/20
		9	—	—	—
		8	—	3/3	3/5
		7	—	15/20	—
		6	1/1	5/20	2/8
		5	1/14	0/20	0/20
		4	2/16	0/20	—
		3	0/20, 0/20	—	—
		2	0/20	—	—

TABLE 5. (Continued)

Material	Temperature (°C)	Level (kg–m)	Test Results		
			WSTF	MSFC	SSFL
Rulon A®	amb	10	1/1, 4/20	7/20	1/20
		9	1/1	2/20	3/20
		8	1/4	1/20, 2/8[b]	2/20
		7	1/1	0/20	0/20
		6	1/15	—	—
		5	1/2, 1/1[a]	—	—
		4	3/20, 0/20[a]	—	—
		3	1/20, 0/2[a]	—	—
		2	1/20, 0/20[a]	—	—
		1	0/20, 0/2[a]	—	—

a. Retest
b. Level Confirmation

43

DISCUSSION

During the initial planning stages of this test program, it was recognized that careful precautions to keep variables to a minimum would be required so that differences between each test apparatus could be determined rather than differences caused by cleaning procedures, test conditions (e.g. pressure and temperature), material lot variability, etc. Because of the diligent efforts to eliminate these variables, the data presented in this report are considered valid for determining energy delivery by a mechanical impact test system and for determining the reaction sensitivity of materials to mechanical impact in oxygen.

It was known throughout the test program that basic design differences between the high pressure WSTF-and Rocketdyne-designed test systems could possibly create differences in test results; however, the extent or the trend of test results caused by these differences was unknown. Therefore, two additional objectives with regard to energy delivery were planned: (1) the reproducibility of the Rocketdyne designed testers would be determined, and (2) the WSTF design could be compared to that of the Rocketdyne design. The detailed design differences are listed in Appendix C; however, the basic distinctions are the base, the mounting of the sample cup, and the striker pin assembly. These differences can be seen in the details shown in Figures 2 and 3.

Another variable in design which could affect energy delivery inherent only to the Rocketdyne SSFL/MSFC testers was the effect of frictional energy losses from the Omniseals® during the dynamic response of the striker assembly. A previous study (performed by Rocketdyne) of this energy loss due to the seals, determined by a similar test method (see Appendix D), showed an energy loss of 9 to 16 percent. Figures 21 and 22 also show that energy losses caused by these seals appear to be independent of energy levels. As explained in a previous section of this report (Phase I: Energy Input Study), anomalies in the data were found in that the "seals" data fell below the "no-seal" data during one test series at MSFC and one at SSFL. The reasons for this remain unknown; however, the trend suggested in this report and supported by previous data presented in Appendix D shows that frictional energy losses below 5 kg-m do not seem to differ significantly from those at levels greater than 5 kg-m.

Figures 16 through 23 graphically present results obtained by the individual testers. These results were as expected in that the higher the temperature the greater the indentation. Figures 16 through 20 also show the individual data points demonstrating the reproducibility of each tester at any

44

given energy level. In general, the two Rocketdyne-designed testers showed excellent correlation. The WSTF tester also had excellent correlation with the Rocketdyne-designed testers at ambient pressure and temperature, but as the temperature decreased and the pressure increased, considerable data scatter was observed. (See Table 2 for exact correlation factor calculations.)

Figures 24, 25, and 26 give direct comparison curves of the high-pressure impact testers using the calculated penetration functions (Appendix B). As stated before, the MSFC/SSFL testers showed greater impact indentations than WSTF, and the MSFC tester gave greater impact indentations than the SSFL tester except at LOX conditions. Also, Figures 27, 28, and 29 show comparative curves demonstrating that the MSFC/SSFL testers closely approach the energy delivered by the ABMA test system.

When correlating this energy input with the material round-robin test series (Phase II), some rather unexpected results were found. From all the graphs and curves generated from high-pressure tester data (Figs. 16 through 29), it was anticipated that the MSFC/SSFL testers would produce the most reactions while the WSTF tester would produce the least. A summary of the high-pressure energy thresholds of the materials involved in round-robin tests is contained in Table 4 with all individual test series data presented in Table 5. As can be seen from these test results, the MSFC and SSFL energy thresholds are within 1 kg-m of each other. As explained further in this report, these data correlate very well with the energy input curves. Surprisingly, WSTF produced lower energy thresholds for Rulon A$^{\circledR}$, FEP Teflon$^{\circledR}$, and in one case much lower thresholds for TFE Teflon$^{\circledR}$ at ambient temperature. During the initial test series, WSTF had determined a threshold of 1 kg-m at 3.4×10^{7} Pa ambient temperature GOX while MSFC and SSFL determined the threshold to be 10 kg-m at identical conditions. Upon subsequent retests of TFE Teflon$^{\circledR}$ at the same conditions, WSTF found the threshold to be 10 kg-m two different times. The reason for this difference in data is unknown; however, sample or test system contamination was discounted as a possible cause. Threshold determinations by WSTF for the remaining materials were essentially equal to those obtained by MSFC and SSFL.

Analysis of Figure 28 shows that for the WSTF high-pressure tester at ambient temperature, a change of 2 kg-m in the indicated energy level resulted in a change of only 1 kg-m in the actual energy level (ABMA equivalent). Similar analysis of Figure 29 for the WSTF high-pressure tester at cryogenic temperatures implies a change of 4 kg-m in indicated energy level is required to provide a change of 1 kg-m in the actual energy level.

Figures 28 and 29 show that MSFC and Rocketdyne testers actual energy level is approximately 80 percent of the indicated energy level.

45

One possible explanation for the lower energy transfer found with the WSTF tester is the way the unit is placed on the drop tower. The unit is supported in the drop tower by a hollow pipe on which the threaded anvil nut (Fig. 3) is not directly supported. This nut may deflect slightly due to thread deformation, thereby absorbing some increment of the impact energy delivered by the plummet. Modification of the test stand such that the nut is fully supported by the base plate or an anvil plate may eliminate many of the differences noted in the energy input study.

All ABMA impact test data from Phase I and Phase II gave excellent reproducibility. Figures 7 through 15 demonstrate the tester-to-tester reproducibility and minimal data scatter per any given energy level. The round-robin test results (Table 3) support the consistency of the ABMA tester with all energy thresholds being essentially equal between the four participating test facilities.

There are a number of variables in the high pressure test systems, such as the dynamic response of the striker assemblies, seal friction, and the energy associated with rebounds, which are still not totally understood. However, through standardization of procedures and test apparatus, an excellent screening device could be obtained for determining the reaction sensitivity of materials to mechanical impact in high pressure oxygen systems.

CONCLUSIONS

Data obtained in the energy input study (Phase I) and the subsequent round-robin material tests (Phase II) indicated the following:

ABMA Test System —

1) The ABMA test systems delivered more energy than the high pressure test systems.

2) ABMA mechanical impact testers operated by KSC, MSFC, Rocketdyne (SSFL), and WSTF produced essentially identical results in Phase I and Phase II tests.

3) Generally, the accuracy of the data produced in Phase I (energy input study) and material energy thresholds from Phase II (round-robin material tests) have an accuracy of at least ±1 kg-m.

Rocketdyne-Designed High Pressure Test System —

    1) The MSFC and Rocketdyne (SSFL) high-pressure impact testers delivered nearly the same amount of energy to the test samples in both 3.4×10^7 Pa LOX and GOX.

    2) Reproducibility of the testers for actual material energy thresholds and energy input seems to have an accuracy of ± 1 kg-m.

    3) In comparison to the amount of energy delivered by the ABMA tester, the tester delivered at least the following:

        a) 75 percent at 3.4×10^7 Pa, LOX

        b) 80 percent at 3.4×10^7 Pa, GOX

        c) 80 percent at ambient pressure and temperature.

WSTF-Designed High Pressure Test System —

    1) In comparison to the amount of energy delivered by the ABMA tester, the WSTF tester delivered the following:

        a) 25 percent at the 3.4×10^7 Pa, LOX

        b) 55 percent at the 3.4×10^7 Pa, GOX

        c) 75 percent at ambient pressure and temperature.

    2) The WSTF high-pressure mechanical impact tester produced material reactions at the same or lower energy levels (i.e., lower plummet heights) than did the MSFC and Rocketdyne testers. This is contrary to the trend suggested by the energy input study, and indicates that factors other than total input energy to the sample influenced material reactivity.

General —

    1) The use of energy input and penetration measurements is a good method for analyzing the performance of an impact tester but does not provide a measurement of other parameters which may contribute to a materials reactivity.

2) As shown by the ABMA test data, standardization of procedures and apparatus can lead to consistently reproducible results.

RECOMMENDATIONS

The following recommendations will improve the reproducibility, reduce the maintenance, and ensure the accuracy of each test system without changing previous oxygen-compatibility data now considered to be valid.

General —

Procedure (s) for the calibration of all impact test systems should be implemented. Calibration procedures could classify, establish, and measure critical parameters which could be used to evaluate system performance at any time.

ABMA Test System —

A design review of the basic ABMA drop tester should be performed to eliminate several inherent design difficiencies and make the following improvements:

1) An improved guide rail system for more rigidity and ensured alignment.

2) The spider assembly should incorporate correct bearing design to withstand and properly distribute rebound loads (this has to be implemented with the guide rail improvement).

3) Increase the mass of the baseplate to improve system rigidity at maximum impact loading (and to eliminate the need for special foundations)

4) To maintain consistency between the high pressure and ABMA test procedures, it is recommended that rebound catchers be used in all systems. Even though test results may differ from previous published ABMA data, incorporation of a catcher would be necessary for standardization of test methods.

5) Use local test site gravity constants for establishing drop heights and timing values.

48

High Pressure Test System —

     A standard mechanical impact tester should be developed and utilized to qualify materials for service in high-pressure oxygen systems. Use of a standard tester configuration by all facilities performing high pressure impact testing would permit better comparison of test data, reduce the incidence of redundant testing of materials, and permit development of a standard universal test procedure.

REFERENCES

1. Specification, Testing Compatibility of Materials for Liquid Oxygen Systems, MSFC-SPEC-106B (Amendment 1).

2. Compatibility of Materials with Liquid Oxygen (Impact Threshold Technique), ASTM-D-2512.

3. Specification, Flammability, Odor, and Offgassing Requirements and Test Procedures for Materials in Environments that Support Combustion. NHB 8060.1A. National Aeronautics and Space Administration, Office of Manned Space Flight, Washington, D.C., February 1974.

APPENDIX A

FINAL REPORT — SPECIAL TASK ASSIGNMENT 033

1. INTRODUCTION

Five different lots of E. I. DuPont's Vespel SP-211 and the 3M Company's Kel-F (molded into raw stock by the Fluorocarbon Company) were procured and supplied to NASA/MSFC by Rocketdyne for the evaluation of oxygen compatibility lot-to-lot variability and test result reproducibility between MSFC and SSFL facilities oxygen impact testers. Rocketdyne's Material and Processes Oxygen Laboratory (SSFL) performed LOX compatibility impact testing per MSFC-SPEC-101B to determine energy thresholds at predetermined test conditions.

The purpose of this report is to present and compare the test results submitted by MSFC to those obtained by Rocketdyne.

2. RESULTS

E. I. DuPont's Vespel SP-211 (Lot Numbers 1569, 1646, 9184, 1888, and 1896) and Fluorocarbon's Kel-F (Lot Numbers 683, 686, 687, 689, and 693[1]) were procured and machined to 11/16-in. diameter impact specimens. Vespel SP-211 lots were tested at a specimen thickness of 0.050 in. and 0.015 in., while all lots of Kel-F were machined to a sample thickness of 0.050 in. Table A-1 presents all test results submitted by MSFC and SSFL with minimal receiving/inspection data received from White Sands Test Facility (WSTF). The arrows in the table point out comparable data between test facilities from which conclusions were drawn. As can be seen, only 17 data points could be used for comparison purposes. Table A-1 also summarizes the data for lot-to-lot and tester-to-tester variation determinations.

SSFL test results for five lots of Vespel SP-211 showed excellent consistency (see Table A-1); i.e., all passed at 8800 psi, LOX, 5 kg-m. MSFC results were to the contrary, however, with four out of five lots failing at the preceding test conditions. (Note that the fifth lot was only tested at the 4 kg-m energy level.) A reduction in sample thickness produced increased lot variation with 60 percent of the lots passing and 40 percent failing at SSFL while

---

1. Kel-F lot numbers are supplied from Minnesota Mining Co. for the basic resin.

MSFC failed all five. The five lots of Kel-F had a wider spread of energy thresholds, ranging from - 2.08 to 5 kg-m with only one lot passing the 5 kg-m level at 8800 psi, LOX at SSFL.

Comparable test data between test facilities listed in Table A-2 determined interesting but disturbing differences in test results of identical lots of material. SSFL and WSTF had 100 percent agreement of results. WSTF and MSFC test results agreed 40 percent and SSFL and MSFC concurred with only 35 percent of the test results.

3. DISCUSSION

The causes for the poor reprodicibility of impact testing remains largely unexplained. There are, however, a number of possibilities which should be explored. Some of these concerns include:

a) Temperature controls and monitors.

b) Methods of examining impact test specimens and interpretation of results.

c) Contamination control.

d) Differences in the impact testers at MSFC, SSFL, and WSTF, i.e., seal loading drag, friction losses, etc.

4. CONCLUSIONS

The following conclusions resulted from reviewing data contained in Table A-1:

a) Lot-to-lot oxygen compatibility variation for Vespel SP-211 was minimal according to test results attained by the SSFL impact tester. Test results were consistent, in that, no reaction in 20 drops occurred for each of the five lots at test conditions of 8800 psi, LOX, 5 kg-m with a sample thickness of 0.050 in. A reduction in sample thickness did, however, increase variation to the extent of one lot failing to meet the same temperature and pressure levels at 2 kg-m. MSFC results showed a greater lot-to-lot variance with energy thresholds at 0.050 in. being ≤ 4 kg-m and all five lots failing the 5 kg-m energy level with a sample thickness of 0.015 in.

52

b) Lot-to-lot oxygen compatibility variation of Kel-F was considerably more than Vespel SP-211. Energy thresholds determinations made from MSFC and SSFL ranged from - 2.08 to 5 kg-m at 8800 psi, LOX with a sample thickness of 0.050 in.

c) Tester-to-tester test result reproducibility of identical lots of Kel-F and Vespel SP-211 to the same test parameters was poor. From comparable data, MSFC failed 65 percent of the materials passing impact testing at SSFL.

5. RECOMMENDED ACTION

Rocketdyne concurs with the recommendation that a meeting be held with the appropriate MSFC, Rocketdyne, and White Sands Test Facility personnel to discuss the causes for the wide discrepancy in test results. Rocketdyne suggests that this meeting be held before the end of the year 1976 due to the importance of the conclusions reached by the results of this task.

TABLE A-1. OXYGEN COMPATIBILITY IMPACT TEST RESULTS

Material	Thickness (inches)	Pressure (psi)	Energy (Kg-m)	MSFC Results	SSFL Results	WSTF Results
Vespel SP-211 Batch 1569	0.050	8800	7	---	0/20	---
	0.045	8800	5	---	---	0/20
			4	0/20	---	---
	0.015	8800	5	3/3	2/7	---
			4	---	2/20	---
			3	---	1/2	---
			2	---	2/33	---
Vespel SP-211 Batch 1646	0.050	8800	7	1/6	0/20	---
			5	1/17	---	0/20
			4	0/20	---	---
	0.015	8800	5	3/3	2/24	---
			4	---	0/20	---
Vespel SP-211 Batch 9184	0.050	8800	5	1/9	---	0/20
			4	1/14	---	---
	0.015	8800	5	3/3	0/20	---
Vespel SP-211 Batch 1888	0.050	8800	5	2/2	0/20	---
	0.015	8800	5	2/2	0/20	---
Kel-F Lot 689	0.050	8800	5	2/2	2/4	---
			4	---	1/20	---
			3	0/20	---	---
	0.050	5500	7	2/2	---	---

TABLE A-1. (Continued)

Material	Thickness (inches)	Pressure (psi)	Energy (Kg-m)	MSFC Results	SSFL Results	WSTF Results
Kel-F Lot 687	0.050	8800	10	---	1/1	---
			8	---	1/1	---
			6	---	2/2	---
			5	4/4	0/20	---
		5500	7	2/2	---	---
			5	---	0/20	---
Kel-F Lot 693	0.050	8800	5.54	2/2	---	---
			5	---	1/6	---
			4.86	2/3	---	---
			4.17	2/3	---	---
			4	---	2/11	---
			3	---	0/22	---
Vespel SP-211 Batch 1896	0.050	8800	5	1/11	0/20	---
	0.015	8800	5	1/11	0/20	---
Kel-F Lot 683	0.050	8800	10	1/1	---	---
			7.62	1/1	---	---
			5.54	1/1	---	---
			5	---	2/24	---
			4.86	1/1	---	---
			2.08	1/1	---	---
	0.050	5500	6.95	1/1	---	---
			5.54	1/1	---	---
			4.86	3/5	---	---

TABLE A-1. (Concluded)

Material	Thickness (inches)	Pressure (psi)	Energy (Kg-m)	MSFC Results	SGFL Results	MSTF Results
Kel-F Lot 686	0.050	8800	5	3/3	2/26	---
	0.050	5500	4	---	---	---
			7	2/2	---	---
			5	2/2	---	---
			4	2/2	---	---
			3	0/20	---	---

TABLE A-2. COMPARABLE LOX IMPACT DATA OF TESTER FACILITIES

Material	Thickness (inches)	Pressure (psi)	Energy (Kg-m)	MSFC Results	SSFL Results	WSTF Results
Vespel SP-211 Batch 1569	0.050	8800	5	--	0/20	0/20
	0.045	8800	4	0/20	0/20	0/20
	0.015	8800	5	3/3	2/7	--
Vespel SP-211 Batch 1646	0.050	8800	7	1/6	0/20	--
	0.050	8800	5	1/17	0/20	0/20
	0.050	8800	4	0/20	0/20	0/20
	0.015	8800	5	3/3	2/24	--
Vespel SP-211 Batch 9184	0.050	8800	5	1/9	0/20	0/20
	0.050	8800	4	1/14	0/20	0/20
	0.015	8800	5	3/3	0/20	--
Vespel SP-211 Batch 1888	0.050	8800	5	2/2	0/20	--
	0.015	8800	5	2/2	0/20	--
Vespel SP-211 Batch 1896	0.050	8800	5	1/11	0/20	--
	0.015	8800	5	1/11	0/20	--
Kel-F Lot 693	0.050	8800	5	3/3	2/26	--
Kel-F Lot 609	0.050	8800	5	2/2	2/4	--
Kel-F Lot 687	0.050	8800	5	4/4	0/20	--

Percentage of Agreements

SSFL & WSTF - 100%; WSTF & MSFC - 40%; SSFL & MSFC - 35%

APPENDIX B

ENERGY INPUT STUDY RAW DATA

Appendix B contains all the raw data from KSC, WSTF, MSFC and Rocketdyne (SSFL) from which all graphs to the body of this report were determined. Table B-1 summarizes the raw data contained in Table B-2. Comments have also been included to provide pertinent information regarding a particular test series.

TABLE B-1. SUMMARY OF RAW DATA

Disc No's	Source	Tester	Test Condition			Comments
			°C	PSI	MN/M²	
1-14	KSC	ABMA	AMB	AMB	AMB	Initial tests showing low penetration data resulting from an improperly shimed base
15-44	KSC	ABMA	AMB	AMB	AMB	Retest at same conditions as disc numbers 1-14 after problem was corrected giving higher penetration data
45-59	KSC	ABMA	LOX	AMB	AMB	No temperature measurement capability
60-90	MSFC	ABMA	AMB	AMB	AMB	
91-118	MSFC	ABMA	LOX	AMB	AMB	No temperature measurement capability
119-145	SSFL	ABMA	AMB	AMB	AMB	
146-163	SSFL	ABMA	AMB	AMB	AMB	
164-195	WSTF	ABMA	AMB	AMB	AMB	With cups
196-222	MSFC	HP	AMB	AMB	AMB	
223-228	MSFC	HP	AMB	AMB	AMB	With seals
229-257	MSFC	HP	AMB	5000	34.5	Without seals
258-283	MSFC	HP	-145	AMB	AMB	With seals
284-304	MSFC	HP	-145	5000	34.5	With seals
305-316	SSFL	HP	74	AMB	AMB	With seals
317-340	SSFL	HP	AMB	AMB	AMB	With seals
341-352	SSFL	HP	-145	AMB	AMB	With seals
353-364	SSFL	HP	74	AMB	AMB	Without seals

59

TABLE B-1. (Concluded)

Disc No's	Source	Tester	Test Condition			Comments
			°C	PSI	MN/M^2	
365-376	SSFL	HP	AMB	AMB	AMB	Without seals
377-388	SSFL	HP	-145	AMB	AMB	Without seals
389-399	SSFL	HP	74	5000	34.5	With seals
400-423	SSFL	HP	AMB	5000	34.5	With seals
424-445	SSFL	HP	-145	5000	34.5	With seals
446-475	WSTF	HP	AMB	AMB	AMB	
476-503	WSTF	HP	AMB	5000	34.5	
504-530	WSTF	HP	LOX	5000	34.5	WSTF does not have temperature measurement capabilities for the high pressure tester

TABLE B-2. RAW DATA FROM KSC, WSTF, MSFC AND SSFL

Source	Disc #	Tester	Temperature, (°C)	Pressure, (Pa)	Energy Level, (Kg-M)	Diameter, (In.)	Diameter, (mm)	Calculated Penetration, (mm)	Calculated Penetration, Squared, (mm²)
KSC	0	ABMA	AMB	AMB	1	0.1780	4.5212	0.4160	0.1731
KSC	1	ABMA	AMB	AMB	1	0.1760	4.4704	0.4064	0.1652
KSC	2	ABMA	AMB	AMB	1	0.1720	4.3688	0.3875	0.1502
KSC	3	ABMA	AMB	AMB	3	0.2280	5.7912	0.6986	0.4381
KSC	4	ABMA	AMB	AMB	3	0.2270	5.7658	0.6921	0.4791
KSC	5	ABMA	AMB	AMB	3	0.2310	5.8674	0.7183	0.5160
KSC	6	ABMA	AMB	AMB	5	0.2580	6.5532	0.9107	0.8293
KSC	7	ABMA	AMB	AMB	5	0.2540	6.4516	0.8804	0.7751
KSC	8	ABMA	AMB	AMB	5	0.2550	6.4770	0.8879	0.7884
KSC	9	ABMA	AMB	AMB	7	0.2860	7.2644	1.1414	1.3028
KSC	10	ABMA	AMB	AMB	7	0.2850	7.2390	1.1326	1.2827
KSC	11	ABMA	AMB	AMB	7	0.2880	7.3152	1.1592	1.3437
KSC	12	ABMA	AMB	AMB	10	0.2940	7.4676	1.2137	1.4731
KSC	13	ABMA	AMB	AMB	10	0.2960	7.5184	1.2323	1.5185
KSC	14	ABMA	AMB	AMB	10	0.2960	7.5184	1.2323	1.5185
KSC	15	ABMA	AMB	AMB	1	0.1840	4.6736	0.4456	0.1986
KSC	16	ABMA	AMB	AMB	1	0.1850	4.6990	0.4506	0.2031
KSC	17	ABMA	AMB	AMB	1	0.1840	4.6736	0.4456	0.1986
KSC	18	ABMA	AMB	AMB	1	0.1810	4.1810	0.4307	0.1855
KSC	19	ABMA	AMB	AMB	1	0.1830	4.6482	0.4406	0.1941
KSC	20	ABMA	AMB	AMB	3	0.2350	5.9690	0.7451	0.5551
KSC	21	ABMA	AMB	AMB	3	0.2370	6.0198	0.7587	0.5756
KSC	22	ABMA	AMB	AMB	3	0.2360	5.9944	0.7518	0.5653

61

TABLE B-2. (Continued)

Source	Disc #	Tester	Temperature, (°C)	Pressure, (Pa)	Energy Level, (Kg-M)	Diameter, (In.)	Diameter, (mm)	Calculated Penetration, a (mm)	Calculated Penetration, Squared (mm²)
KSC	23	ABMA	AMB	AMB	3	0.2380	6.0452	0.7655	0.5860
KSC	24	ABMA	AMB	AMB	3	0.2360	5.9944	0.7518	0.5653
KSC	25	ABMA	AMB	AMB	5	0.2660	6.7564	0.9732	0.9471
KSC	26	ABMA	AMB	AMB	5	0.2650	6.7310	0.9652	0.9316
KSC	27	ABMA	AMB	AMB	5	0 2660	6.7564	0.9732	0.9471
KSC	28	ABMA	AMB	AMB	5	0.2640	6.7056	0.9573	0.9164
KSC	29	ABMA	AMB	AMB	5	0.2650	6.7310	0.9652	0.9316
KSC	30	ABMA	AMB	AMB	7	0.2860	7.2644	1.1414	1.3028
KSC	31	ABMA	AMB	AMB	7	0.2840	7.2136	1.1238	1.2629
KSC	32	ABMA	AMB	AMB	7	0.2830	7.1882	1.1150	1.2433
KSC	33	ABMA	AMB	AMB	7	0.2850	7.2390	1.1326	1.2827
KSC	34	ABMA	AMB	AMB	7	0.2840	7.2136	1.1238	1.2629
KSC	35	ABMA	AMB	AMB	9	0.3010	7.6454	1.2795	1.6372
KSC	36	ABMA	AMB	AMB	9	0.3000	7.6200	1.2700	1.6129
KSC	37	ABMA	AMB	AMB	9	0.3010	7.6454	1.2795	1.6372
KSC	38	ABMA	AMB	AMB	9	0.2980	7.5692	1.2510	1.5651
KSC	39	ABMA	AMB	AMB	9	0.3000	7.6200	1.2700	1.6129
KSC	40	ABMA	AMB	AMB	10	0.3080	7.8232	1.3478	1.8166
KSC	41	ABMA	AMB	AMB	10	013060	7.7724	1.3281	1.7637
KSC	42	ABMA	AMB	AMB	10	0.3080	7.8232	1.3478	1.8166
KSC	43	ABMA	AMB	AMB	10	0.3070	7.7978	1.3379	1.7900
KSC	44	ABMA	AMB	AMB	10	0.3080	7.8232	1.3478	1.8166

TABLE B-2. (Continued)

Source	Disc #	Tester	Temperature, (°C)	Pressure, (Pa)	Energy Level, (Kg-M)	Diameter, (In.)	Diameter, (mm)	Calculated Penetration, (mm)	Calculated Penetration, Squared (mm^2)
KSC	45	ABMA	LOX	AMB	1	0.1610	4.0894	0.3382	0.1144
KSC	46	ABMA	LOX	AMB	1	0.1590	4.0386	0.3296	0.1087
KSC	47	ABMA	LOX	AMB	1	0.1600	4.0640	0.3339	0.1115
KSC	48	ABMA	LOX	AMB	1	0.1590	4.0386	0.3296	0.1087
KSC	49	ABMA	LOX	AMB	1	0.1600	4.0640	0.3339	0.1115
KSC	50	ABMA	LOX	AMB	5	0.2350	5.9690	0.7451	0.5551
KSC	51	ABMA	LOX	AMB	5	0.2340	5.9436	0.7383	0.5451
KSC	52	ABMA	LOX	AMB	5	0.2340	5.9436	0.7383	0.5451
KSC	53	ABMA	LOX	AMB	5	0.2340	5.9436	0.7383	0.5451
KSC	54	ABMA	LOX	AMB	5	0.2330	5.9182	0.7316	0.5353
KSC	55	ABMA	LOX	AMB	10	0.2760	7.0104	1.0551	1.1132
KSC	56	ABMA	LOX	AMB	10	0.2750	6.9850	1.0467	1.0956
KSC	57	ABMA	LOX	AMB	10	0.2760	7.0104	1.0551	1.1132
KSC	58	ABMA	LOX	AMB	10	0.2750	6.9850	1.0467	1.0956
KSC	59	ABMA	LOX	AMB	10	0.2760	7.0104	1.0551	1.1132
MSFC	60	ABMA	AMB	AMB	1	0.1916	4.8666	0.4847	0.2350
MSFC	61	ABMA	AMB	AMB	1	0.1920	4.8768	0.4868	0.2370
MSFC	62	ABMA	AMB	AMB	1	0.1926	4.8920	0.4900	0.2401
MSFC	63	ABMA	AMB	AMB	2	0.2165	5.4991	0.6261	0.3921
MSFC	64	ABMA	AMB	AMB	2	0.2152	5.4661	0.6183	0.3822
MSFC	65	ABMA	AMB	AMB	2	0.2155	5.4737	0.6201	0.3845

TABLE B-2. (Continued)

Source	Disc #	Tester	Temperature, (°C)	Pressure, (Pa)	Energy Level, (Kg-M)	Diameter, (In.)	Diameter, (mm)	Calculated Penetration, (mm)	Calculated Penetration, Squared (mm²)
MSFC	66	ABMA	AMB	AMB	3	0.2322	5.8979	0.7263	0.5275
MSFC	67	ABMA	AMB	AMB	3	0.2373	6.0274	0.7607	0.5787
MSFC	68	ABMA	AMB	AMB	3	0.2366	6.0096	0.7559	0.5714
MSFC	69	ABMA	AMB	AMB	4	0.2508	6.3703	0.8566	0.7338
MSFC	70	ABMA	AMB	AMB	4	0.2629	6.6777	0.9487	0.8999
MSFC	71	ABMA	AMB	AMB	4	0.2508	6.3703	0.8566	0.7338
MSFC	72	ABMA	AMB	AMB	5	0.2647	6.7234	0.9628	0.9271
MSFC	73	ABMA	AMB	AMB	5	0.2635	6.6929	0.9534	0.9089
MSFC	74	ABMA	AMB	AMB	5	0.2647	6.7234	0.9628	0.9271
MSFC	75	ABMA	AMB	AMB	6	0.2774	7.0460	1.0669	1.1383
MSFC	76	ABMA	AMB	AMB	6	0.2775	7.0485	1.0678	1.1401
MSFC	77	ABMA	AMB	AMB	6	0.2739	6.9571	1.0375	1.0765
MSFC	78	ABMA	AMB	AMB	7	0.2840	7.2136	1.1238	1.2629
MSFC	79	ABMA	AMB	AMB	7	0.2842	7.2187	1.1255	1.2668
MSFC	80	ABMA	AMB	AMB	7	0.2830	7.1882	1.1150	1.2433
MSFC	81	ABMA	AMB	AMB	7	0.2846	7.2288	1.1290	1.2747
MSFC	82	ABMA	AMB	AMB	8	0.2913	7.3990	1.1890	1.4137
MSFC	83	ABMA	AMB	AMB	8	0.2912	713965	1.1881	1.4115
MSFC	84	ABMA	AMB	AMB	8	0.2932	7.4473	1.2064	1.4553
MSFC	85	AMBA	AMB	AMB	9	0.3027	7.6886	1.2959	1.6794
MSFC	86	ABMA	AMB	AMB	9	0.2966	7.5336	1.2379	1.5324
MSFC	87	ABMA	AMB	AMB	9	0.3022	7.6759	1.2911	1.6669
MSFC	88	ABMA	AMB	AMB	10	0.3020	7.6708	1.2891	1.6619

Source	Disc #	Tester	Temperature, (°C)	Pressure, (Pa)	Energy Level, (Kg-M)	Diameter, (In.)	Diameter, (mm)	Calculated Penetration, (mm)	Calculated Penetration, Squared (mm^2)
MSFC	89	ABMA	AMB	AMB	10	0.3071	7.8003	1.3389	1.7926
MSFC	90	ABMA	AMB	AMB	10	0.3047	7.7394	1.3153	1.7301
MSFC	91	ABMA	LOX	AMB	1	0.1760	4.4704	0.4064	0.1652
MSFC	92	ABMA	LOX	AMB	1	0.1683	4.2748	0.3705	0.1373
MSFC	93	ABMA	LOX	AMB	1	0.1631	4.1427	0.3473	0.1206
MSFC	94	ABMA	LOX	AMB	2	0.1901	4.8285	0.4768	0.2274
MSFC	95	ABMA	LOX	AMB	2	0.1873	4.7574	0.4624	0.2138
MSFC	96	ABMA	LOX	AMB	2	0.1943	4.9352	0.4991	0.2491
MSFC	97	ABMA	LOX	AMB	3	0.2106	5.3492	0.5907	0.3490
MSFC	98	ABMA	LOX	AMB	3	0.2048	5.2019	0.5571	0.3104
MSFC	99	ABMA	LOX	AMB	3	0.2029	5.1537	0.5464	0.2985
MSFC	100	ABMA	LOX	AMB	4	0.2241	5.6921	0.6735	0.4536
MSFC	101	ABMA	LOX	AMB	4	0.2219	5.6363	0.6596	0.4351
MSFC	102	ABMA	LOX	AMB	5	0.2332	5.9233	0.7330	0.5372
MSFC	103	ABMA	LOX	AMB	5	0.2348	5.9639	0.7437	0.5531
MSFC	104	ABMA	LOX	AMB	6	0.2401	6.0985	0.7800	0.6084
MSFC	105	ABMA	LOX	AMB	6	0.2409	6.1189	0.7856	0.6172
MSFC	106	ABMA	LOX	AMB	6	0.2391	6.0731	0.7731	0.5977
MSFC	107	ABMA	LOX	AMB	7	0.2498	6.3449	0.8493	0.7213
MSFC	108	ABMA	LOX	AMB	7	0.2526	6.4160	0.8699	0.7568
MSFC	109	ABMA	LOX	AMB	7	0.2497	6.3424	0.8485	0.7200

TABLE B-2. (Continued)

Source	Disc #	Tester	Temperature, (°C)	Pressure, (Pa)	Energy Level, (Kg-M)	Diameter, (In.)	Diameter, (mm)	Calculated Penetration, (mm)	Calculated Penetration, Squared (mm^2)
MSFC	110	ABMA	LOX	AMB	8	0.2599	6.6015	0.9253	0.8561
MSFC	111	ABMA	LOX	AMB	8	0.2617	6.6472	0.9393	0.8822
MSFC	112	ABMA	LOX	AMB	8	0.2584	6.5634	0.9137	0.8349
MSFC	113	ABMA	LOX	AMB	9	0.2651	6.7335	0.9660	0.9331
MSFC	114	ABMA	LOX	AMB	9	0.2612	6.6245	0.9354	0.8749
MSFC	115	ABMA	LOX	AMB	9	0.2663	6.7640	0.9756	0.9517
MSFC	116	ABMA	LOX	AMB	10	0.2749	6.9825	1.0459	1.0939
MSFC	117	ABMA	LOX	AMB	10	0.2729	6.9317	1.0292	1.0594
MSFC	118	ABMA	LOX	AMB	10	0.2712	6.8885	1.0152	1.0307
SSFL	119	ABMA	AMB	AMB	1	0.1788	4.5415	0.4199	0.1763
SSFL	120	ABMA	AMB	AMB	1	0.1783	4.5288	0.4175	0.1743
SSFL	121	ABMA	AMB	AMB	1	0.1790	4.5466	0.4209	0.1771
SSFL	122	ABMA	AMB	AMB	2	0.2143	5.4432	0.6128	0.3755
SSFL	123	ABMA	AMB	AMB	2	0.2124	5.3950	0.6014	0.3617
SSFL	124	ABMA	AMB	AMB	2	0.2135	5.4229	0.6080	0.3697
SSFL	125	ABMA	AMB	AMB	3	0.2305	5.8547	0.7150	0.5112
SSFL	126	ABMA	AMB	AMB	3	0.2310	5.8674	0.7183	0.5160
SSFL	127	ABMA	AMB	AMB	3	0.2319	5.8903	0.7243	0.5246
SSFL	128	ABMA	AMB	AMB	4	0.2469	6.2613	0.8282	0.6859
SSFL	129	ABMA	AMB	AMB	4	0.2520	6.4008	0.8655	0.7491
SSFL	130	ABMA	AMB	AMB	4	0.2462	6.2535	0.8232	0.6776

TABLE B-2. (Continued)

Source	Disc #	Tester	Temperature, (°C)	Pressure, (Pa)	Energy Level, (Kg-M)	Diameter, (In.)	Diameter, (mm)	Calculated Penetration, (mm)	Calculated Penetration, Squared (mm^2)
SSFL	131	ABMA	AMB	AMB	5	0.2604	6.6142	0.9292	0.8633
SSFL	132	ABMA	AMB	AMB	5	0.2608	6.6243	0.9322	0.8691
SSFL	133	ABMA	AMB	AMB	5	0.2627	6.6726	0.9471	0.8970
SSFL	134	ABMA	AMB	AMB	6	0.2760	7.0104	1.0551	1.1132
SSFL	135	ABMA	AMB	AMB	6	0.2688	6.8275	0.9957	0.9914
SSFL	136	ABMA	AMB	AMB	6	0.2725	6.9210	1.0258	1.0522
SSFL	137	ABMA	AMB	AMB	7	0.2817	7.1552	1.1037	1.2182
SSFL	138	ABMA	AMB	AMB	7	0.2811	7.1399	1.0985	1.2068
SSFL	139	ABMA	AMB	AMB	7	0.2808	7.1323	1.0959	1.2011
SSFL	140	ABMA	AMB	AMB	8	0.2881	7.3177	1.1601	1.3458
SSFL	141	ABMA	AMB	AMB	8	0.2881	7.3177	1.1601	1.3458
SSFL	142	ABMA	AMB	AMB	8	0.2878	7.3101	1.1574	1.3396
SSFL	143	ABMA	AMB	AMB	10	0.3025	7.6835	1.2940	1.6744
SSFL	144	ABMA	AMB	AMB	10	0.3080	7.8232	1.3478	1.8166
SSFL	145	ABMA	AMB	AMB	10	0.2980	7.5692	1.2510	1.5651
SSFL	146	ABMA	AMB	AMB	1	0.1746	4.4348	0.3997	0.1598
SSFL	147	ABMA	AMB	AMB	1	0.1767	4.4882	0.4098	0.1679
SSFL	148	ABMA	AMB	AMB	2	0.2093	5.3162	0.5831	0.3400
SSFL	149	ABMA	AMB	AMB	2	0.2105	5.3467	0.5902	0.3483
SSFL	150	ABMA	AMB	AMB	3	0.2324	5.9030	0.7276	0.5294

67

TABLE B-2. (Continued)

Source	Disc #	Tester	Temperature, (°C)	Pressure, (Pa)	Energy Level, (Kg-M)	Diameter, (In.)	Diameter, (mm)	Calculated Penetration, (mm)	Calculated Penetration, Squared (mm^2)
SSFL	151	ABMA	AMB	AMB	3	0.2288	5.8115	0.7038	0.4954
SSFL	152	ABMA	AMB	AMB	4	0.2484	6.3094	0.8391	0.7040
SSFL	153	ABMA	AMB	AMB	4	0.2488	6.3195	0.8420	0.7089
SSFL	154	ABMA	AMB	AMB	5	0.2599	6.6015	0.9253	0.8561
SSFL	155	ABMA	AMB	AMB	5	0.2616	6.6446	0.9385	0.8807
SSFL	156	ABMA	AMB	AMB	6	0.2697	6.8504	1.0030	1.0060
SSFL	157	ABMA	AMB	AMB	6	0.2730	6.9342	1.0301	1.0610
SSFL	158	ABMA	AMB	AMB	7	0.2797	7.1044	1.0865	1.1805
SSFL	159	ABMA	AMB	AMB	7	0.2824	7.1730	1.1098	1.2317
SSFL	160	ABMA	AMB	AMB	8	0.2848	7.2339	1.1308	1.2787
SSFL	161	ABMA	AMB	AMB	8	0.2890	7.3406	1.1682	1.3646
SSFL	162	ABMA	AMB	AMB	10	0.2990	7.5946	1.2605	1.5889
SSFL	163	ABMA	AMB	AMB	10	0.3001	7.6225	1.2710	1.6153
WSTF	164	ABMA	AMB	AMB	1	0.1810	4.5974	0.4307	0.1855
WSTF	165	ABMA	AMB	AMB	1	0.1832	4.6533	0.4416	0.1950
WSTF	166	ABMA	AMB	AMB	1	0.1826	4.6380	0.4386	0.1924
WSTF	167	ABMA	AMB	AMB	1	0.1818	4.6177	0.4346	0.1889
WSTF	168	ABMA	AMB	AMB	1	0.1845	4.6863	0.4481	0.2008
WSTF	169	ABMA	AMB	AMB	1	0.1805	4.5847	0.4282	0.1834
WSTF	170	ABMA	AMB	AMB	3	0.2375	6.0325	0.7621	0.5808
WSTF	171	ABMA	AMB	AMB	3	0.2375	6.0325	0.7621	0.5808
WSTF	172	ABMA	AMB	AMB	3	0.2365	6.0071	0.7553	0.5704

TABLE B-2. (Continued)

Source	Disc #	Tester	Temperature, (°C)	Pressure, (Pa)	Energy Level, (Kg-M)	Diameter, (In.)	Diameter, (mm)	Calculated Penetration, (mm)	Calculated Penetration, Squared (mm²)
WSTF	173	ABMA	AMB	AMB	3	0.2345	5.9563	0.7417	0.5501
WSTF	174	ABMA	AMB	AMB	3	0.2368	6.0147	0.7573	0.5735
WSTF	175	ABMA	AMB	AMB	5	0.2668	6.7767	0.9796	0.9595
WSTF	176	ABMA	AMB	AMB	5	0.2640	6.7056	0.9573	0.9164
WSTF	177	ABMA	AMB	AMB	5	0.2650	6.7310	0.9652	0.9316
WSTF	178	ABMA	AMB	AMB	5	0.2650	6.7310	0.9652	0.9316
WSTF	179	ABMA	AMB	AMB	5	0.2650	6.7310	0.9652	0.9316
WSTF	180	ABMA	AMB	AMB	7	0.2845	7.2263	1.1282	1.2727
WSTF	181	ABMA	AMB	AMB	7	0.2865	7.2771	1.1458	1.3129
WSTF	182	ABMA	AMB	AMB	7	0.2850	7.2390	1.1326	1.2827
WSTF	183	ABMA	AMB	AMB	7	0.2850	7.2390	1.1326	1.2827
WSTF	184	ABMA	AMB	AMB	7	0.2870	7.2898	1.1503	1.3231
WSTF	185	ABMA	AMB	AMB	8	0.2950	7.4930	1.2230	1.4957
WSTF	186	ABMA	AMB	AMB	8	0.2936	7.4574	1.2100	1.4642
WSTF	187	ABMA	AMB	AMB	8	0.2975	7.5565	1.2463	1.5534
WSTF	188	ABMA	AMB	AMB	8	0.2970	7.5438	1.2416	1.5417
WSTF	189	ABMA	AMB	AMB	8	0.2942	7.4727	1.2156	1.4777
WSTF	190	ABMA	AMB	AMB	10	0.3090	7.8486	1.3578	1.8435
WSTF	191	ABMA	AMB	AMB	10	0.3100	7.8740	1.3678	1.8708
WSTF	192	ABMA	AMB	AMB	10	0.3085	7.8359	1.3528	1.8300
WSTF	193	ABMA	AMB	AMB	10	0.3100	7.8740	1.3678	1.8708
WSTF	194	ABMA	AMB	AMB	10	0.3085	7.8359	1.3528	1.8300
WSTF	195	ABMA	AMB	AMB	10	0.3131	7.9527	1.3991	1.9576

TABLE B-2. (Continued)

Source	Disc #	Tester	Temperature, (°C)	Pressure, (Pa)	Energy Level, (Kg-M)	Diameter, (In.)	Diameter, (mm)	Calculated Penetration, (mm)	Calculated Penetration, Squared (mm^2)
MSFC	196	H.P.	AMB	AMB	1	0.1848	4.6939	0.4496	0.2022
MSFC	197	H.P.	AMB	AMB	1	0.1871	4.7523	0.4613	0.2128
MSFC	198	H.P.	AMB	AMB	1	0.1879	4.7727	0.4655	0.2167
MSFC	199	H.P.	AMB	AMB	2	0.2238	5.6845	0.6716	0.4511
MSFC	200	H.P.	AMB	AMB	2	0.2206	5.6032	0.6514	0.4244
MSFC	201	H.P.	AMB	AMB	2	0.2217	5.6312	0.6583	0.4334
MSFC	202	H.P.	AMB	AMB	3	0.2417	6.1392	0.7912	0.6260
MSFC	203	H.P.	AMB	AMB	3	0.2423	6.1544	0.7954	0.6327
MSFC	204	H.P.	AMB	AMB	3	0.2439	6.1951	0.8067	0.6508
MSFC	205	H.P.	AMB	AMB	4	0.2590	6.5786	0.9183	0.8433
MSFC	206	H.P.	AMB	AMB	4	0.2582	6.5583	0.9122	0.8321
MSFC	207	H.P.	AMB	AMB	4	0.2587	6.5710	0.9160	0.8391
MSFC	208	H.P.	AMB	AMB	5	0.2713	6.8910	1.0160	1.0324
MSFC	209	H.P.	AMB	AMB	5	0.2713	6.8910	1.0160	1.0324
MSFC	210	H.P.	AMB	AMB	5	0.2714	6.8936	1.0169	1.0341
MSFC	211	H.P.	AMB	AMB	6	0.2795	7.0993	1.0848	1.1768
MSFC	212	H.P.	AMB	AMB	6	0.2823	7.1704	1.1089	1.2297
MSFC	213	H.P.	AMB	AMB	6	0.2796	7.1018	1.0856	1.1786
MSFC	214	H.P.	AMB	AMB	7	0.2904	7.3762	1.1808	1.3943
MSFC	215	H.P.	AMB	AMB	7	0.2875	7.3025	1.1547	1.3334
MSFC	216	H.P.	AMB	AMB	8	0.2942	7.4727	1.2156	1.4777
MSFC	217	H.P.	AMB	AMB	8	0.2960	7.5184	1.2323	1.5185
MSFC	218	H.P.	AMB	AMB	9	0.3034	7.7064	1.3027	1.6970

TABLE B-2. (Continued)

Source	Disc #	Tester	Temperature, (°C)	Pressure, (Pa)	Energy Level, (Kg-M)	Diameter, (In.)	Diameter, (mm)	Calculated Penetration, (mm)	Calculated Penetration, Squared (mm^2)
MSFC	219	H.P.	AMB	AMB	9	0.2964	7.5286	1.2360	1.5278
MSFC	220	H.P.	AMB	AMB	10	0.3031	7.6987	1.2998	1.6894
MSFC	221	H.P.	AMB	AMB	10	0.3068	7.7927	1.3359	1.7847
MSFC	222	H.P.	AMB	AMB	10	0.2940	7.4676	1.2137	1.4731
MSFC	223	H.P.	AMB	AMB	1	0.1916	4.8666	0.4847	0.2350
MSFC	224	H.P.	AMB	AMB	5	0.2618	6.6497	0.9400	0.8837
MSFC	225	H.P.	AMB	AMB	8	0.2879	7.3127	1.1583	1.3417
MSFC	226	H.P.	AMB	AMB	8	0.2848	7.2339	1.1308	1.2787
MSFC	227	H.P.	AMB	AMB	10	0.3025	7.6835	1.2940	1.6744
MSFC	228	H.P.	AMB	AMB	10	0.3038	7.7165	1.3066	1.7071
MSFC	229	H.P.	AMB	3.4×10^7	1	0.2076	5.2730	0.5732	0.3286
MSFC	230	H.P.	AMB	3.4×10^7	1	0.2073	5.2654	0.5715	0.3266
MSFC	231	H.P.	AMB	3.4×10^7	3	0.2413	6.1290	0.7884	0.6216
MSFC	232	H.P.	AMB	3.4×10^7	3	0.2389	6.0681	0.7717	0.5956
MSFC	233	H.P.	AMB	3.4×10^7	3	0.2404	6.1062	0.7821	0.6117
MSFC	234	H.P.	AMB	3.4×10^7	5	0.2812	7.1425	1.0994	1.2087
MSFC	235	H.P.	AMB	3.4×10^7	5	0.2702	6.8631	1.0071	1.0142
MSFC	236	H.P.	AMB	3.4×10^7	5	0.2687	6.8250	0.9949	0.9898
MSFC	237	H.P.	AMB	3.4×10^7	7	0.2895	7.3533	1.1727	1.3752

71

TABLE B-2. (Continued)

Source	Disc #	Tester	Temperature, (°C)	Pressure, (Pa)	Energy Level, (Kg-M)	Diameter, (In.)	Diameter, (mm)	Calculated Penetration, (mm)	Calculated Penetration, Squared (mm^2)
MSFC	238	H.P.	AMB	3.4×10^7	7	0.2733	6.9418	1.0325	1.0661
MSFC	239	H.P.	AMB	3.4×10^7	7	0.2727	6.9266	1.0276	1.0559
MSFC	240	H.P.	AMB	3.4×10^7	9	0.2883	7.3228	1.1619	1.3500
MSFC	241	H.P.	AMB	3.4×10^7	9	0.2993	7.6022	1.2633	1.5960
MSFC	242	H.P.	AMB	3.4×10^7	9	0.2973	7.5514	1.2445	1.5487
MSFC	243	H.P.	AMB	3.4×10^7	10	0.2932	7.4473	1.2064	0.4553
MSFC	244	H.P.	AMB	3.4×10^7	10	0.2961	7.5209	1.2332	1.5208
MSFC	245	H.P.	AMB	3.4×10^7	1	0.1721	4.3713	0.3880	0.1505
MSFC	246	H.P.	AMB	3.4×10^7	1	0.1668	4.2367	0.3638	0.1323
MSFC	247	H.P.	AMB	3.4×10^7	3	0.2256	5.7302	0.6831	0.4666
MSFC	248	H.P.	AMB	3.4×10^7	3	0.2191	5.5651	0.6421	0.4123
MSFC	249	H.P.	AMB	3.4×10^7	5	0.2512	6.3805	0.8596	0.7389
MSFC	250	H.P.	AMB	3.4×10^7	5	0.2614	6.6396	0.9369	0.8778
MSFC	251	H.P.	AMB	3.4×10^7	7	0.2763	7.0180	1.0576	1.1185
MSFC	252	H.P.	AMB	3.4×10^7	7	0.2812	7.1425	1.0994	1.2087
MSFC	253	H.P.	AMB	3.4×10^7	7	0.2773	7.0434	1.0660	1.1365
MSFC	254	H.P.	AMB	3.4×10^7	9	0.2926	7.4320	1.2008	1.4420
MSFC	255	H.P.	AMB	3.4×10^7	9	0.2938	7.4625	1.2119	1.4687
MSFC	256	H.P.	AMB	3.4×10^7	10	0.3027	7.6886	1.2959	1.6794
MSFC	257	H.P.	AMB	3.4×10^7	10	0.2996	7.6098	1.2662	1.6032
MSFC	258	H.P.	LOX	AMB	1	0.1719	4.3663	0.3871	0.1498
MSFC	259	H.P.	LOX	AMB	1	0.1676	4.2570	0.3674	0.1350

72

TABLE B-2. (Continued)

Source	Disc #	Tester	Temperature, (°C)	Pressure, (Pa)	Energy Level, (Kg-M)	Diameter, (In.)	Diameter, (mm)	Calculated Penetration, (mm)	Calculated Penetration, Squared (mm²)
MSFC	260	H.P.	LOX	AMB	1	0.1701	4.3205	0.3788	0.1435
MSFC	261	H.P.	LOX	AMB	3	0.2139	5.4331	0.6104	0.3726
MSFC	262	H.P.	LOX	AMB	3	0.2203	5.5959	0.6496	0.4220
MSFC	263	H.P.	LOX	AMB	3	0.2215	5.6261	0.6571	0.4318
MSFC	264	H.P.	LOX	AMB	5	0.2394	6.0808	0.7752	0.6009
MSFC	265	H.P.	LOX	AMB	5	0.2265	5.7531	0.6889	0.4746
MSFC	266	H.P.	LOX	AMB	5	0.2313	5.8750	0.7203	0.5188
MSFC	267	H.P.	LOX	AMB	7	0.2477	6.2916	0.8340	0.6955
MSFC	268	H.P.	LOX	AMB	7	0.2412	6.1265	0.7877	0.6205
MSFC	269	H.P.	LOX	AMB	7	0.2436	6.1874	0.8046	0.6474
MSFC	270	H.P.	LOX	AMB	7	0.2395	6.0833	0.7759	0.6020
MSFC	271	H.P.	LOX	AMB	7	0.2391	6.0731	0.7731	0.5977
MSFC	272	H.P.	LOX	AMB	7	0.2404	6.1062	0.7821	0.6117
MSFC	273	H.P.	LOX	AMB	9	0.2586	6.5684	0.9152	0.6377
MSFC	274	H.P.	LOX	AMB	9	0.2574	6.5380	0.9061	0.8210
MSFC	275	H.P.	LOX	AMB	10	0.2797	7.1044	1.0865	1.1805
MSFC	276	H.P.	LOX	AMB	10	0.2736	6.9494	1.0350	1.0713
MSFC	277	H.P.	LOX	AMB	10	0.2776	7.0510	1.0686	1.1419
MSFC	278	H.P.	LOX	AMB	10	0.2554	6.4872	0.8909	0.7937
MSFC	279	H.P.	LOX	AMB	10	0.2585	6.5659	0.9145	0.8363
MSFC	280	H.P.	LOX	AMB	10	0.2641	6.7081	0.9581	0.9179
MSFC	281	H.P.	LOX	AMB	10	0.2619	6.6523	0.9408	0.8851
MSFC	282	H.P.	LOX	AMB	10	0.2614	6.6396	0.9369	0.8778

TABLE B-2. (Continued)

Source	Disc #	Tester	Temperature, (°C)	Pressure, (Pa)	Energy Level, (Kg-M)	Diameter, (In.)	Diameter, (mm)	Calculated Penetration, (mm)	Calculated Penetration, Squared (mm^2)
MSFC	283	H.P.	LOX	AMB	10	0.2614	6.6396	0.0360	0.8778
MSFC	284	H.P.	LOX	3.4×10^7	1	0.1684	4.2774	0.3710	0.1376
MSFC	285	H.P.	LOX	3.4×10^7	1	0.1358	3.4493	0.2387	0.0570
MSFC	286	H.P.	LOX	3.4×10^7	1	0.1682	4.2723	0.3701	0.1370
MSFC	287	H.P.	LOX	3.4×10^7	3	0.2120	5.3848	0.5990	0.3589
MSFC	288	H.P.	LOX	3.4×10^7	3	0.2240	5.6896	0.6729	0.4528
MSFC	289	H.P.	LOX	3.4×10^7	3	0.2413	6.1290	0.7884	0.6216
MSFC	290	H.P.	LOX	3.4×10^7	5	0.2194	5.5728	0.6440	0.4147
MSFC	291	H.P.	LOX	3.4×10^7	5	0.2260	5.7404	0.6857	0.4702
MSFC	292	H.P.	LOX	3.4×10^7	5	0.2274	5.7760	0.6947	0.4827
MSFC	293	H.P.	LOX	3.4×10^7	7	0.2410	6.1214	0.7863	0.6183
MSFC	294	H.P.	LOX	3.4×10^7	7	0.2425	6.1595	0.7968	0.6349
MSFC	295	H.P.	LOX	3.4×10^7	7	0.2443	6.2052	0.8096	0.6554
MSFC	296	H.P.	LOX	3.4×10^7	9	0.2532	6.4313	0.8744	0.7646
MSFC	297	H.P.	LOX	3.4×10^7	9	0.2530	6.4262	0.8729	0.7620
MSFC	298	H.P.	LOX	3.4×10^7	9	0.2522	6.4059	0.8670	0.7516
MSFC	299	H.P.	LOX	3.4×10^7	10	0.2596	6.5938	0.9229	0.8518
MSFC	300	H.P.	LOX	3.4×10^7	10	0.2598	6.5989	0.9245	0.8547
MSFC	301	H.P.	LOX	3.4×10^7	10	0.2576	6.5430	0.9076	0.8237
MSFC	302	H.P.	LOX	3.4×10^7	10	0.2506	6.3652	0.8551	0.7313
MSFC	303	H.P.	LOX	3.4×10^7	10	0.2616	6.6446	0.9385	0.8807
MSFC	304	H.P.	LOX	3.4×10^7	10	0.2538	6.4465	0.8789	0.7724

TABLE B-2. (Continued)

Source	Disc #	Tester	Temperature, (°C)	Pressure, (Pa)	Energy Level, (Kg-M)	Diameter, (In.)	Diameter, (mm)	Calculated Penetration, (mm)	Calculated Penetration, Squared (mm²)
SSFL	305	H.P.	HIGH	AMB	1	0.1889	4.7981	0.4706	0.2215
SSFL	306	H.P.	HIGH	AMB	1	0.1887	4.7930	0.4696	0.2205
SSFL	307	H.P.	HIGH	AMB	1	0.1857	4.7168	0.4542	0.2063
SSFL	308	H.P.	HIGH	AMB	5	0.2714	6.8936	1.0169	1.0340
SSFL	309	H.P.	HIGH	AMB	5	0.2656	6.7462	0.9700	0.9409
SSFL	310	H.P.	HIGH	AMB	5	0.2677	6.7996	0.9868	0.9738
SSFL	311	H.P.	HIGH	AMB	7	0.2849	7.2365	1.1317	1.2807
SSFL	312	H.P.	HIGH	AMB	7	0.2870	7.2898	1.1503	1.3231
SSFL	313	H.P.	HIGH	AMB	7	0.2909	7.3889	1.1853	1.4050
SSFL	314	H.P.	HIGH	AMB	10	0.3175	8.0645	0.4445	2.0867
SSFL	315	H.P.	HIGH	AMB	10	0.3110	7.8994	1.3778	1.8984
SSFL	316	H.P.	HIGH	AMB	10	0.3119	7.9223	1.3869	1.9236
SSFL	317	H.P.	AMB	AMB	1	0.1765	4.4831	0.4088	0.1671
SSFL	318	H.P.	AMB	AMB	1	0.1781	4.5237	0.4165	0.1735
SSFL	319	H.P.	AMB	AMB	1	0.1778	4.5161	0.4150	0.1723
SSFL	320	H.P.	AMB	AMB	2	0.2039	5.1791	0.5520	0.3047
SSFL	321	H.P.	AMB	AMB	2	0.2008	5.1003	0.5346	0.2858
SSFL	322	H.P.	AMB	AMB	2	0.2024	5.1410	0.5435	0.2954
SSFL	323	H.P.	AMB	AMB	3	0.2241	5.6921	0.6735	0.4536
SSFL	324	H.P.	AMB	AMB	3	0.2256	5.7302	0.6831	0.4666
SSFL	325	H.P.	AMB	AMB	3	0.2276	5.7810	0.6960	0.4844
SSFL	326	H.P.	AMB	AMB	4	0.2353	5.9766	0.7471	0.5581

TABLE B-2. (Continued)

Source	Disc #	Tester	Temperature, (°C)	Pressure, (Pa)	Energy Level, (Kg-M)	Diameter, (In.)	Diameter, (mm)	Calculated Penetration, (mm)	Calculated Penetration, Squared (mm²)
SSFL	327	H.P.	AMB	AMB	4	0.2373	6.0274	0.7607	0.5787
SSFL	328	H.P.	AMB	AMB	4	0.2377	6.0376	0.7635	0.5829
SSFL	329	H.P.	AMB	AMB	5	0.2564	6.5126	0.8985	0.8073
SSFL	330	H.P.	AMB	AMB	5	0.2581	6.5557	0.9114	0.8307
SSFL	331	H.P.	AMB	AMB	5	0.2589	6.5761	0.9176	0.8419
SSFL	332	H.P.	AMB	AMB	7	0.2579	6.8047	0.9884	0.9770
SSFL	333	H.P.	AMB	AMB	7	0.2717	6.9012	1.0193	1.0391
SSFL	334	H.P.	AMB	AMB	7	0.2701	6.8605	0.0062	1.0125
SSFL	335	H.P.	AMB	AMB	8	0.2855	7.2517	1.1370	1.2827
SSFL	336	H.P.	AMB	AMB	8	0.2870	7.2898	1.1503	1.3231
SSFL	337	H.P.	AMB	AMB	8	0.2862	7.2695	0.1432	1.3068
SSFL	338	H.P.	AMB	AMB	10	0.2948	7.4879	1.2211	1.4912
SSFL	339	H.P.	AMB	AMB	10	0.2966	7.5336	1.2379	1.5324
SSFL	340	H.P.	AMB	AMB	10	0.2938	7.4625	1.2119	1.4687
SSFL	341	H.P.	LOX	AMB	1	0.1485	3.7719	0.2865	0.0821
SSFL	342	H.P.	LOX	AMB	1	0.1500	3.8100	0.2925	0.0855
SSFL	343	H.P.	LOX	AMB	1	0.1506	3.8252	0.2949	0.0870
SSFL	344	H.P.	LOX	AMB	5	0.2239	5.6871	0.6723	0.4519
SSFL	345	H.P.	LOX	AMB	5	0.2249	5.7125	0.6786	0.4605
SSFL	346	H.P.	LOX	AMB	5	0.2249	5.7125	0.6786	0.4605
SSFL	347	H.P.	LOX	AMB	7	0.2412	6.1265	0.7877	0.6205
SSFL	348	H.P.	LOX	AMB	7	0.2395	6.0833	0.7759	0.6020

TABLE B-2. (Continued)

Source	Disc #	Tester	Temperature, (°C)	Pressure, (Pa)	Energy Level, (Kg-M)	Diameter, (In.)	Diameter, (mm)	Calculated Penetration, (mm)	Calculated Penetration, Squared (mm²)
SSFL	349	H.P.	LOX	AMB	7	0.2438	6.1925	0.8060	0.6497
SSFL	350	H.P.	LOX	AMB	10	0.2657	6.7488	0.9708	0.9424
SSFL	351	H.P.	LOX	AMB	10	0.2642	6.7107	0.9589	0.9194
SSFL	352	H.P.	LOX	AMB	10	0.2626	6.6700	0.9463	0.8955
SSFL	353	H.P.	HIGH	AMB	1	0.1806	4.5872	0.4287	0.1838
SSFL	354	H.P.	HIGH	AMB	1	0.1841	4.6761	0.4461	0.1990
SSFL	355	H.P.	HIGH	AMB	1	0.1857	4.7168	0.4542	0.2063
SSFL	356	H.P.	HIGH	AMB	5	0.2592	6.5837	0.9199	0.8462
SSFL	357	H.P.	HIGH	AMB	6	0.2694	6.8428	1.0005	1.0011
SSFL	358	H.P.	HIGH	AMB	5	0.2695	6.8453	1.0014	1.0027
SSFL	359	H.P.	HIGH	AMB	7	0.2914	7.4016	1.1899	1.4158
SSFL	360	H.P.	HIGH	AMB	7	0.2922	7.4219	1.1972	1.4333
SSFL	361	H.P.	HIGH	AMB	7	0.2915	7.4041	1.1908	1.4180
SSFL	362	H.F.	HIGH	AMB	10	0.3139	7.9731	1.4073	1.9806
SSFL	363	H.P.	HIGH	AMB	10	0.3060	7.7724	1.3281	1.7637
SSFL	364	H.P.	HIGH	AMB	10	0.3184	8.0874	1.4540	2.1140
SSFL	365	H.P.	AMB	AMB	1	0.1766	4.4856	0.4093	0.1675
SSFL	366	H.P.	AMB	AMB	1	0.1756	4.4602	0.4045	0.1636
SSFL	367	H.P.	AMB	AMB	1	0.1738	4.4145	0.3960	0.1568
SSFL	368	H.P.	AMB	AMB	5	0.2630	6.6802	0.9494	0.9014
SSFL	369	H.P.	AMB	AMB	5	0.2611	6.6319	0.9346	0.8734

TABLE B-2. (Continued)

Source	Disc #	Tester	Temperature, (°C)	Pressure, (Pa)	Energy Level, (Kg-M)	Diameter, (In.)	Diameter, (mm)	Calculated Penetration, (mm)	Calculated Penetration, Squared (mm^2)
SSFL	370	H.P.	AMB	AMB	5	0.2631	6.6827	0.9502	0.9029
SSFL	371	H.P.	AMB	AMB	7	0.2821	7.1653	1.1072	1.2259
SSFL	372	H.P.	AMB	AMB	7	0.2824	7.1730	1.1098	1.2317
SSFL	373	H.P.	AMB	AMB	7	0.2836	7.2034	1.1203	1.2550
SSFL	374	H.P.	AMB	AMB	10	0.3004	7.6302	1.2738	1.6226
SSFL	375	H.P.	AMB	AMB	10	0.3071	7.8003	1.3389	1.7926
SSFL	376	H.P.	AMB	AMB	10	0.3077	7.8156	1.3448	1.8086
SSFL	377	H.P.	LOX	AMB	1	0.1513	3.8430	0.2977	0.0886
SSFL	378	H.P.	LOX	AMB	1	0.1545	3.9243	0.3108	0.0966
SSFL	379	H.P.	LOX	AMB	1	0.1583	4.0208	0.3266	0.1067
SSFL	380	H.P.	LOX	AMB	5	0.2183	5.5448	0.6372	0.4060
SSFL	381	H.P.	LOX	AMB	5	0.2215	5.6261	0.6571	0.4318
SSFL	382	H.P.	LOX	AMB	5	0.2135	5.4229	0.6080	0.3697
SSFL	383	H.P.	LOX	AMB	7	0.2447	6.2154	0.8124	0.6600
SSFL	384	H.P.	LOX	AMB	7	0.2455	6.2357	0.8181	0.6693
SSFL	385	H.P.	LOX	AMB	7	0.2440	6.1976	0.8074	0.6520
SSFL	386	H.P.	LOX	AMB	10	0.2676	6.7970	0.9860	0.9722
SSFL	387	H.P.	LOX	AMB	10	012695	6.8453	1.0014	1.0027
SSFL	388	H.P.	LOX	AMB	10	012662	6.7615	0.9748	0.9502
SSFL	389	H.P.	HIGH	3.4 x 10^7	1	0.1878	4.7701	0.4649	0.2162
SSFL	390	H.P.	HIGH	3.4 x 10^7	1	0.1841	4.6761	0.4461	0.1990

TABLE B-2. (Continued)

Source	Disc #	Tester	Temperature, (°C)	Pressure, (Pa)	Energy Level, (Kg-M)	Diameter, (In.)	Diameter, (mm)	Calculated Penetration, (mm)	Calculated Penetration, Squared (mm^2)
SSFL	391	H.P.	HIGH	3.4×10^7	1	0.1898	4.8209	0.4753	0.2259
SSFL	392	H.P.	HIGH	3.4×10^7	5	0.2687	6.8250	0.9949	0.9898
SSFL	393	H.P.	HIGH	3.4×10^7	5	0.2697	6.8504	1.0030	1.0060
SSFL	394	H.P.	HIGH	3.4×10^7	7	0.2913	7.3990	1.1890	1.4137
SSFL	395	H.P.	HIGH	3.4×10^7	7	0.2929	7.4397	1.2036	1.4487
SSFL	396	H.P.	HIGH	3.4×10^7	7	0.3046	7.7368	1.3143	1.7275
SSFL	397	H.P.	HIGH	3.4×10^7	10	0.3467	8.8062	1.7745	3.1488
SSFL	398	H.P.	HIGH	3.4×10^7	10	0.3085	7.8359	1.3528	1.8300
SSFL	399	H.P.	HIGH	3.4×10^7	10	0.3119	7.9223	1.3869	1.9236
SSFL	400	H.P.	AMB	3.4×10^7	1	0.1708	4.3383	0.3820	0.1459
SSFL	401	H.P.	AMB	3.4×10^7	1	0.1734	4.4044	0.3941	0.1553
SSFL	402	H.P.	AMB	3.4×10^7	1	0.1705	4.3307	0.3806	0.1449
SSFL	403	H.P.	AMB	3.4×10^7	2	0.2043	5.1892	0.5543	0.3072
SSFL	404	H.P.	AMB	3.4×10^7	2	0.2038	5.1765	0.5514	0.3041
SSFL	405	H.P.	AMB	3.4×10^7	2	0.2044	5.1918	0.5548	0.3079
SSFL	406	H.P.	AMB	3.4×10^7	3	0.2269	5.7633	0.6915	0.4782
SSFL	407	H.P.	AMB	3.4×10^7	3	0.2252	5.7201	0.6806	0.4632
SSFL	408	H.P.	AMB	3.4×10^7	3	0.2247	5.7074	0.6774	0.4588
SSFL	409	H.P.	AMB	3.4×10^7	4	0.2482	6.3043	0.8376	0.7016
SSFL	410	H.P.	AMB	3.4×10^7	4	0.2469	6.2713	0.8282	0.6859
SSFL	411	H.P.	AMB	3.4×10^7	4	0.2477	6.2916	0.8340	0.6955
SSFL	412	H.P.	AMB	3.4×10^7	5	0.2592	6.5837	0.9199	0.8462

TABLE B-2. (Continued)

Source	Disc #	Tester	Temperature, (°C)	Pressure, (Pa)	Energy Level, (Kg-M)	Diameter, (In.)	Diameter, (mm)	Calculated Penetration, (mm)	Calculated Penetration, Squared (mm^2)
SSFL	413	H.P.	AMB	3.4×10^7	5	0.2566	6.5176	0.9000	0.8100
SSFL	414	H.P.	AMB	3.4×10^7	5	0.2607	6.6218	0.9315	0.8676
SSFL	415	H.P.	AMB	3.4×10^7	7	0.2779	7.0587	1.0712	1.1474
SSFL	416	H.P.	AMB	3.4×10^7	7	0.2753	6.9926	1.0492	1.1008
SSFL	417	H.P.	AMB	3.4×10^7	7	0.2742	6.9647	1.0400	1.0817
SSFL	418	H.P.	AMB	3.4×10^7	8	0.2841	7.2161	1.1246	1.2648
SSFL	419	H.P.	AMB	3.4×10^7	8	0.2803	7.1196	1-0916	1.1917
SSFL	420	H.P.	AMB	3.4×10^7	8	0.2770	7.0358	1.0635	1.1311
SSFL	421	H.P.	AMB	3.4×10^7	10	0.2883	7.3228	1.1619	1.3500
SSFL	422	H.P.	AMB	3.4×10^7	10	0.2936	7.4574	1.2100	1.4642
SSFL	423	H.P.	AMB	3.4×10^7	10	0.2969	7.5413	1.2407	1.5394
SSFL	424	H.P.	LOX	3.4×10^7	1	0.1486	3.7744	0.2869	0.0823
SSFL	425	H.P.	LOX	3.4×10^7	1	0.1485	3.7719	0.2865	0.0821
SSFL	426	H.P.	LOX	3.4×10^7	1	0.1478	3.7541	0.2838	0.0805
SSFL	427	H.P.	LOX	3.4×10^7	2	0.1790	4.5466	0.4209	0.1771
SSFL	428	H.P.	LOX	3.4×10^7	2	0.1762	4.4755	0.4074	0.1659
SSFL	429	H.P.	LOX	3.4×10^7	2	0.1769	4.4933	0.4107	0.1687
SSFL	430	H.P.	LOX	3.4×10^7	3	0.2011	5.1079	0.5362	0.2876
SSFL	431	H.P.	LOX	3.4×10^7	3	0.1959	4.9759	0.5077	0.2577
SSFL	432	H.P.	LOX	3.4×10^7	3	0.1945	4.9403	0.5001	0.2501
SSFL	433	H.P.	LOX	3.4×10^7	4	0.2149	5.4585	0.6164	0.3800
SSFL	434	H.P.	LOX	3.4×10^7	4	0.2135	5.4229	0.6080	0.3697

TABLE B-2. (Continued)

Source	Disc #	Tester	Temperature (°C)	Pressure (Pa)	Energy Level (Kg-M)	Diameter (In.)	Diameter (mm)	Calculated Penetration (mm)	Calculated Penetration Squared (mm^2)
SSFL	435	H.P.	LOX	3.4×10^7	4	0.2085	5.2959	0.5784	0.3346
SSFL	436	H.P.	LOX	3.4×10^7	5	0.2296	5.8318	0.7091	0.5028
SSFL	437	H.P.	LOX	3.4×10^7	7	0.2425	6.1595	0.7968	0.6349
SSFL	438	H.P.	LOX	3.4×10^7	7	0.2431	6.1747	0.8011	0.6417
SSFL	439	H.P.	LOX	3.4×10^7	7	0.2431	6.1747	0.8011	0.6417
SSFL	440	H.P.	LOX	3.4×10^7	8	0.2510	6.3754	0.8581	0.7363
SSFL	441	H.P.	LOX	3.4×10^7	8	0.2486	6.3144	0.8405	0.7064
SSFL	442	H.P.	LOX	3.4×10^7	8	0.2521	6.4033	0.8662	0.7503
SSFL	443	H.P.	LOX	3.4×10^7	10	0.2595	6.5913	0.9222	0.8504
SSFL	444	H.P.	LOX	3.4×10^7	10	0.2616	6.6446	0.9385	0.8807
SSFL	445	H.P.	LOX	3.4×10^7	10	0.2588	6.5735	0.9168	0.8405
WSTF	446	H.P.	AMB	AMB	1	0.1718	4.3637	0.3866	0.1495
WSTF	447	H.P.	AMB	AMB	1	0.1718	4.3637	0.3866	0.1495
WSTF	448	H.P.	AMB	AMB	1	0.1735	4.4069	0.3946	0.1557
WSTF	449	H.P.	AMB	AMB	1	0.1705	4.3307	0.3806	0.1449
WSTF	450	H.P.	AMB	AMB	1	0.1700	4.3180	0.3783	0.1431
WSTF	451	H.P.	AMB	AMB	3	0.2162	5.4915	0.6243	0.3898
WSTF	452	H.P.	AMB	AMB	3	0.2172	5.5169	0.6304	0.3974
WSTF	453	H.P.	AMB	AMB	3	0.2150	5.4610	0.6170	0.3807
WSTF	454	H.P.	AMB	AMB	3	0.2200	5.5880	0.6477	0.4195
WSTF	455	H.P.	AMB	AMB	3	0.2213	5.6210	0.6558	0.4301
WSTF	456	H.P.	AMB	AMB	5	0.2455	6.2357	0.8181	0.6693

TABLE B-2. (Continued)

Source	Disc #	Tester	Temperature, (°C)	Pressure, (Pa)	Energy Level, (Kg-M)	Diameter, (In.)	Diameter, (mm)	Calculated Penetration, (mm)	Calculated Penetration, Squared (mm^2)
WSTF	457	H.P.	AMB	AMB	5	0.2500	6.3500	0.8507	0.7238
WSTF	458	H.P.	AMB	AMB	5	0.2498	6.3449	0.8493	0.7213
WSTF	459	H.P.	AMB	AMB	5	0.2455	6.2357	0.8181	0.6693
WSTF	460	H.P.	AMB	AMB	5	0.2475	6.2865	0.8325	0.6931
WSTF	461	H.P.	AMB	AMB	7	0.2670	6.7818	0.9812	0.9627
WSTF	462	H.P.	AMB	AMB	7	0.2680	6.8072	0.9892	0.9785
WSTF	463	H.P.	AMB	AMB	7	0.2683	6.8148	0.9916	0.9833
WSTF	464	H.P.	AMB	AMB	7	0.2640	6.7056	0.9573	0.9164
WSTF	465	H.P.	AMB	AMB	7	0.2745	6.9723	1.0425	1.0869
WSTF	466	H.P.	AMB	AMB	8	0.2767	7.0282	1.0610	1.1257
WSTF	467	H.P.	AMB	AMB	8	0.2775	7.0485	1.0678	1.1401
WSTF	468	H.P.	AMB	AMB	8	0.2772	7.0409	1.0652	1.1347
WSTF	469	H.P.	AMB	AMB	8	0.2777	7.0536	1.0695	1.1437
WSTF	470	H.P.	AMB	AMB	8	0.2795	7.0993	1.0848	1.1768
WSTF	471	H.P.	AMB	AMB	10	0.2943	7.4752	1.2165	1.4799
WSTF	472	H.P.	AMB	AMB	10	0.2828	7.1831	1.1133	1.2394
WSTF	473	H.P.	AMB	AMB	10	0.2880	7.3152	1.1592	1.3437
WSTF	474	H.P.	AMB	AMB	10	0.2850	7.2390	1.1326	1.2827
WSTF	475	H.P.	AMB	AMB	10	0.2935	7.4549	1.2091	1.4620
WSTF	476	H.P.	AMB	3.4×10^7	1	0.0740	1.8796	0.0699	0.0049
WSTF	477	H.P.	AMB	3.4×10^7	1	0.0749	1.9025	0.0717	0.0051
WSTF	478	H.P.	AMB	3.4×10^7	1	0.0790	2.0066	0.0798	0.0064

TABLE B-2. (Continued)

Source	Disc #	Tester	Temperature (°C)	Pressure (Pa)	Energy Level (Kg-M)	Diameter (In.)	Diameter (mm)	Calculated Penetration (mm)	Calculated Penetration, Squared (mm²)
WSTF	479	H.P.	AMB	3.4×10^7	3	0.1880	4.7752	0.4660	0.2171
WSTF	480	H.P.	AMB	3.4×10^7	3	0.1945	4.9403	0.5001	0.2501
WSTF	481	H.P.	AMB	3.4×10^7	3	0.1840	4.6736	0.4456	0.1986
WSTF	482	H.P.	AMB	3.4×10^7	3	0.1950	4.9530	0.5028	0.2528
WSTF	483	H.P.	AMB	3.4×10^7	3	0.1965	4.9911	0.5109	0.2611
WSTF	484	H.P.	AMB	3.4×10^7	5	0.2335	5.9309	0.7350	0.5402
WSTF	485	H.P.	AMB	3.4×10^7	5	0.2168	5.5067	0.6280	0.3944
WSTF	486	H.P.	AMB	3.4×10^7	5	0.2233	5.6718	0.6684	0.4468
WSTF	487	H.P.	AMB	3.4×10^7	5	0.2362	5.9995	0.7532	0.5673
WSTF	488	H.P.	AMB	3.4×10^7	5	0.2322	5.8979	0.7263	0.5275
WSTF	489	H.P.	AMB	3.4×10^7	7	0.2518	6.3957	0.8640	0.7465
WSTF	490	H.P.	AMB	3.4×10^7	7	0.2475	6.2865	0.8325	0.6931
WSTF	491	H.P.	AMB	3.4×10^7	7	0.2518	6.3957	0.8640	0.7465
WSTF	492	H.P.	AMB	3.4×10^7	7	0.2543	6.4592	0.8826	0.7790
WSTF	493	H.P.	AMB	3.4×10^7	7	0.2600	6.6040	0.9260	0.8576
WSTF	494	H.P.	AMB	3.4×10^7	8	0.2630	6.6802	0.9494	0.9014
WSTF	495	H.P.	AMB	3.4×10^7	8	0.2587	6.5710	0.9160	0.8391
WSTF	496	H.P.	AMB	3.4×10^7	8	0.2680	6.8072	0.9892	0.9785
WSTF	497	H.P.	AMB	3.4×10^7	8	0.2625	6.6675	0.9455	0.8940
WSTF	498	H.P.	AMB	3.4×10^7	8	0.2560	6.5024	0.8954	0.8018
WSTF	499	H.P.	AMB	3.4×10^7	10	0.2713	6.8910	1.0160	1.0324
WSTF	500	H.P.	AMB	3.4×10^7	10	0.2763	7.0180	1.0576	1.1185
WSTF	501	H.P.	AMB	3.4×10^7	10	0.2740	6.9596	1.0384	1.0782
WSTF	502	H.P.	AMB	3.4×10^7	10	0.2758	7.0053	1.0534	1.1097

TABLE B-2. (Continued)

Source	Disc #	Tester	Temperature, (°C)	Pressure, (Pa)	Energy Level, (Kg-M)	Diameter, (In.)	Diameter, (mm)	Calculated Penetration, (mm)	Calculated Penetration, Squared (mm^2)
WSTF	503	H.P.	AMB	3.4×10^7	10	0.2810	7.1374	1.0977	1.2049
WSTF	504	H.P.	LOX	3.4×10^7	3	0.1525	3.8735	0.3026	0.0915
WSTF	505	H.P.	LOX	3.4×10^7	3	0.1300	3.3020	0.2184	0.0477
WSTF	506	H.P.	LOX	3.4×10^7	3	0.1045	2.6543	0.1402	0.0197
WSTF	507	H.P.	LOX	3.4×10^7	3	0.1570	3.9878	0.3212	0.1031
WSTF	508	H.P.	LOX	3.4×10^7	5	0.1630	4.1402	0.3469	0.1203
WSTF	509	H.P.	LOX	3.4×10^7	5	0.1750	4.4450	0.4016	0.1613
WSTF	510	H.P.	LOX	3.4×10^7	5	0.1350	3.4290	0.2358	0.0556
WSTF	511	H.P.	LOX	3.4×10^7	5	0.1535	3.8989	0.3066	0.0940
WSTF	512	H.P.	LOX	3.4×10^7	5	0.1790	4.5466	0.4209	0.1771
WSTF	513	H.P.	LOX	3.4×10^7	5	0.1205	3.0607	0.1872	0.0350
WSTF	514	H.P.	LOX	3.4×10^7	7	0.1863	4.7320	0.4572	0.2091
WSTF	515	H.P.	LOX	3.4×10^7	7	0.1355	3.4417	0.2376	0.0565
WSTF	516	H.P.	LOX	3.4×10^7	7	0.1950	4.9530	0.5028	0.2528
WSTF	517	H.P.	LOX	3.4×10^7	7	0.1874	4.7600	0.4629	0.2143
WSTF	518	H.P.	LOX	3.4×10^7	7	0.1775	4.5085	0.4136	0.1711
WSTF	519	H.P.	LOX	3.4×10^7	8	0.1745	4.4323	0.3993	0.1594
WSTF	520	H.P.	LOX	3.4×10^7	8	0.1890	4.8006	0.4711	0.2220
WSTF	521	H.P.	LOX	3.4×10^7	8	0.1715	4.3561	0.3852	0.1484
WSTF	522	H.P.	LOX	3.4×10^7	8	0.2155	5.4737	0.6201	0.3845
WSTF	523	H.P.	LOX	3.4×10^7	8	0.1935	4.9149	0.4948	0.2448
WSTF	524	H.P.	LOX	3.4×10^7	8	0.1935	4.9149	0.4948	0.2448

TABLE B-2. (Concluded)

Source	Disc #	Tester	Temperature, (°C)	Pressure, (Pa)	Energy Level, (Kg-M)	Diameter, (In.)	Diameter, (mm)	Calculated Penetration, (mm)	Calculated Penetration, Squared (mm^2)
WSTF	525	H.P.	LOX	3.4×10^7	8	0.1930	4.9022	0.4921	0.2422
WSTF	526	H.P.	LOX	3.4×10^7	10	0.2116	5.3746	0.5967	0.3560
WSTF	527	H.P.	LOX	3.4×10^7	10	0.2156	5.4762	0.6207	0.3852
WSTF	528	H.P.	LOX	3.4×10^7	10	0.1810	4.5974	0.4307	0.1855
WSTF	529	H.P.	LOX	3.4×10^7	10	0.2156	5.4762	0.6207	0.3852
WSTF	530	H.P.	LOX	3.4×10^7	10	0.1932	4.9073	0.4932	0.2432

APPENDIX C

COMPARISON OF HIGH PRESSURE IMPACT TESTERS AND PROCEDURES

	MSFC	SSFL	WSTF
I. Apparatus:			
A. Pins			
Material	Inconel 718	Inconel 718	17-4
Hardness	Rc 43-45	Rc 36-45	Rc 43-45
Diameter	1/2"	1/2"	1/2"
Finish	16 micro in/in	16 micro in/in	16 micro in/in
Reuse	Every 5 drops on metallics	Changed when necessary	Change each drop
B. Shaft			
Material	Inconel 718	Inconel 718	Inconel 718
Diameter	0.625"	0.625"	0.375"
Hardness	Rc 43-45	Rc 36-45	Rc 43-45
Design	1 piece	1 piece	2 pieces
C. Seals	3 omni seals, Teflon for cryogenic, 15% graphite filled for RT & above	3 omni seals, Teflon & moly filled TFE	2 15% graphite filled ball seals
D. Bore Tightness	Empirical Check (through balance pressure)	Empirical Check (through balance pressure)	Spring Gauge Check
E. Blanks	Optional	One/day	Optional
F. Thermocouple	Within 0.090" of wall	Within 0.090" of wall	In chamber
G. Oxygen	99.5%	99.5%	99.5%
H. Free Fall		Velocity Checked each drop	

	MSFC	SSFL	WSTF
I. Apparatus:			
I. Base	Each verify and hardness	Composition	Thickness
J. Mountings	Floor and pedestal	Concrete block and pedestal	Cylindrical pedestal, floor separate block
II. Measurements:			
A. Temperature	Fe/Const TC	Fe/Const TC	Ch/Al TC
B. Pressure	Strain Gauge	Transducer	Strain Gauge
C. Flash	No	No	Yes
III. Evaluation:			
A. Reaction	Visual, cup, sample, striker	Visual, cup, sample, striker	Visual/flash detector
B. Rebound	Catcher	Catcher	No Catcher
IV. Procedure:			
A. Cleaning -			
Cups, Pins	MSFC-164A	RL10001	WSTF-1-3.14
Block	F-33	Freon	Freon
O_2 Lines	--	Flushed with Freon	--
Sample	Detergent (F-33)	Elastomers	No Trichloroethylene
	Distilled (H_2O)	Freon	On non-metallics
	Freon	(Material dependent)	Distilled (H_2O)
	Dry/150° overnight		GN_2, Dry/RT

	MSFC	SSFL	WSTF
IV. **Procedure:**			
Between Drops	Kimwipe	Flush with Freon, GN_2	Flush with Freon
B. Preload	Preload until striker down then back off pressure	Preload until striker down	Preload to 60 lb. force, check periodically with forge gauge

APPENDIX D

ROCKETDYNE REPORT No. MPR 74-751, "CORRECTION FACTOR FOR THE HIGH PRESSURE OXYGEN IMPACT TESTER"

Rockwell
International
Rocketdyne Division

21 May 1974   MPR 74-751

D. L. Fulton   llw'   Chemistry & Nonmetallic
D/596-175, AC10   Materials

                                      2340

CORRECTION FACTOR FOR THE HIGH PRESSURE OXYGEN IMPACT TESTER

INTRODUCTION

The High Pressure Oxygen Compatibility Impact Tester, two of which are installed at MSFC and one at Rocketdyne, differ from the conventional unpressurized ABMA LOX Impact Tester in that a special head (Figure 1) is utilized to test under oxygen pressures up to 10,000 psi. A balanced pressure on each end of the striker pin in the head theoretically eliminates the need for an impact energy correction factor to be applied because of the high pressure alone. However, the Teflon Omniseals used in the test head introduce a frictional resistance to pin movement, and the higher the pressure the higher the friction. Friction data provided by the seal supplier show that this resistance is low at room temperature and is reported to be less than 125 lbs for 3 seals, even at high pressure. However, MSFC M&P Laboratory personnel reported that it required about 1000 lbs to move the piston when the seals were chilled down to cryogenic temperatures without the test head being pressurized. (This increase in resistance could be due to the differential coefficient of thermal expansion, which would make the seals shrink down onto the piston.) Concern was expressed by MSFC personnel that friction considerations may be even more significant at low temperature under high pressure, especially when threshold determinations are conducted which might result in fairly low impact energy ratings for some materials. Working simultaneously, both MSFC and Rocketdyne conducted a test program to determine the effects of tester seal friction. This report summarizes Rocketdyne's work to date. MSFC's study has not been reported.

CONCLUSIONS

1. Testing at -160C and 8800 psi resulted in a maximum seal frictional resistance of 1200 lbs when the 20 lb plummet was dropped from a height of 15 inches. Extrapolated to a drop height of 21 inches, the friction value was 1380 lbs. Friction energy losses from 9-16 percent were calculated.

2. Some discrepant data points were obtained which have not been fully explained. Retesting at these levels produced data points which fell in line with others considered good; however,   89

D. L. Fulton
21 May 1974
Page 2

MPR 74-751

additional testing will be conducted to isolate the cause of the discrepancy. The data obtained so far is still considered useful for applying a meaningful correction factor to test data.

3. It is recommended that a safety factor of 1½:1 be applied to the friction data until more precise data can be obtained from more closely controlled tests.

PROCEDURE AND RESULTS

Theoretical

Energy is imparted to a specimen by dropping the tester plummet having a fixed weight of 20 lbs from some height, h, onto the striker pin which rests directly on the specimen. Without the seals installed in the test head the total energy of the drop, $E_t = 20 \times h$, is approximately equal to the energy, E_s, received by the specimen since the friction is negligible. With the seals installed, however, the only way that the specimen can receive the same amount of energy, E_s, is to increase the drop height so that a new total energy, $E_t' = 20 \times h'$, less the energy, E_f, lost to friction, equals E_s.

Expressing the above as equations:

$$E_s = E_t = 20h \quad \text{(without seals)} \qquad (1)$$

$$E_s = E_t' - E_f = 20h' - E_f \quad \text{(with seals)} \qquad (2)$$

$$\therefore \quad E_t = E_t' - E_f \qquad (3)$$

$$\text{or} \quad E_f = E_t' - E_t = 20h' - 20h = 20 \Delta h \qquad (4)$$

The key to the solution of the above equations is to have some way of knowing when the same energy, E_s, is imparted to the test specimens with and without seals installed. There is no easy way of measuring E_s directly, but it can be represented by measuring the amount of deformation in the specimen after impact. Since the higher the drop height the greater the deformation, curves can be developed of drop height vs specimen deformation for both conditions, with and without seals installed. Then, for a given deformation, which represents the same E_s, the difference in drop height, Δh, between the 2 curves represents the loss to the seals. This difference, Δh, multiplied by the weight of the plummet (20 lbs) is the energy, E_f, lost in the seals (Equation (4)).

The energy loss can also be expressed as the product of the friction force, E_f, and the total displacement, Δ_s, of the striker pin. Neglecting the effects of elastic deformation in the striker pin and the specimen, Δ_s can be approximated by measuring the permanent vertical deformation in the specimen.

Then

$$20 \Delta h = F_f \times \Delta_s \qquad (5)$$

or $\qquad F_f = \dfrac{20 \Delta h}{\Delta_s} \qquad (6)$

Thus, the friction force can be calculated from experimental data.

Experimental

A standard Inconel 718 striker pin was modified by machining its flat tip to form a ½ inch diameter hemisphere so that, when impacted, a Brinnel-type indentation is made in a test specimen (Figure 2). The test specimens were 7/8 inch diameter x 3/16 inch thick disks of 6061-0 and 6061-T6 aluminum alloy. Data were then generated and plots were made of drop height vs the circular diameter of the indentation, both with and without seals and with the 2 heat conditions of 6061 alloy noted above. The diameters were measured in 2 directions, 90 degrees apart, using a Mitutoyo Type Bi-4 tool maker's microscope which was calibrated to the nearest 0.0001 inch. For friction force, F_f, calculations, the pin displacement, Δ_s, was taken as the depth of the hemispherical indentation, the value for which was determined from the geometrical relationship of the depth to the measured circular diameter of the hemispherical depression.

It is apparent that the relationship, between plummet drop height and the indentation diameter of the hemispherical striker tip, is a curve with a lower bound of 0,0 (i.e., zero drop height, zero indentation diameter) and an upper bound equal to the diameter of the hemispherical striker tip. The curve is illustrated as follows:

91
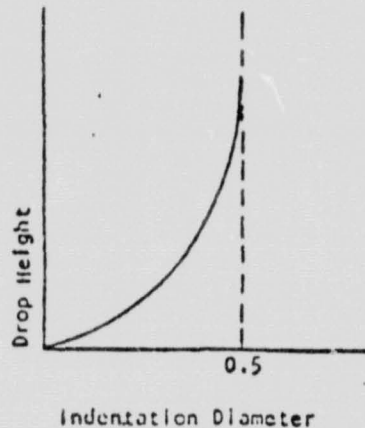
D. L. Fulton
21 May 1974
Page 4

HPR 74-751

Using the tester generated data (omitting the discrepant data points discussed below) a computer generated exponential curve fit equation, $y = ax^b$, was determined. This was done for each of the four test conditions shown in Figure 3.

Figure 3 also shows the discrepant data points, noticeably at the 9-inch drop height level for the 6061-0 curves. Retesting, however, produced data points having good alignment with those obtained at other drop heights. (The possible causes of the discrepancies are discussed later.)

From equation (6) it is obvious that, for the friction force to remain constant (as theoretically it should), Δh should vary as some function of Δ_s. The convergence of the curves toward the 0,0 bound bears this out except that the calculations at several indentation diameters indicate the friction is less at lower drop heights. The maximum Δh and therefore the maximum friction within the range of the actual data points occurs at an indentation diameter of 0.30 inch, representing a Δh of 3 inches and a deflection of 0.05 inch. Substituting these values in Equation (6):

$$F_f = \frac{20 \times 3}{.05} = 1200 \text{ lbs}$$

Similarly, by extrapolating the same set of curves to the point where the curve for seals installed crosses the 21 inch drop height level, a Δh of approximately 4 inches and a deflection of .058 inch (for 0.3215 inch indentation diameter) are obtained. In this case the friction force is approximately

$$F_f \approx \frac{20 \times 4}{.058} \approx 1380 \text{ lbs}$$

The above values are considered sufficiently accurate for certain conclusions to be drawn.

DISCUSSION

Various factors which might have caused the discrepancies noted above have been considered. Among these are wobble and drag in the plummet tracks, sideways movement in the specimen at impact, sideways movement in the striker pin when seals are not installed, and the pressure on the pin from the automatic pressure balancing system at time of plummet release. It is known that the automatic pressure balancing system on the pin (designed to apply a positive pressure on the pin to hold it against the specimen) works against the friction force, and its magnitude depends on what the downward pressure is at time of impact. An attempt will be made to determine the maximum and minimum pressures on the pin resulting from the automatic balancing system and investigate the effects of other variables.

APPENDIX D

D. L. Fulton
21 May 1974
Page 5

MPR 74-751

PAGE 5 OF 8

In spite of these discrepancies, the alignment of the data points is considered to be accurate enough to draw some meaningful conclusions. Assuming a friction force of 1380 lbs (for drop height of approximately 21 inches) and a full pin travel through a 0.050 inch test specimen, the friction energy loss is 1380 x 0.050 or 69 in-lb (5.75 ft-lb). For a material such as Vespel SP-211, which has an impact threshold level of 36 ft-lb (approximately a drop height of 21 inches) in that thickness under the same temperature and pressure, the percent loss is about 16. Similarly, making the same assumption for 0.015 inch thick specimens, the loss is 20.7 inch-lb (1.7 ft-lb). Again, the threshold level for Vespel SP-211 in that thickness is 18 ft-lb, or the energy loss to friction is approximately 9½ percent. (The value is even less for friction actually determined for a drop height of 9 inches.)

An energy loss of 9-16 percent is considered conservative (somewhat higher than the actual value) from the standpoint of assuming a deformation equal to the thickness of the material and the fact that elastic deformation was neglected in calculating the friction force. (A larger Δ_s in equation (6) would result in a smaller F_f.) On the other hand, since some data points were obviously discrepant, it has to be assumed that other points may be somewhat inaccurate but to a much lesser degree. It is possible, therefore, that the curves for the pressurized tests (Figure 3) could shift slightly (to the left, for example, if the data were not obtained at minimum pressure differential on the pressure balancing system on the pin).

Until more precise data points can be obtained by refining the test procedure and exercising tighter controls, on the tester, it is recommended that a safety factor be applied to the friction loss. A factor of 1½:1 is more than enough to spread out the curves for tests with and without seals (Figure 3) so that all of the good data points fall between them. It is recommended that this value (equivalent of a maximum percent loss of 24) be used for the development of rationale for the use of Vespel SP-211 and other materials for which threshold determinations have been made. The correction factor can be updated when additional testing has been completed.

R. Bodemeijer

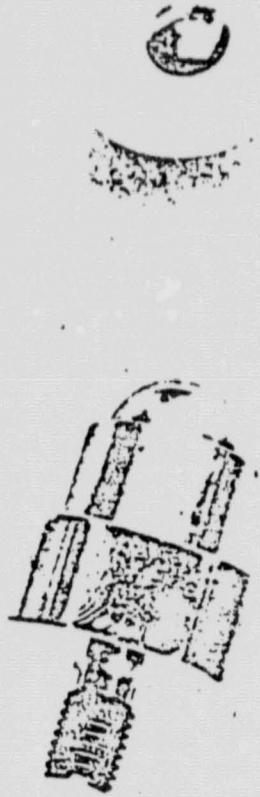R. Bodemeijer

G. E. Williams

G. E. Williams

J. H. Lieb, Manager
Chemistry & Nonmetallic Materials
Materials and Processes

JHL:GEW:cb

94

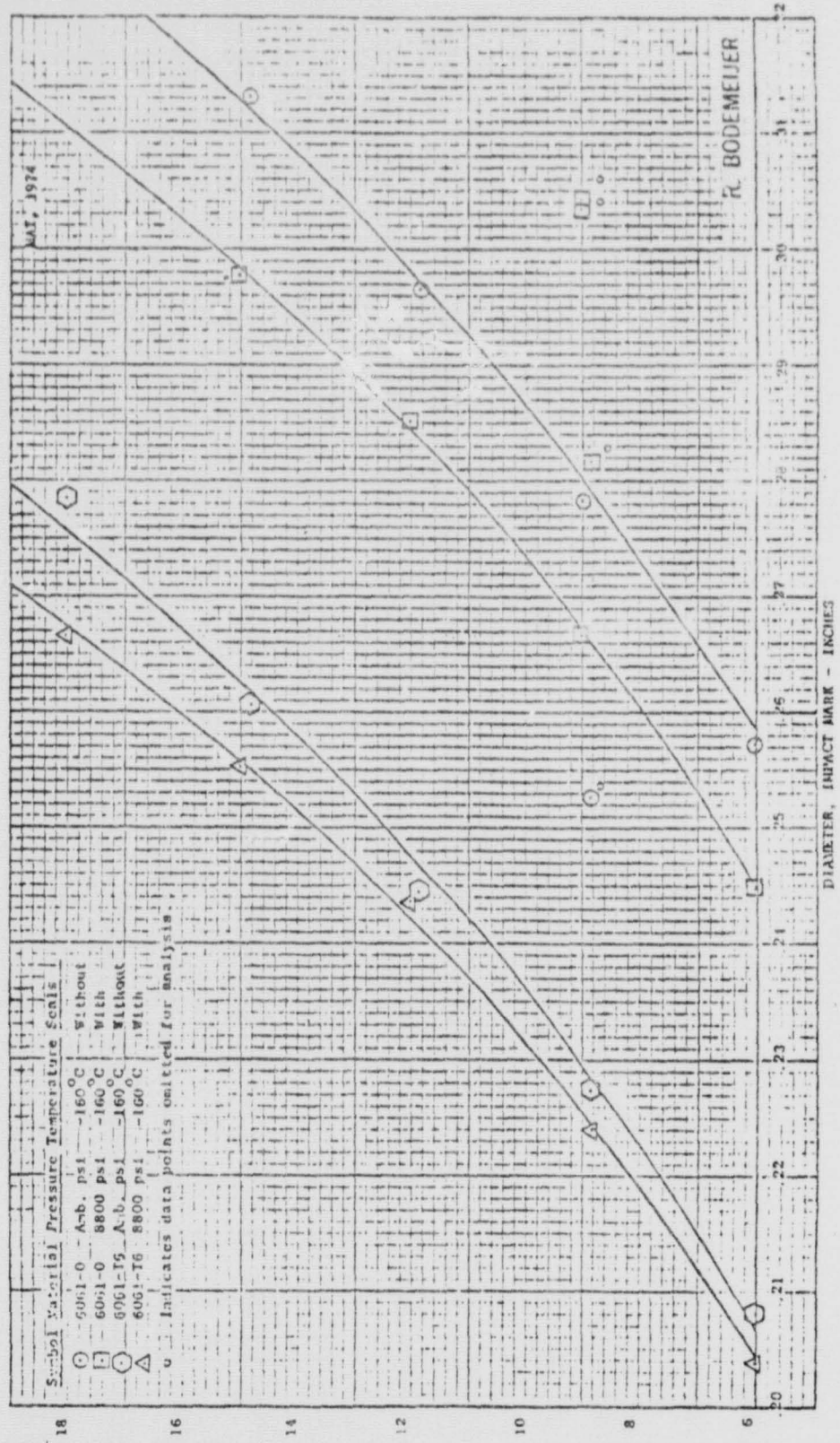# HIGH PRESSURE OXYGEN IMPACT TESTER
- FRICTION LOSS DETERMINATION -

MODIFIED STRIKER TIP — IMPACTED SPECIMEN

Figure 2

APPENDIX D.